Instituto Tecnológico y de Estudios Superiores de Monterrey

Campus Monterrey

School of Engineering and Sciences

Folates, amino acids, and phenotypic analyses of Methionine Synthase *Arabidopsis thaliana* T-DNA mutants

A thesis presented by

Jorge Alberto Alcudia Zamudio

Submitted to the

School of Engineering and Sciences

in partial fulfillment of the requirements for the degree of

Master of Science

In Biotechnology

Monterrey Nuevo León, **June 15th, 2020**

Dedication

Acknowledgements

Content

List of Figures

List of Tables

Abbreviations

10-CHO-THF: 10-formyl-tetrahydrofolate

1C: one carbon metabolism

5,10-CH=THF: 5,10-Methenyltetrahydrofolate

5,10-CH_2-THF: 5,10-Methylenetetrahydrofolate

5-CH3-THF: 5-methyl-tetrahydrofolate

5-CHO-THF: 5-formyl-tetrahydrofolate

ABRC: The Arabidopsis Biological Resource Center

ACC: Aminocyclopropane-1-carboxylic acid

ACO: ACC oxidase

ADC: 4-amino-4deoxychorismate

Arg: Arginine

Asn: Asparagine

Asp: Aspartic acid

ATMS1: *A. thaliana* methionine synthase 1

ATMS2: *A. thaliana* methionine synthase 2

ATMS3: *A. thaliana* methionine synthase 3

ATP: Adenine triphosphate

CHES: 2-(Cyclohexylamino)ethanesulfonic acid

CTAB: Cetyltrimethylammonium bromide

CTP: Cytidine triphosphate

Cys: Cysteine

dCTP: 2'deoxycytidine-5'-triphosphate

DEPC: Diethyl pyrocarbonate

DHF: Dihydrofolate

DHM: 7,8-dihydromonapterin

DHN-P3: 7,8-dihydropneopterin 3'-triphosphate

dTMP: Thymidylate

DTPA: Diethylenetriaminepentaacetic acid

dTTP: Thymidine triphosphate

dUTP: 2'-deoxyuridine-5'-triphosphate

EDTA: Ethylenediaminetetraacetic acid

FA: Folic acid

FPGS: Folypolyglutamate synthase

FW: Fresh weight

GGH: γ-glutamyl hydrolase

Gln: Glutamine

Glu: Glutamic acid

Gly: Glycine

Gly: Glycine

GTP: guanosine tri-phosphate

GTPCHI: GTP cyclohydrolase I

H_3PO_4: Phosporic acid

Hcy: Homocysteine

HEPES: (4-(2-hydroxyethyl)-1-piperazineethanesulfonic acid

His: Histidine

Hm: Homozygous

HMDHP: 6-hydroxymethyl-7,8-dihydropterin

HMDHP-P_2: Hydroxymethyldihydropterin pyrophosphate

HPLC: High performance liquid chromatography

Hz: Heterozygous

Ile: Isoleucine

K_2HPO_4: Dipotassium phosphate

KH_2PO_4: Potassium dihydrogen phosphate

Leu: Leucine

Lys: Lysine

Met: Methionine

MS: Methionine synthase

M&S: Murashige and Skoog

NADH: Nicotinamide adenine dinucleotide

NaH_2PO_4: Monosodium phosphate

NDP: Nucleotide diphosphates

NTP: Nucleotide triphosphates

p-ABA: p-aminobenzoic acid

PCR: Polymerase chain reaction

Phe: phenylalanine

Pro: Proline

PRPP: Phosphoribosyl pyrophosphate

PVP: Polyvinylpyrrolidone

SAM: s-adenosylmethionine

Ser: Serine

Ser: Serine

TAIR: The Arabidopsis Information Resource

THF: tetrahydrofolate

Thr: Threonine

Tyr: Tyrosine

UDP: Uridine diphosphate

UPLC: Ultra performance liquid chromatography

UTP: Uridine triphosphate

Val: Valine

WT: Wild type

Folates, amino acids, and phenotypic analyses of Methionine Synthase *Arabidopsis thaliana* T-DNA mutants

by

Jorge Alberto Alcudia Zamudio

Resumen

Las plantas son la principal fuente de micronutrientes para humanos. Los folatos (vitamina B9) y los aminoácidos esenciales, como la metionina, están presentes en niveles limitados en las plantas. Además, los folatos y la metionina interactúan en el metabolismo de un carbono (1C), por lo tanto, estas moléculas tienen un rol clave en el crecimiento y desarrollo de las plantas. *Arabidopsis thaliana* tiene tres isoenzimas de metionina sintasa (ATMS1, ATMS2 y ATMS3), enzimas responsables de la síntesis de metionina. ATMS1 y ATMS2 están localizadas en citosol y ATMS3 en plástidos. El presente trabajo tuvo como objetivo comprender el rol de cada isoenzima en el fenotipo visual de crecimiento y el contenido de metabolitos en ocho mutantes de T-DNA de *A.thaliana*. Se realizó una selección de mutantes de T-DNA para aislar plantas homocigotas y heterocigotas para cada isoforma. Subsecuentemente se realizó un estudio fenotípico *in vitro*, se cosecharon las plantas, y finalmente, se cuantificó el perfil de aminoácidos por HPLC-fluorescencia y folatos por HPLC-electroquímico. Interesantemente sólo se identificaron plantas homocigotas para ATMS2 y ATMS3, indicando que las líneas mutantes homocigotas de ATMS1 son letales debido a que sólo se encontraron plantas heterocigotas. Diferencias significativas fueron encontradas en germinación, peso de plántulas, desarrollo de la planta, tamaño de cotiledón y de raíz, y peso de semillas de las líneas mutantes con respecto a las plantas control. También, el perfil de aminoácidos se vio diferencialmente afectado en aminoácidos de las familias de síntesis de aspartato, glutamato, y aminoácidos aromáticos. 5-CH_3-THF fue el principal tipo de folato caracterizado en todas las plantas de *Arabidopsis*, el cual mostró diferencias significativas con incrementos de hasta 46% en los contenidos de las líneas mutantes de ATMS3 con respecto a las plantas control. Además, resultados preliminares indican cambios en el perfil de poliglutamilación de 5-CH_3-THF en las plantas mutantes en las cuales se encontró que acumulan mayoritariamente de 6 a 9 residuos de glutamato a diferencia de las plantas control que acumula principalmente 1 residuo de glutamato. Estos resultados sirven como los primeros pasos para un estudio de genómica funcional y conducen a un interesante trabajo futuro de aspectos de funcionalidad aún desconocidos de las isoenzimas de metionina sintasa en plantas.

Abstract

Plants are the main source of micronutrients for humans. Folates (Vitamin B9) and essential amino acids, such as methionine, are present in limited levels in plants. Furthermore, folates and methionine interact in one carbon metabolism (1C), therefore, these molecules have a key role in plant growth and development. *Arabidopsis thaliana* has three methionine synthase isoenzymes (ATMS1, ATMS2 and ATMS3), enzymes that are responsible for methionine biosynthesis. ATMS1 and ATMS2 are localized in cytosol and ATMS3 in plastids. Therefore, the objective of the present work was to understand the role of each isoenzyme in the visual growth phenotype and metabolite content in eight *A. thaliana* T-DNA mutants. A selection of T-DNA mutants was performed to isolate homozygous and heterozygous plants for each isoenzyme. Subsequently, an *in vitro* phenotypic study was performed, the plants were harvested, and finally, the amino acid content was characterized by fluorescence-HPLC and folate profile was characterized by electrochemical-HPLC. Interestingly, only homozygous plants for ATMS2 and ATMS3 were identified, indicating that the homozygous mutant lines of ATMS1 could be lethal because only heterozygous plants were found. Significant differences were found in germination, seedling weight, plant development, cotyledon and root size, and seed weight of the mutant lines in comparison to control plants. Also, the amino acid profile was differentially affected in amino acids from the aspartate, glutamate, and aromatic biosynthetic families. 5-CH_3-THF was the main type of folate characterized in all *Arabidopsis* plants, which showed significant differences with increases of up to 46% in ATMS3 mutant lines with respect to control plants. Furthermore, preliminary results indicate changes in the polyglutamylation profile of 5-CH_3-THF in mutant lines in which it was found that they accumulate mostly from 6 to 9 glutamate residues unlike the control plants that accumulates 1 glutamate residue. These results serve as the first steps for a functional genomic study and lead to interesting future work on still unknown aspects of functionality of methionine synthase isoenzymes in plants.

1. Introduction

Methionine is an essential amino acid in all organisms, its production depends on the enzyme Methionine synthase (MS), which takes homocysteine as a substrate and uses 5-methyl-tetrahydrofolate (5-CH_3-THF) as a donor of a methyl group to form methionine. There are three isoforms of methionine synthase in *Arabidopsis thaliana*, two are located in the cytosol (ATMS1; At5g17920 and ATMS2; At3g03780), and another in chloroplasts (ATMS3; At5g20980) (Ravanel *et al*., 2004). The ATMS1 and ATMS2 isoforms are involved in the regeneration of methionine from homocysteine, while the ATMS3 isoform is responsible for *de novo* synthesis of methionine in plant cells (Stéphane Ravanel et al., 2004). On the other hand, the methionine synthase enzyme participates in a step compromised by the metabolic pathway of ethylene biosynthesis and one carbon metabolism (1C) (Baur & Yang, 1972; García-Salinas, Ramos-Parra, & de la Garza, 2016).

One-carbon metabolism is an important metabolic process involved in cellular functions and development as well as glycine-serine interconversion, purines; thymidylate methionine and ethylene biosynthesis, etc; which are essential molecules for life (García-Salinas, Ramos-Parra, & de la Garza, 2016; Ramos-Parra, Urrea-López, & Díaz de la Garza, 2013). Ethylene and methionine biosynthesis metabolic pathways require the participation of compounds known as folates. Folates, also known as tetrahydrofolates (THF) and their derivatives, are a family of enzymatic co-factors that participate in important metabolic reactions (Crider, Yang, Berry, & Bailey, 2012).

Folate deficiency is associated with abnormalities in the metabolism of 1C, which causes chronic diseases and the development of disorders, such as autism, Alzheimer's disease, senile dementia and neural tube defects (Fox & Stover, 2008; Saini, Nile, & Keum, 2016). Because of this, a diet rich in folates is highly recommended for pregnant women, in order to prevent disease and improve the proper development of the fetus.

The main source of folates in developed countries is folic acid, the synthetic form of folates, although there are possible adverse effects associated with their consumption , for example, folic acid can mask risk symptoms for prostate cancer and vitamin deficiencies B12 (Hanson & Gregory III, 2011). For this reason, the best way to combat folate deficiencies by

preventing side effects to health is by increasing the consumption of fruits and vegetables rich in this vitamin (Maharaj, Prasad, Devi, & Gopalan, 2015).

The main focus of this research work was to investigate the relationship of the disabling (knockout) of the three isoforms of methionine synthase in *Arabidopsis thaliana*, with observable phenotypic effects and metabolic phenotypes associated with amino acids and folates biosynthesis pathways. For this purpose, the study of insertional mutants (Knockout mediated by T-DNA insertion) for ATMS1, ATMS2 and ATMS3 isoforms were carried out to assess the impact on their metabolism and development.

1.1 Justification

Methionine synthase is a key enzyme for the development of plants and prokaryotes, since it is the only way for *de novo* methionine synthesis (Ravanel *et al.,* 2004), unlike plants, animal cells cannot synthesize methionine, therefore, it should be acquire it through food (Hanson & Gregory III, 2011). Methionine is an amino acid present and indispensable for protein synthesis, in addition to being involved in one carbon metabolism (1C) and in important biological processes such as methylation, responsible for genetic regulation in the cell (González & Vera, 2019; Lieberman, Kunishi, Mapson, & Wardale, 1965; Stéphane Ravanel, Gakière, Job, & Douce, 1998; Sauter, Moffatt, Saechao, Hell, & Wirtz, 2013; Yan *et al*., 2019). The processes of addition of 1C units are of vital importance in the synthesis of numerous metabolites such as thymidylate, serine, glycine, purine rings, 5-methyl-tetrahydrofolate, and s-adenosylmethionine (SAM) (Fox & Stover, 2008; Jabrin, Ravanel, Gambonnet, Douce, & Rébeillé, 2003). There are three known isoenzymes of methionine synthase which are ATMS1, ATMS2, and ATMS3 (Ravanel et al., 2004). Therefore, to know what impact each isoform in the plant and the importance of their localization in the growing phenotype has, in this work, *A. thaliana* insertion mutant lines were selected, analyzed, and compared with the wild variety. This is part of an approach of the classic strategy of functional genomics, in which by eliminating an isoenzyme, it will be known what impact it has globally on the plant. This work is going to provide basic knowledge of vital importance to future research work to unravel the functional destinations of each isoenzyme and their relationship in plant development.

This knowledge will give us information about agricultural importance and will also eventually lay the foundations of knowledge to be able to use metabolic engineering tools to design more nutritious foods that can impact human nutrition worldwide

1.2 Hypothesis

The lack of one methionine synthase isoforms could alter *Arabidopsis thaliana* at several levels, including phenotypic, metabolic and plant development.

1.3 Objectives

1.3.1 General Objective

- To evaluate the overall phenotypic and metabolic impact of the individual absence of each of the methionine synthase isoforms on the development of *Arabidopsis thaliana.*

1.3.2 Specific objectives

- To identify homozygous plants for ATMS1, ATMS2 and ATMS3 T-DNA insertion knockouts.
- To characterize the development phenotype *in vitro* of ATMS1, ATMS2 and ATMS3 T-DNA insertion knockouts
- To characterize the amino acid profile of the ATMS1, ATMS2 and ATMS3 T-DNA insertion knockouts
- To characterize the folates profile of the ATMS1, ATMS2 and ATMS3 T-DNA insertion knockouts

2. Background

2.1 Folates and one carbon metabolism

Tetrahydrofolate and its derivatives, known as folates, belong to a family of enzyme co-factors that participate in a number of important metabolic reactions as mediators of the transfer of one-carbon (C1) (Mehrshahi *et al*., 2010). Tetrahydrofolate is the natural form of vitamin B9 and they are present in plant foods, mainly green leaves, legume seeds, fruits; while folic acid is the synthetic form of this vitamin, which is used in fortified foods and dietary supplements(Fox & Stover, 2008).

Because folates are present in low amounts in food sources, the primary source of dietary folate in developed countries is the synthetic folic acid. Although the consumption of this synthetic form arise some possible adverse effects, for example the synthetic folate form can mask symptoms of prostate cancer risk and Vitamin B_{12} deficiency (Araghi *et al*., 2019; Hanson & Gregory III, 2011; Hirsch *et al*., 2019). Therefore, the best way to combat the folate deficiency complications, avoiding health concerns is to increase the consumption of fruits and vegetables with folate-rich content and enhanced bioavailability (Crider *et al*., 2012). Due to the low amounts of folates in foods and significant losses reported during food processing , such as boiling (10-64%) and frying (1-36%) (Maharaj *et al*., 2015), different approaches have been performed to increase the folate content of fruits and vegetables to accomplish the dietary intake requirements (Saini *et al*., 2016).

Additionally, photorespiration and chlorophyll synthesis in plants require folates; also the 1C product, SAM, is required for the production of molecules such as ethylene, nicotinamide and polyamines, and also, for DNA methylation (Stephane Ravanel, Douce, & Rebeille, 2011). Now it is clear that folates have an essential role in plant cell development, but folates biosynthesis is a complex process in which are involved several enzymes, products and precursors (Jabrin *et al*., 2003); the importance of these processes are going to be described in the next sections.

2.1.2 Folates biosynthesis in plants

Naturally, the plant folates are formed by three molecules, including a pterin ring, p-aminobenzoic acid (pABA) and glutamate tail (**Figure 2.1**). This polyglutamate tail (-Glu_n) is created by the action of folypolyglutamate synthase (FPGS), which performs the sequential addition of γ-linked glutamate residues to THF. Many forms of folates differ in the one carbon unit which is linked at N_5-and/or N_{10} position of the ptering moiety (**Figure 2.1**), such as methyl (5-CH_3-), methylene (5,10-CH_2-), formimino (5-CHNH-), formyl (5-or 10-CHO-), and methenyl (5,10-CH=) (Hanson & Gregory III, 2011). Folates are converted into the animal cells in many forms such as dihydrofolate, tetrahydrofolate, L-methyl folate, and other derivatives. Each folate form participates in important and specified biological activities, such as methionine regeneration from homocysteine, nucleotide synthesis, oxidation and reduction of 1C units that are required for normal cell division and growth, and DNA methylations (Crider *et al*., 2012).

The folate biosynthetic pathway in plants has been extensively described (Hanson & Gregory III, 2011; Saini *et al*., 2016). Biosynthesis of pteridine moieties starts with the breakdown of guanosine triphosphate (GTP) in the cytosol as shown in **Figure 2.2** (Steps 1-4). A product, 7,8-dihydroneopterin 3'–triphosphate (DHN-P_3) is formed and mediated by GTP cyclohydrolase I (GTPCHI). DHN-P_3 is used to create 7,8-dihydroneopterin mediated by DHN-P_3 pyrophosphatase and non-specific phosphatase in two steps dephosphorylation. 6-hydroxymethyl-7,8-dihydropterin (HMDHP) and glycolaldehyde are formed cleaving the side chain of DHN by dihydroneptering aldolase; also, this enzyme facilitates the epimerization of the second carbon of the DHN side chain, a product from this reaction is 7,8-dihydromonapterin (DHM), this compound finally is cleaved to form HMDHP (Hanson & Gregory III, 2011; Saini *et al*., 2016).

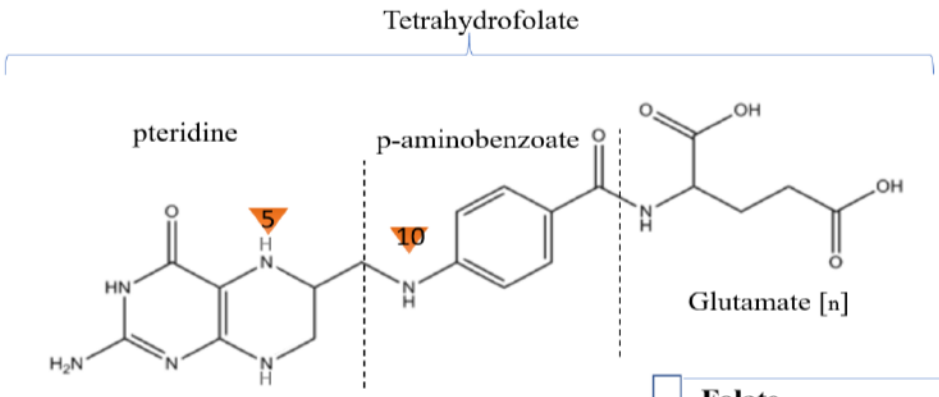

Folate name	Position	
	N_5	N_{10}
THF	-H	-H
10-CHO-THF	-H	-CHO
5-CH_3-THF	-CH_3	-H
5-CHO-THF	-CHO	-H
Folic acid	-	-H

Stability

Folate cofactor	Products
THF	Glycine
5,10-CH_2-THF	Thymidylate, pantothenate and serine
10-CHO-THF	Purines, formate and formylmethionyl tRNA
5-CH_3-THF	**Methionine**
5-CHO-THF	Not 1C donor

Figure 2.1. Chemical structure of Tetrahydrofolate (THF) and their derivatives. In this figure is shown the basic structure of folates molecules. The table show examples of products of metabolic processes that uses folates as precursors. This figure is modified from (Saini *et al*., 2016).

The p-amino benzoic acid is synthesized from chorismate in plastids by two steps reaction catalyzed by amino deoxychorismate synthase and amino deoxychorismate lyase as shown in **Figure 2.2** (Steps 5 and 6). The first step is the transfer of amide nitrogen of glutamine to chorismate, this reaction form 4-amino-4deoxychorismate (ADC). Subsequently, the second step consists of the elimination and aromatization of pyruvate giving rise to p-ABA.

Finally, the last step is the assembling of HMDHP and p-ABA moieties into THF, this reaction occurs in the mitochondrion as shown in **Figure 2.2** (steps 7 to 10). The first step in the formation of 6-hydroxymethyldihydropterin pyrophosphate (HMDHP-P_2) consists on the activation of HMDHP by HMDHP pyrophosphokinase, subsequently, HMDHP-P_2 is attached to p-ABA mediated by C-N bonding to produce dihydropteroate (DHP); this condensation process is catalyzed by dihydropteroate synthase. Then, DHP and glutamate are linked by dihydrofolate synthase to produce dihydrofolate (DHF).

The last step consists on the reduction of DHF to THF mediated by the bifunctional enzyme DHF reductase-thymidylate synthase. The formation of the polyglutamate tail of THF-Glu_n occurs by sequential addition of γ-lined glutamate residues to THF mediated by the action of folypolyglutamate synthase (FPGS). These mechanisms of folate biosynthesis are regulated at different levels, and it is a matter of great importance in order to be efficiently utilized for enhancement of folates in plants (Saini *et al*., 2016).

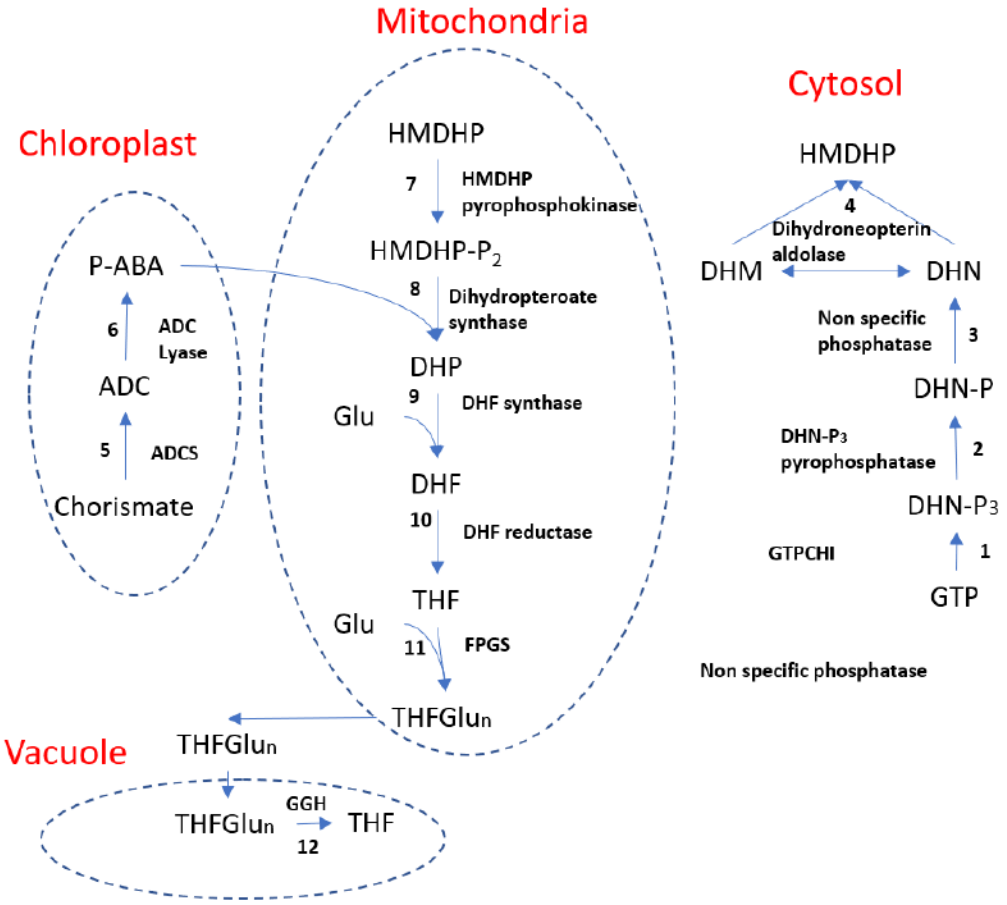

Figure 2.2 Compartmentalization of folate biosynthesis pathway in plant cells. A schematic representation of the folate moieties synthesized in different cellular compartments. It shown the enzymes involved in each metabolic step. ADC, 4-amino-4deoxychorismate; ADCS, 4-amino-4deoxychorismate synthetase; p-ABA, p-aminobenzoic acid; HMDHP, 6-hydroxymethyl-7,8-dihydropterin; HMDHP-P_2, hydroxymethyldihydropterin pyro-phosphate; DHP, dihydropterin; DHF, dihydrofolate; THF, tetrahydrofolate; FPGS, folypolyglutamate synthase; DHN, dihydropneopterin; GTP, guanosine tri-phosphate. This figure is modified from (Hanson & Gregory III, 2011; Saini *et al*., 2016).

From folates species, 5-CH_3-THF is an important folate derivative, which plays an essential role as a methyl donor for the regeneration of methionine from homocysteine. This folate derivative is produced in the methylation cycle occurring in one carbon metabolism (Fox & Stover, 2008). Due to methylation reactions are important mechanisms of gene regulation in eukaryotic cells, 5-CH_3-THF is the main biologically active form of folate that plays an important role at cellular level in the transfer of methyl group to homocysteine mediated by the action of methionine synthase (MS) and the generation of methionine. Also 5-CH_3-THF is responsible for the synthesis one carbon metabolism end products such as interconversion serine/glycine, thymidylate, pantothenate, purines, formate, formylmethionyl tRNA, ethylene, polyamines, proteins, etc.

2.1.2 One carbon metabolism

As previously stated, the addition or removal of one-carbon moieties, which is known as one-carbon (1C) metabolism, coordinates the production of numerous biological compounds and regulate many metabolic processes. The 1C units for transfer reactions come from tetrahydrofolate (THF) cofactors which are required in major cellular processes that will be detailed next. Methionine is the source of S-adenosyl-methionine (SAM), this molecule represents the principal substrate to obtain methyl units which are required for the synthesis of molecules such as chlorophyll, choline, and lignin required for plant growth and development (Jabrin *et al*., 2003).

2.1.2.1. Glycine and serine interconversion

Glycine is one of the proteinogenic amino acids, this compound is biosynthesized in different pathways. The major pathway in most organisms uses L-serine to yield glycine catalyzed by glycine hydroxymethyltransferase. Additionally, this process represents the main source for one-carbon units, which are stored in using 5,10-methylene-THF(5,10-CH_2-THF) mono-L-glutamate. In eukaryotic cells, there is an opposite process mediated by serine hydroxymethyltransferase 2 (SHMT2) and serine hydroxymethyltransferase 1 (SHMT1), both isoenzymes are localized in cytosol and mitochondria, respectively; in this process, serine is converted to glycine and one carbon groups are used for purine synthesis. Also, glycine can be formed using glyoxylate as substrate to produce glyoxylate cycle mediated by alanine-glyoxylate transaminase. Other mechanism involved in glycine biosynthesis consists on using L-threonine mediated by low-specificity L-threonine aldolase (Kastanos, Woldman,

& Appling, 1997). Moreover, serine and glycine are sources of one-carbon units required for necessary cellular components such as purines, pyrimidines, amino acids, and lipids.

2.1.2.2. Purines and thymidylate biosynthesis

Deoxyribonucleic acid (DNA) is the molecule responsible for storing and transmission of genetic information. The nucleotides are the building blocks that constitute DNA, and these are molecules created by a nucleoside linked to a phosphate group. These molecules are divided into purines (adenine and guanine) and pyrimidines (thymine, cytosine, and uracil). Purine nucleotides play a key role in many aspects of cellular metabolism such as enzyme cofactors, cellular signaling, phosphate group donors, and generating cellular energy (Rolfes, 2006). A review of nucleotides metabolism has been extensively described by Witte & Herde (2020), briefly nucleotides monophosphates are synthesized *de novo* from phosphoribosyl pyrophosphate (PRPP), glutamine, aspartic acid, bicarbonate, glycine, and 5-formyl-tetrahydrofolate, in which 5-formyl-tetrahydrofolate serve as storage form of folate due to its stability and regulate folate-dependent one carbon metabolism by enzymes inhibition targeting folate-dependent *de novo* purine biosynthesis enzymes (Field *et al*., 2006).

Then, nucleotides monophosphates are phosphorylated to yield nucleotide diphosphates (NDPs) and triphosphates (NTPs). NTPs are building blocks to synthesize RNA and serve as precursors for the biosynthesis of metabolites such as SAM, UDP-glucose, and NADH. Moreover, nucleotides are essential stores of chemical energy, which is contained in the phosphoanhydride bonds used in several energetic coupling reactions, also serve as important donors of phosphate in kinase reactions. NDPs yield dNDPs when undergoing reduction process, then dNDPs follow a phosphorylation reaction to produce dNTPs which serve as precursors for DNA biosynthesis (Witte & Herde, 2020).

In another hand, 5,10-methylene-THF is a by-product from serine metabolism, which is required in thymidylate synthesis. This reaction belongs to pyrimidine nucleotide biosynthesis. In this metabolic process, there are two convergent pathways; the first starts with cytidine-triphosphate (CTP) and formate, both substrates are reduced to produce 2'deoxycytidine-5'-triphosphate (dCTP), followed by a reaction catalyzed by dCTP deaminase (EC 3.5.4.13) to yield 2'-deoxyuridine-5'-triphosphate (dUTP); the second

pathway comes from the reaction of formate and uridine-triphosphate (UTP) to produce dUTP. From this convergent step, dUTP is used to produce 2'-deoxyuridine 5'-phosphate, 2'-deoxyuridine 5- monophosphate (dUMP), the subsequent reaction uses 5,10-methylene-THF and dUMP catalyzed by thymidylate synthase (EC 2.1.1.45) to yield thymidylate (dTMP). Finally, two phosphorylation reactions occur to yield thymidine triphosphate (dTTP).

2.1.2.3. Pantothenate biosynthesis

Pantothenate, also known as B5, is the universal precursor molecule required to synthesize 4'-phosphopantetheine, this compound is an essential moiety of coenzyme A and acyl carrier protein. In plants and microorganisms, pantothenate can be synthesized *de novo*. The biosynthesis of pantothenate starts with 3-methyl-2-oxobutanoate and 5,10-methylenetetrahydrofolate in a reaction catalyzed by ketopantoate hydroxymethyl-transferase (EC 2.1.2.11) to yield 2-dehydropantoate and tetrahydrofolate. Then, 2-dehydropantoate undergo reduction process by 2-dehydropantoate (EC 1.1.1.169) reductase to produce (R)-pantoate; β-alanine and (R)-pantoate are ligated by patoate:β-alanine ligase to form (R)-pantothenate. Finally, (R) pantothenate is used to produce (R)-4'-phosphopantothenate (Jones, Dancer, Smith, & Abell, 1994; Raman & Rathinasabapathi, 2004)

2.2 Methionine synthase- A central metabolism enzyme between 5-CH_3-THF, methionine, SAM and ethylene.

As previously described, one-carbon metabolism is responsible for providing essential molecules for plant growth and development. Also, there is a common metabolic step in the biosynthesis of methionine, SAM, ethylene, and one-carbon metabolism, which is mediated by the action of methionine synthase. This process is one of the most important metabolic pathways on plant cells because it is the only way that plant cells can synthesize methionine *de novo* (García-Salinas, Ramos-Parra, & Díaz de la Garza, 2016; Ravanel *et* al., 2004). This enzyme utilizes polyglutamylated 5-methyl-THF as a methyl donor in the synthesis of methionine from homocysteine in plastids and also in the regeneration of the methyl group of SAM after the methylation reactions that occur in the cytosol such as methylation of mRNa, proteins and hormones, unlike methylations in the nucleus which occur in DNA and histones (Rahikainen et al., 2018). Also, SAM is used as substrate by the action of

Aminocyclopropane-1-carboxylic acid (ACC) synthase (ACS) to produce ACC, later this molecule is oxidized by ACC oxidase (ACO) to produce ethylene (Ravanel *et al.*, 2004). Ethylene acts as a gaseous hormone that coordinates several important processes such as ripening in climacteric fruits when it is produced endogenously or when it is applied exogenously (Sauter *et al.*, 2013). This process is shown in **Figure 2.3** The biosynthetic pathways of methionine, SAM and ethylene will be discussed next.

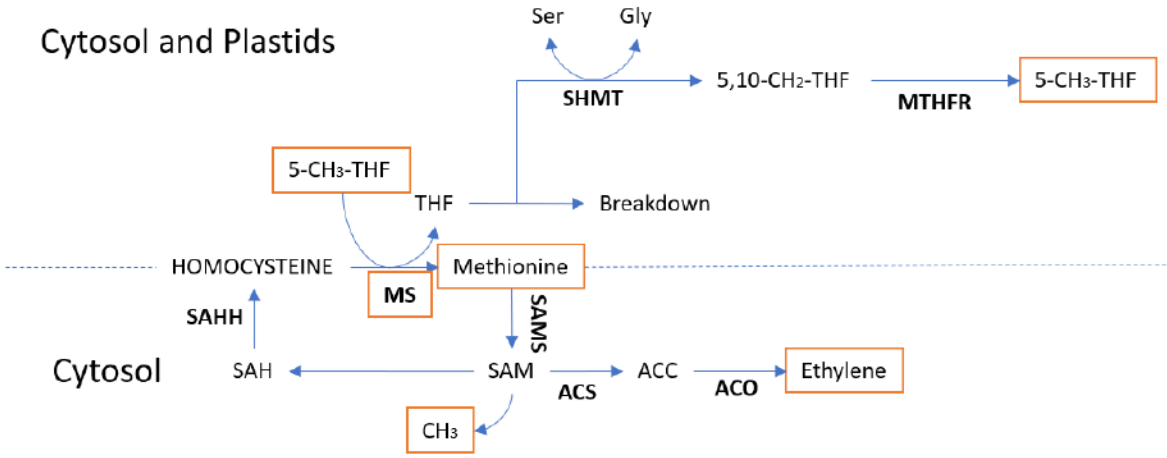

Figure 2.3. One carbon metabolism and ethylene crossroads. Methionine synthase (MS) is represented in this scheme as a central enzyme in the biosynthesis of ethylene, folates, and methionine. This figure is modified from (García-Salinas, Ramos-Parra, & Díaz de la Garza, 2016)

There are three isoforms of methionine synthase in *Arabidopsis thaliana*, two are located in the cytosol (ATMS1, At5g17920, and ATMS2, At3g03780), and another in chloroplasts (ATMS3, At5g20980)) (TAIR, 2018). The ATMS1 and ATMS2 isoforms are involved in the regeneration of methionine from homocysteine, while the ATMS3 isoform is responsible for the synthesis of methionine in plant cells (Ravanel *et al.*, 2004).

The role of methionine synthase in the methionine biosynthesis is widely known, but its detailed mechanism on the regulation of the production of ethylene, THF, 5-CH_3-THF, and SAM remains unknown. In previous research the differential genes expression when plant tissues were treated with exogenous ethylene was evaluated, the principal findings revealed a positive correlation between the increment in exogenous ethylene concentration and the expression level of methionine synthase (García-Salinas, 2016). Moreover,

methionine synthase is involved in regulating important biological compounds that will be discussed.

2.2.1 Cysteine biosynthesis- a precursor of methionine biosynthesis

Cysteine biosynthesis in plants is an essential process in fixing inorganic sulfur as sulfate from the soil or as sulfur dioxide and hydrogen sulfide from the atmosphere (Leustek, Martin, Bick, & Davies, 2000). Sulfide is incorporated into cysteine in the chloroplast, mitochondria, and the cytoplasm. Then γ-glutamylcysteine is synthesized from glutamate and cysteine by glutamate-cysteine ligase which will serve as the precursor for glutathione which is a molecule required for homocysteine synthesis Therefore, cysteine biosynthesis pathway provides the only metabolic sulfide donor required for the production of methionine, glutathione, phytochelatins, iron-sulfur clusters, vitamin cofactors and a number of secondary metabolites, moreover, it has an important role in protein structure (Bonner, Cahoon, Knapke, & Jez, 2005).

This process is catalyzed by action of two enzymes. Serine acetyltransferase (SAT;) transfers acetate from acetyl-CoA to serine, generating O-acetylserine. O-Acetylserine sulfhydrylase (OASS or O-acetylserine (thiol) lyase) uses pyridoxal 5' phosphate (PLP) as a cofactor to catalyze the production of cysteine from O-acetylserine and sulfide. These two enzymes associate each other to make the assembly cysteine synthase complex, which is responsible for sulfate assimilation and modulates cysteine synthesis at the cellular level (Droux, Ruffet, Douce, & Job, 1998; Kredich, Becker, & Tomkins, 1969). Extensive research on molecular basis of cysteine biosynthesis, structural analysis of SAT and OASS in plants is provided by Bonner and colleagues (Bonner *et al*., 2005).

2.2.2 Methionine biosynthesis

Methionine belongs to sulfur amino acids, in 1966, it was established that most of the inorganic sulfate assimilated and reduced by plants comes from cysteine and methionine, containing about 90% of the total sulfur content in most plants (Allaway, 1970; Giovanelli, Mudd, & Datko, 1980). Mammals cannot produce *de novo* synthesis of cysteine and methionine, but plants can perform this process, and because this reason, Allaway and fellows (1970) mentioned that is considered "one of the key reactions in biology, comparable

in importance with the reduction of carbon in photosynthesis". There are two methionine biosynthesis pathways, *de novo* synthesis, and methionine recycling.

2.2.2.1 *De novo* methionine synthesis

Three convergent pathways are required for *de novo* synthesis of methionine. Firstly, the carbon backbone is obtained from aspartate; secondly, cysteine provides the sulfur atom; finally, the methyl group is obtained from the β-carbon of serine (Ravanel *et al*., 1998). Specifically, in plants, this process starts with substrate O-phosphohomoserine (OPH), subsequently, three consecutive reactions occur that are catalyzed in order by cystathionine γ-synthase, cystathionine β-lyase, and finally methionine synthase; the last one, represents the unique way to synthesize methionine in plant metabolism (Giovanelli *et al*., 1980). In the two first reactions, pyridoxal 5'-phosphate (PLP)-dependent enzymes are required as catalyzers, this constitutes the trans-sulfuration pathway, which is the transfer of the sulfur atom of cysteine to homocysteine using the thioether cystathionine as intermediate. In detail, the first step involves cystathionine γ-synthase for the synthesis of cystathionine from cysteine and OPH substrates by a γ-replacement reaction.

Accordingly to available information, this is the only enzyme that is capable of catalyzing a replacement reaction at the γ-carbon of amino acids (Ravanel *et al*., 1998). The second reaction step involves Cystathionine β-lyase which catalyzes an α, β-elimination of cystathionine to yield homocysteine, pyruvate, and ammonia. The third step involves the transfer of the methyl group from polyglutamylated 5-methyl-tetrahydrofolate to homocysteine. It has been previously reported that this step is performed by a cobalamin independent methionine synthase (EC 2.1.1.14) (Eichel, González, Hotze, Matthews, & Schröder, 1995). Methionine is a central molecule used in cellular metabolisms such as protein synthesis, methyl-group transfer trough s-adenosyl-methionine, polyamines, and ethylene synthesis; these metabolic processes are inter-regulated.

2.2.2.2 Recycling methionine

The mechanism of methionine recycling was extensively described (Ravanel *et al*., 2004). The unique process which is capable of utilizing the complete methionine molecule is protein synthesis, other processes consist in recycling methionine moieties, for example, 80% of methionine molecules are used for s-adenosyl-methionine (SAM) synthesis

(Giovanelli, Mudd, & Datko, 1985). In plants, there are two pathways using the methyl group or the 4-carbon moiety of methionine, both involve SAM as a first intermediate. In the first reaction, approximately 90% of SAM is used for transmethylation reactions, this process consists in the transference of the methyl group of methionine to methyl acceptors; major end products from this reaction are choline and its derivatives such as phosphatidylcholine (Giovanelli *et al*., 1985; Ravanel *et al*., 2004). Then, the reaction is followed by recycling of the homocysteine moiety to regenerate methionine.

In another hand, s-adenosyl-L-homocysteine, that is produced during methylation reactions, is converted into homocysteine in a reaction which is catalyzed by S-adenosyl-homocysteine hydrolase. Therefore, methionine is regenerated through the methylation of homocysteine. To denote, methionine synthase not only is responsible for catalyzing the last reaction in *de novo* methionine synthases but also serves to regenerate the methyl group of SAM. The second pathway consists in the use of the 4-carbon moiety of SAM to yield polyamines and, in some plant tissues, ethylene; this is accompanied by recycling of the methylthio moiety and methionine regeneration. Additionally, 5-methylthioadenosine is a by-product that is used to yield methionine mediated by the use of intermediates such as 5-methylthioribose, 5-methylthioribose-1-phosphate, and 2-keto4-methylthiobutyrate; in consecutive reactions that produce the methylthio and 4-carbon moieties of methionine (McKeon, Fernández-Maculet, & Yang, 1995). Methionine recycling is also important due to it represents approximately one-third of the amount of methionine accumulating in proteins (Giovanelli *et al*., 1980).

2.2.3. S-adenosyl methionine synthesis

The SAM synthesis was previously described and explained in detail (Stéphane Ravanel et al., 2004). To produce SAM, methionine is used as substrate in a reaction catalyzed by S-adenosyl methionine synthetase (EC 2.5.1.6). In this process is required inorganic tripolyphosphate, an enzyme-bound intermediate, which is cleaved by a tripolyphosphatase activity of the enzyme, in this reaction the α- and β-phosphate groups of ATP release PPi, whereas the terminal γ-phosphate is released as inorganic phosphate (Aarnes, 1977). Experimental evidence demonstrated that the activity of the yeast and bacterial SAM synthetases are modulated by SAM in a complex manner because high concentrations of SAM inhibit the enzyme, in another hand, low concentrations of SAM

allosterically activate the enzyme by performing tripolyphosphate cleavage reaction (Giovanelli *et al*., 1980; Saint-Girons *et al*., 1988). Other findings demonstrated that partially purified enzyme from pea seedlings is strongly inhibited by tripolyphosphate, this suggests that the reaction is catalyzed by the plant enzyme following the same mechanism as the yeast and bacterial SAM synthetases (Aarnes, 1977). The genes that encode plant SAM synthetase have been cloned from various species, the characterization of these genes provided information that plant SAM synthetase is highly conserved in all organisms and they are encoded by a gene family. Some studies demonstrated that the absence of signal sequence at the N-terminal part of SAM synthetase isoforms predicted from rice and *C. roseus* cDNA sequences, this demonstrated that these isoenzymes are located in cytosol (Schröder, Eichel, Breinig, & Schröder, 1997). Thus, if SAM synthetases are localized in cytosolic compartments, this arises the problem of SAM transport across the limiting border of mitochondria and chloroplasts to maintain internal transmethylation reactions (Ravanel *et al*., 2004). In an experiment, the properties of three *C. roseus* isoenzymes were compared after heterologous expression of the individual enzymes in recombinant bacteria, specifically, the inhibition by the action of tripolyphosphate intermediate and the SAM reaction product was observed; although from this study it is unclear if plant SAM synthetase is activated by low concentrations of SAM, as it has been demonstrated for the bacterial and yeast enzymes. Also, similarities in physicochemical properties such as optima temperature, pH, dependence of cations, and inhibition by reaction products of the *C. roseus* isoenzymes suggested that the presence of several isoforms of plant SAM synthetase is because of specificities in the interaction with enzymes that use SAM (Schröder *et al*., 1997).

2.2.4. Ethylene production

The first milestone to discover the relation between methionine and ethylene was established in 1965 (Lieberman *et al*., 1965), but the specific mechanism was unknown. Two years later, studies demonstrated that methionine conversion to form ethylene was the major flux for methionine metabolism (Burg & Clagett, 1967). It was until eight years later when the metabolic pathway of methionine conversion to form ethylene was first described by (Baur & Yang, 1972), briefly, methionine is degraded to produce ethylene, this step release a methylmercapto group which is transferred to a serine derivative to form S-methylcysteine. In this step, the methyl group and the sulfur atom of methionine are transferred as a unit.

Additionally, in the conversion of S-methylcysteine to methionine, sulfur is incorporated over the methyl group. In order to occur this, S-Methylcysteine is firsts demethylated to yield cysteine which then donates its sulfur to form methionine trough cysthathionine and homocysteine. Cysteine, homoserine, and homocysteine are converted to methionine, although the most efficient methionine precursor is homocysteine, and finally, methionine is the most efficient precursor of ethylene.

It was until 1972 when was well established that methionine is a precursor of ethylene and that the sulfur atom of this amino acid is not volatilized during the conversion but is retained in the tissue and metabolized. Also, it was demonstrated that apples maintain a substantial rate of ethylene production for extended periods, but it has low methionine levels (Lieberman *et al*., 1965). Therefore, this arises the idea that the apple, in order to continue to produce ethylene, the sulfur of methionine must be recycled to provide an adequate supply of methionine for continued ethylene production.

These studies led to discover the firsts approaches of what is known today as methionine salvage or methionine recycling (Baur & Yang, 1972). This idea was confirmed and demonstrated that when methionine is degraded to yield ethylene, the methylmercapto group is transferred presumably to a serine derivative to form S-methylcysteine. In this process, the methyl group and the sulfur atom of methionine are transferred as a unit. In the conversion of S-methylcysteine to methionine, sulfur is incorporated preferentially over the methyl group. In this step, S-Methylcysteine is first demethylated to yield cysteine which then donates its sulfur to form methionine presumably through cystathionine and homocysteine.

Such a view is supported by the observations that cysteine, homoserine, and homocysteine are converted to methionine with homocysteine being the most efficient precursor of ethylene. Though homoserine, homocysteine and methionine are all converted into ethylene, methionine is the most efficient precursor and is therefore, closest to the immediate precursor of ethylene (Baur & Yang, 1972).

2.3 Functional genomics of methionine synthase

Arabidopsis germplasms for methionine synthase genes are available in Arabidopsis Biological Resource Center (ABRC). There are 23, 14, and 6 mutant lines for ATMS1,

ATMS2, and ATMS3, respectively. Between them, few mutant lines have been characterized for ATMS1, ATMS2 and ATMS3, these mutant lines are going to be described next. In the case of ATMS1, the three available germplasms that have been studied are ATMS1-1, SAIL_655_B04, and SAIL_136_C12. (Yan *et al*., 2019) reported the polymorphisms identified as *atms1-1*(germplasm atms1-1), *atms2* (germplasm GABI_359D10), and *atms3* (germplasm SALK_088429)*;* main results of this research demonstrated that the homozygous mutation of G>A substitution leading to mutation of Gly(7) amino acid to Glu(7) in *atms1-1* mutant line, and a significant decrease in the ratio of s-adenosylmethionine to s-adenosylhomocysteine, a key index of methylation status, leading to decreased levels of DNA methylation and affecting the chromatin silencing. They reported that the mutation of ATMS1 lead to affect the expression levels of 1,556 protein-coding genes and 571 TE (transposable elements). Further analyses demonstrated that this phenotype could be alleviated by the supplementation with methionine, moreover, they found significant changes ($P<0.05$) in methionine content of *atms1-1* mutants which was lower when compared to wild type; also they found that SAM, Hcy, and SAH levels were higher when compared to wild type while in the complementation line ATMS1 (mutant line which produce methionine synthase 1) their levels where recovered to the wild type content. Therefore, they demonstrated the relationship of ATMS1 in DNA and histone methylation due to its functions in one-carbon metabolism pathway. Also, in this study, methionine content was evaluated in *atms1-1*, *atms2*, and *atms3*, showed significant decreases in all mutant lines when compared to control, moreover, similar trends in reduction of SAM contents were observed for *atms2-1* and *atms3-1*. The role of ATMS1 in DNA methylation was also studied using the SAIL_655_B04 and SAIL_136_C12 mutant lines for ATMS1 (González & Vera, 2019). The authors found the relationship between DNA methylation and plant immunity response against bacterial infection. They were able to demonstrate that ATMS1 overexpression leads to increase DNA methylation which has an impact on repressing plant immune response.

Similarly, an investigation conducted by (Ju *et al*., 2020) used the T-DNA insertion lines SALK_205174, CS480822, and CS828436, which are ATMS1 mutant lines. They observed that L-methionine is required by AtGLR3.5 (Arabidopsis glutamate receptor homolog 3.5) and Ca^{2+} signaling to regulate seed germination. In this study, they reported that AtGLR3.5 play a regulation role in cytosolic Ca^{2+} due to a positive relationship between

AtGLR3.5-dependent increase in cytosolic Ca^{2+}, also they observed that the expression of AtGLR3.5 is mostly up-regulated during 24-36 h after imbibition, in the other hand, a knock-down of AtGLR3.5 results in reduced germination (Kong *et al*., 2015). In the first experiments to get this conclusion, they performed seed germination test using physiological concentrations of amino acids (10 µm and 30 µm) whose levels increase during germination such as L-methionine, D-Serine, L-Asp, and L-threonine; and that have been previously described that activate plan GLR Ca^{2+} (Kong *et al*., 2016; Li *et al*., 2013; Michard *et al*., 2011). From this test, they were able to demonstrated the efficacy of L-methionine in enhancing seed germination in a dose-dependent manner when it is added at 30 µM, this result is in agreement with the previously reported seed germination promotional effect of methionine by Gallardo *et al*. (2002).

Additionally, Ju *et al*. (2020) observed that L-methionine has the same effect that Ca^{+2} treatment reported by Kong *et al.* (2015). Therefore, they designed an experiment in which used a combination of L-methionine with $LaCL_3$ treatment, a Ca^{2+} channel blocker, in order to determine if the effect was related to the amino acid or the Ca^{2+} channels. The result of this experiment demonstrated that $LaCL_3$ eliminated the seed germination enhancing of L-methionine.

Additional experiments were focused on investigated the relationship between AtGLR3.5 with L-methionine-modulated control of germination because of AtGLR3.5 acts as a Ca^{2+} channel (Kong *et al*., 2015). Thus, they have grown AtGLR3.5 T-DNA insertion lines *Atglr3.5-1* and *Atglr3.5-2* using a supplementation strategy with L-methionine. With this experiment, they were able to demonstrate that AtGLR3.5 and Ca^{2+} signal are involved in the regulation of seed germination by L-methionine. Since methionine can be synthesized in plants by three functional isoforms, this arises the question which isoenzyme is most important for the methionine supply into seed germination. Therefore, Ju *et al.* (2020) followed a strategy of qRT-PCR and found that transcript levels of ATMS1 were approximately 12-fold higher than ATMS2 and ATMS3 in wild type seeds. Then, they analyzed methionine content in imbibed seeds of *atms1* mutant line incubated at 22°C for 0 h 24 h, they found significant lower contents of methionine in both treatments than control seeds.

In **Figure 2.4** is represented the insertion location of *Arabidopsis* mutant lines previously reported in literature. In **Table 2.1**a brief summary with the principal findings of the functional genomic studies of methionine synthase isoforms is shown. Accordingly, to the best of our knowledge, there are unknown overall effects of methionine synthase isoforms in plants and would be interesting study the relationship between the one-carbon metabolism and methionine synthase isoforms regarding cellular processes such as plant growth, development, and metabolism.

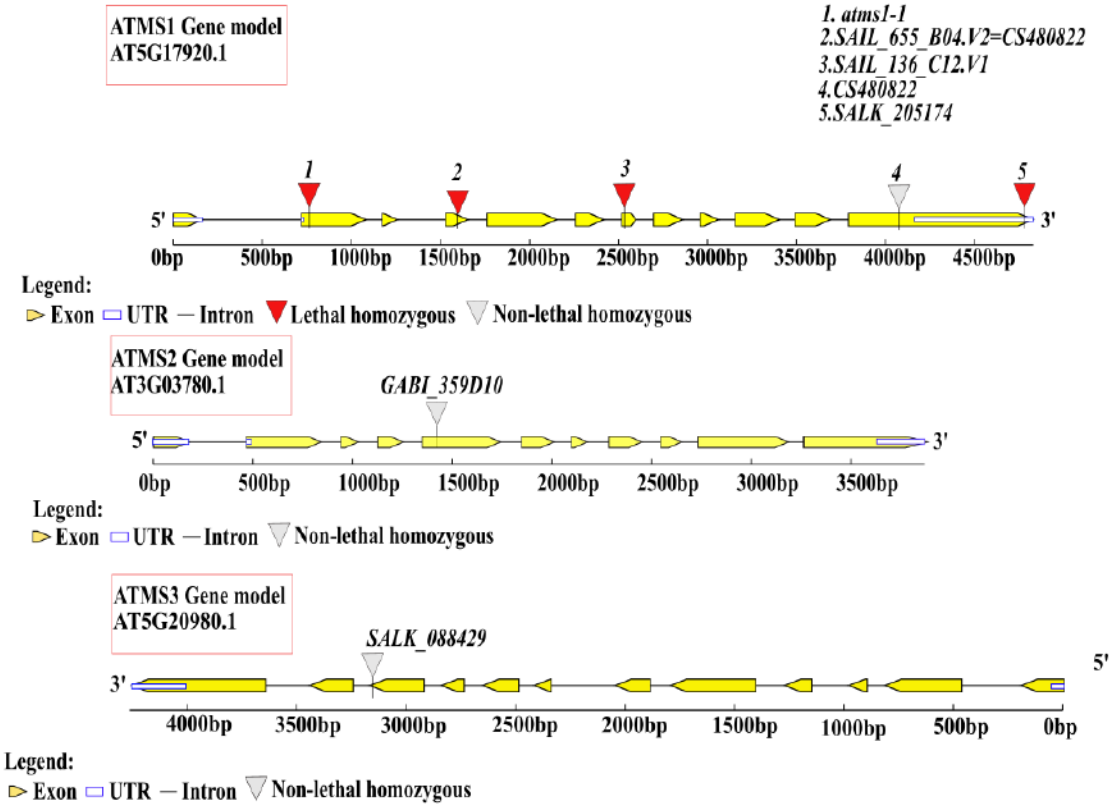

Figure 2.4 Location of previously studied mutant lines in *Arabidopsis thaliana*. Yellow boxes represent exons, blue rectangles represent untranslated regions, black line represent introns, and triangles represent insertion position for each T-DNA insertion mutants.

Table 2.1 Summary of methionine synthase functional genomics in Arabidopsis

Germplasm	Isoenzyme	Phenotype	Insertion position	Reference
atms1-1	ATMS1	Lethal homozygous. Mutation substitution of Gly-7 to Glu-7, lower methionine content, decreased DNA methylation levels, SAM, SAH and Hcy contents increased.	Exon 2, Protein position: G7	Yan *et al*., 2019
SAIL_655_B04 or CS480822	ATMS1	Lethal homozygous, reduction of ATMS1 40-50% gene transcripts, enhanced immune response	Exon 4, Protein position: V159	González & Vera, 2019
SAIL_136_C12	ATMS1	Lethal homozygous, reduction of 40-50% gene transcripts.	Exon 7, Protein position: L384	González & Vera, 2019
SALK_205174	ATMS1	Lethal homozygous, no measurements were performed.	3'-UTR	Ju *et al*.,2020
CS480822	ATMS1	Non-lethal homozygous, delayed germination, lower methionine content, decrease in methionine content during germination, less AtGLR3.5 and more *ABI4* relative expression.	Exon 12, Protein position: E742	Ju *et al*.,2020
SAIL_655_B04 or CS480822	ATMS1	Homozygous lethality, no measurements were performed.	Exon 4, Protein position: V159	Ju *et al*.,2020
GABI_359D10	ATMS2	Non-lethal homozygous, decreased expression levels of ATMS2 gene transcripts, lower methionine content, significant changes in methylation levels.	Exon 4, Protein position: T242	Yan *et al*., 2019
SALK_088429	ATMS3	Non-lethal homozygous, expression levels of target gene decreased, lower methionine content, no significant changes in methylation levels, homozygous.	Exon 10, Protein position: F679	Yan *et al*., 2019

3. Materials and methods

3.1. Biological material

All mutant lines of *Arabidopsis thaliana* were obtained from the Arabidopsis Biological Resource Center (Columbus, OH) with exception of col-0, *ms2-1*, and *ms2-2*. Col-0 seeds were kindly gifted by Dr. Joseph Dubrovsky from Universidad Nacional Autónoma de México, while *ms2-1*, and *ms2-2* homozygous plants were previously isolated in our Lab by Dr. Carolina García (Tecnológico de Monterrey).

In order to choose *ms1* and *ms3* Arabidopsis mutant lines, bioinformatic search based on insertion site was performed at The Arabidopsis Information Resource (TAIR) (https://www.arabidopsis.org/). T-DNA insertional lines SALK_035581 (*ms1-1*), SALK_030047(*ms1-2*), SALK_138706 (*ms1-3*), SALK_018956 (*ms3-1*), SALK_088429 (*ms3-2*), CS852575(*ms3-3*) were selected and obtained from the Arabidopsis Biological Resource Center (Alonso *et al*., 2003). All mutant lines used in this work are shown in **Table 3.1**. Using gene feature information obtained from TAIR , gene maps of the insertion site for each Arabidopsis mutant lines were made using Gene Structure Display Server (http://gsds.cbi.pku.edu.cn/) , and InkScape software (https://inkscape.org/) for minor adjustments.

Table 3.1 Selected Arabidopsis mutant lines

Germplasm	Name	Polymorphism	Insertion position	Chromosome
SALK_035581	*ms1-1*	SALKseq_035581.1	5936505	5
SALK_030047	*ms1-2*	SALKseq_030047.2	5937242	5
SALK_138706	*ms1-3*	SALKseq_138706.8	5938023	5
CS881177	*ms2-1*	SALKseq_66232.2	958426	3
SALK_143628	*ms2-2*	SALK_143628.49.40.x	960443	3
SALK_018956	*ms3-1*	SALK_018956.27.10.x	7125238	5
SALK_088429	*ms3-2*	SALKseq_088429.2	7125153	5
CS852575	*ms3-3*	WiscDsLox356D04.0	7128403	5

3.2. DNA extraction

DNA extractions were performed following cetyltrimethylammonium bromide (CTAB) method (Clarke, 2009) with few modifications. Briefly, DNA extraction buffer was prepared as follow: 2% (w/v) CTAB, 0.1M TRIS-HCl, 20mM EDTA, 1.4M NaCl, and 1% (w/v) PVP. After, DNA extraction was conducted with 1-2 leaves (approximately 10 mg) from 4 weeks old plants in 1.5 mL Eppendorf tubes with 400 uL DNA extraction buffer. Leaves were grinded with a pellet pestle, and later, the tubes were vortexed and placed in a water bath at 65°C for 20 min. Tubes were placed at room temperature for 5 min and 400 µL of chloroform was added to each tube, and then the samples were vortexed and centrifuged for 5 min at 14,000 RPM and 21°C. After that, the supernatant was collected in new tubes followed by the addition of 300 µL isopropanol, tubes were vortexed and incubated at -20°C for 4 h in order to precipitate DNA. Then, tubes were centrifuged for 15 min at 14,000 RPM and 4°C, supernatant was discarded, pellets were washed with 300 uL ethanol, vortexed and centrifuged for 5 min at 14,000 RPM and 4°C. The supernatant was discarded and the DNA extracts were dried at 37°C for 20 min. Finally, DNA pellets were resuspended in 40 µL DEPC treated water.

3.3. Genotyping analysis

In order to isolate homozygous plants genotyping analysis was performed by PCR. First, primers were selected from SIGnAL (Salk Institute Genomic Analysis Laboratory) http://signal.salk.edu/tdnaprimers.2.html. This bioinformatic tool provides specific primers for each mutant line from Salk collection. Selected primers are shown in **Table 3.2**. Two sets of PCRs were used, one using the gene-specific primer pair (LP+RP) and the other using a gene-specific primer and the T-DNA border primer. This strategy could determine whether the individual was homozygous for no T-DNA insertion (wild type), heterozygous for the T-DNA insertion, or homozygous for the T-DNA insertion.

For PCR preparation, DNA extractions were quantified by NanoDrop 1000 (ThermoScientific, Massachusetts, USA) and adjusted to final concentration between 40-100 µg/uL. PCR reactions were prepared as indicated in **Table 3.3**.

Table 3.2 Primer list for Genotyping analysis

ID	Sequence	Tm (°C)	WT Band (bp)	T-DNA band (bp)
LP*ms1-1*	5'-ACCTCCTGCTCTCTTCTCCAC-3'	60.01	1093	489-789
RP*ms1-1*	5'-TGACGGGACCAGTAAGCATAC-3'	60.01		
LP*ms1-2*	5'-CCAGATGTTCCTTCCATCAAC-3'	59.40	1037	521-821
RP*ms1-2*	5'-AATGACCAAGTGGTTCGACAC-3'	59.88		
LP*ms1-3*	5'-ACACCGTCCCTGTACTTGTTG-3'	59.94	1024	467-767
RP*ms1-3*	5'-AGATCTCCTTGAAGCCAAAGC-3'	59.98		
LP*ms2-1*	5'-TCAAACAAAGGGTTCACTTGG-3'	59.99	1138	503-803
RP*ms2-1*	5'-ATGTTTCTGTTTGATGCAGCC-3'	60.13		
LP*ms2-2*	5'-TTGTTGACATCCAAGAGGACC-3'	59.96	1152	523-823
RP*ms2-2*	5-'CCCTCAAAACCTAACTTTGGC-3'	59.99		
LP*ms3-1*	5'-GACTTTGCTGTCCAGAACAGC-3'	60.05	1101	486-786
RP*ms3-1*	5'-AAGCTTCAGGAAGAACTTGGG-3'	59.87		
LP*ms3-2*	5'-ATCACCACCGTTCAACAGAAG-3'	60.02	1161	526-826
RP*ms3-2*	5'-TTTGAGTAGCACATGTGGGTG-3'	59.62		
LP*ms3-3*	5'-TATTTGATTCCAGCATGAGCC-3'	60.05	1149	575-875
RP*ms3-3*	5-'GAGGCTCTGTTACCTGCATTG-3'	59.89		
LBb1	5'-GCGTGGACCGCTTGCTGCAACT-3'	60.00	NA	NA
WiscDsLox LB	5'-TCCTCGAGTTTCTCCATAATAATGT-3'	60.00	NA	NA

Primers LP+RP are used to amplify WT band while primers LB+RP are used to amplify T-DNA band. LP: Left genome primer; RP: Right genome primer; LB: Left border primer.

Table 3.3 PCR reaction preparation

Reaction for WT band	(µL)	Reaction for T-DNA band	(µL)
Green master mix 2X buffer	5.0	Green master mix 2X buffer	5.0
LP primer 10 mM	0.5	LB primer 10 mM	0.5
RP primer 10 mM	0.5	RP primer 10 mM	0.5
H_20 nuclease free	3.0	H_20 nuclease free	3.0
DNA (50-100 ng/uL)	1.0	DNA (50-100 ng/uL)	1.0

Two reactions are performed in order to identified genotype, reaction for WT band use LP and RP primers which result in wild type band; while reaction for T-DNA band use LB and RP primers which result in T-DNA insertion band. The presence of WT band and T-DNA band indicates heterozygous genotype, in the other hand, the presence of WT band or T-DNA indicate wild type and homozygous genotype, respectively.

Once the PCR reactions were prepared, tubes were placed in Maxigen II thermocycler (Axygen, USA) with the following conditions: Initial denaturing step at 94°C for 3 min, following by 30 cycles of denaturing at 94 °C for 30 secs, annealing at 60°C for 30 secs and extension at 72°C for 2 min; and final extension at 72°C for 10 min. These conditions were used for identifying all mutant lines with exception of *ms1-3* mutant line. *ms1-3* required only to modify the annealing temperature to 45°C.

3.5 Plant growth conditions

For initial screening of T-DNA insertion mutants, seeds were cold treated for 3 days at 4°C before being sown in soil with vermiculite and peatmoss (1:1) composition. Seeds were placed in pots by pipetting individual seeds in each pot. Pots were previously labeled for each mutant line. After seeds were sown in soil, the pots were placed in trays containing water and transferred to the growth chamber. Growth chamber conditions were photoperiod of 16 h light and 8 h darkness, relative humidity of 30-40 %.

3.5.1 Plate-based phenotypic analysis

For plate-based phenotypic analysis approximately 450 seeds of *ms1-1* (Hz), *ms1-3* (Hz), *ms2-1* (Hm), *ms2-2* (Hm), *ms3-1* (Hm), *ms3-2* (Hm), *ms3-3* (Hm) were surface sterilized with 70% ethanol for 5 min followed by 30% commercial bleach for 20 min and rinsed seven times with sterile deionized water. Surface-sterilized seeds were sown onto petri dishes (100x20mm) containing 40 mL of sterile medium consisting of 0.5X Murashige and Skoog (1962) salts (Sigma Aldrich), 1% (w/v) sucrose (Sigma Aldrich) and 1% (w/v) Agar (Sigma Aldrich). Plates were placed in a cold room for 3 days at 4°C to synchronize germination. Cold-stratified seeds in plates were transferred into growth chamber with day and night temperature at 22°C under long-day condition (16/8, light/darkness). Each two days, photographs were taken to assess seedling development beginning at removal from the cold room (day 3 after sowing) until the seedlings were harvested on day 14. Shoots and roots were collected separately in cryovials, fast freezing and stored at -80°C until the amino acids and folates analysis.

For each genotype, 50 seeds were sown in each plate. The number of plates for each genotype was *col-0* n=9, *ms1-1* n=9, *ms1-3* n=8, *ms2-1* n=8, *ms2-2* n=7, *ms3-1* 6, *ms3-2* n=9, and *ms3-3* n=9. To evaluate shoots and root weight per plant, the weight of shoots and roots

of 14-days-old plants per plate was recorded and divided by the number of plants produced in the plate. For root, hypocotyl and cotyledon length determination, photographs of vertically incubated plates of 7-days-old plants were analyzed by Image J software (https://imagej.nih.gov/ij/), in this case, the root of each plant in the plate was measure (number of measures for each genotype: *col-0* n=57, *ms1-1* n=25, *ms1-3* n=31, *ms2-1* n=18, *ms2-2* n=43, *ms3-1* n=47, *ms3-2* n=23, and *ms3-3* n=16).

To compare plants developmental stage, photographs of 4-days-old plants were used; For this analysis, each plant was assigned with a number which correspond to the developmental stage (0.1, 0.5, 0.7 and 1.0 to denote dormant seed, seed protrusion, hypocotyl and cotyledon emergence and fully opened cotyledons, respectively) according to methods described by (Boyes *et al.*, 2001). The number of plants per developmental stage was obtained and the percentage of plants in each developmental stage was calculated (each plate contains 50 seeds and n=3 plates were used for each genotype).

3.6 Amino acid analysis

To perform amino acid extraction, 50 mg of 14-days-old *Arabidopsis* shoots (n=3, per genotype) were placed in 2 mL microtubes with lysis bead (6.35 mm zirconium silicate bead) and 1 mL amino acid extraction buffer (0.1M NaH_2PO_4, 10 mM Borate, 1 mM DTPA, pH 8.2). Plant tissue lysis was performed by a cycle of 20 secs at 6 $m*s^{-1}$ in FastPrep-24 system (MP Biomedicals, Shandong, China). Then, the samples were centrifuged at 14,000 RPM at 4°C for 10 min, the supernatant was collected and filtered with 0.45 µm PVDF membrane syringe filters and placed in new microtubes.

For amino acid derivatization was followed the methodology described in previous literature (Cohen & Michaud, 1993) with minor modifications. The derivatization reaction was prepared directly in insert hplc vials with 10 µL of standard solutions, extraction buffer (blank) or amino acid extracts; 30 µL of AccQ-Fluor borate buffer, following by homogenization with vortex for 5 secs and quick spin. Finally, the derivatization began with the addition of 10 µL AccQ-Fluor reagent at 55°C for 10 min on a heating plate.

Amino acid analysis was performed on an UPLC Acquity System (Waters, Massachusetts, USA) and operated by the Empower software version 3 (Waters, Massachusetts, USA).

Separation was performed on 3.9 x 150 mm AccQ-Tag column (Waters, Massachusetts, USA) at 37°C. The amino acids profile was detected using Waters 2475 fluorescence detector with excitation parameter at 250 nm and emission at 395 nm. Mobile phase A (140 mM Sodium acetate, 7 mM Triethylamine, and pH adjusted to 5.8 with H_3PO_4), and mobile phase B (60% acetonitrile (v/v) and 40% water (v/v)) were used at 1 mL/min flow rate with the following gradient: 0-1 min, 100% A; 1-16 min, 98.4% A, 1.6% B; 16-25 min, 95.7% A, 4.3% B; 25-35 min, 90% A, 10% B; 35-40 min, 75.5% A, 24.5% B; 40-51 min, 67%A, 33% B; 51-54 min, 100% B; 54-60 min, 100% A. Amino acid concentrations were calculated by direct comparing with standard curves prepared with commercial amino acid standards (Thermo Scientific).

3.7 Folate analysis

Folates extraction was performed according with methodology described in previous works (Ramos-Parra *et al*., 2013), with minor modifications for *A. thaliana* tissue. Extraction buffer was prepared as follow: 50 mM HEPES, 50 mM CHES, 2% (w/v) sodium ascorbate, 10 mM β-mercaptoethanol, and pH adjusted to 7.85 with KOH. Folate extraction was carry-out using 200 mg of 14-days-old Arabidopsis shoots (n=3, for each genotype) in 5 mL extraction buffer in 15 mL Falcon tubes containing two 6.35 mm zirconium silicate beads. Oxygen was removed from the tube by flushing with gas nitrogen in order to prevent folates degradation by oxidation each time tubes were opened.

Plant tissue lysis was performed by a cycle of 40 secs, at 6 $m*s^{-1}$ in FastPrep-24 system (MP Biomedicals, Shandong, China). Tubes were placed in boiling water for 10 min to completely cell denaturalization and enzyme inactivation. Immediately, tubes were placed on ice for 10 min. Then, tubes were centrifuged at 10,300 RPM, for 10 min at 4°C, and supernatant was collected in new tubes. The pellets were re-extracted with 3 mL of extraction buffer and following same previous steps. Both supernatants were combined and filtered using Whatman qualitative filter paper (No. 1) of 42.5 mm diameter.

Samples were adjusted to pH 6.0 with orthophosphoric acid (1:10 v/v) and 0.1 mg of GGH (gamma-glutamyl hydrolase) per g of sample for folate deglutamylation. Samples were incubated at 37°C for 1 h, folate deglutamylation was stopped by adjusting pH to 7.8 with 5M KOH and placing the samples in boiling water for 10 min. Immediately, samples were

transferred to ice for 10 min. Tubes were centrifuged at 10,300 RPM, 4°C for 10 min, and supernatant was filtered again in filter paper.

Folate purification was performed by affinity chromatography in columns containing Folate Binding Protein isolated of whey protein concentrate (Gregory III & Toth, 1988). Chromatographic steps consisted on: 5 mL of salted phosphate buffer (25 mM $KHPO_4$, 1M NaCl, 1% ascorbic acid and pH adjusted to 7.4 with 5M KOH), 5 mL of desalted phosphate buffer (25 mM $KHPO_4$, pH 7.4), displacement of phosphate buffer with 700 µL of elution buffer (28 mM K_2HPO_4 and 0.59 mM H_3PO_4), and final elution with 3 mL of elution buffer. Eluted samples were filtered using 0.45µm PVDF membrane syringe filters and transferred to 2 mL HPLC vials.

Folates analysis was performed by HPLC Agilent 1290 (Agilent, California, USA) coupled with a four-channel electrochemical detector CoulArray model 5600A (ESA, Massachusetts, USA). Folates were separated with Prodigy C-18, 150 x 4.6 mm, 150 Å column (Phenomenex, California, USA) following a non-linear gradient of 33 min from 90% mobile phase A to 100% mobile phase B at 1 mL/min. Mobile phase A consisted in phosphate buffer (28 mM K_2HPO_4 and 59 mM H_3PO_4, pH 2.5), and mobile phase B (75% phase A (v/v), and 25% acetonitrile (v/v)). Cell potential for folate characterization and quantification was set at four levels: 100, 200, 300 and 400 mV. Cell potential response was calibrated with standard curves of commercial standards of 5-CH_3-THF, 5-CHO-THF (Shircks, Jona, Switzerland), and Folic Acid (Sigma, Missouri, USA). THF was prepared from FA; while 5,10-CH=THF from 5-CHO-THF according to reported protocol (Baggott *et al*., 1995).

3.8 Statistical analysis

All data were analyzed using Minitab software (https://www.minitab.com). For ANOVA tests, significant differences were calculated by Tukey HSD test at p-value ≤ 0.05.

4. Results

4.1. Isolation of T-DNA insertion lines

Using gene feature information obtained from TAIR, gene maps of insertion sites were made (**Figure 4.1**).

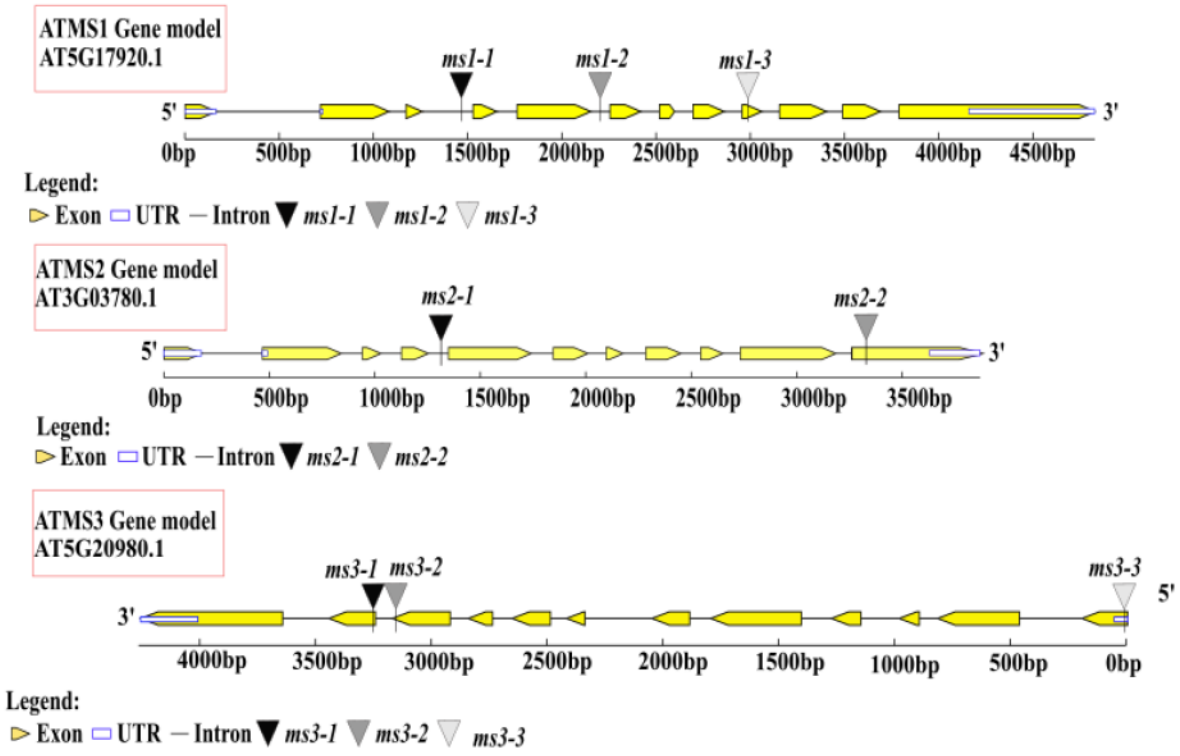

Figure 4.1. Location of T-DNA insertion mutant lines of the three methionine synthase (MS) genes in *Arabidopsis thaliana*. Yellow boxes represent exons, blue rectangles represent untranslated regions, black line represent introns, and triangles represent insertion position for each T-DNA insertion mutants.

Acquired seeds (**Table 3.1**) were segregating for the insertion of T-DNA. Therefore, seeds had to be sown individually in soil and perform genotype screening in order to isolate homozygous plants for T-DNA insertion. In the case of CS881177 (*ms2-1*) and SALK_143628 (*ms2-2*), homozygous plants were previously isolated by Dr. Carolina García and kindly gifted to our research group, because of this, genotype screening was performed only to confirm homozygous genotype for *ms2-1* and *ms2-2*.

T-DNA mutant lines *ms1-1, ms1-3, ms2-1, ms2-2, ms3-1, ms3-2*, and *ms3-3* in Columbia background were identified by PCR screening of individual DNA extractions from plants grown in soil. The primers that were used for amplification of WT and T-DNA band

along with expected PCR products were shown in **Table 3.2**. The PCR products were analyzed by DNA blotting and the results were shown as follows. Genotyping analysis identified heterozygous T-DNA mutant lines for *ms1-1*, *ms1-2* and *ms1-3* (**Figures 4.2, 4.3** and **4.4**, respectively). Homozygous T-DNA mutant lines for *ms2-1*, and *ms2-2* were confirmed (**Figures 4.5** and **4.6,** respectively); and homozygous T-DNA mutant lines were identified for *ms3-1*, *ms3-2*, and *ms3-3* (**Figures 4.7**, **4.8** and **4.9**, respectively).

For ATMS1 mutant lines the genotyping analysis for *ms1-1* SALKseq_030047.2 (**Figure 4.2**) showed that F27 was heterozygous for T-DNA insertion. Plants F23, F28, F29.1, and F30 were identified as wild type due they were homozygous for no T-DNA insertion. For genotyping analysis of *ms1-2* SALKseq_138706.8 (**Figure 4.3**), it was necessary to change the annealing temperature from 60 to 45°C after numerous failure attempts to amplify T-DNA insertion band **(Figure 4.3**). The genotyping analysis identified that D30 was heterozygous for T-DNA insertion. The genotyping analysis of *ms1-3* SALKseq_035581.1 (**Figure 4.4)** showed that A19, and A22 were heterozygous for T-DNA insertion. Plants A4, A9, A11, A13, A18, A28, A35, A38, A42, and A43 were identified as wild type because they were homozygous for no T-DNA insertion. DNA extraction of plant A5 failed to amplify probably due to DNA integrity or quality.

For ATMS2 mutant lines, it was only necessary to confirm the homozygous genotype because these seeds were previously isolated as mentioned above in Chapter 3. The genotyping analysis of SALKseq_66232.2 (**Figure 4.5**) confirmed that samples M1, M2, and M3 were homozygous for T-DNA insertion, whereas genotyping analysis of SALK_143628.49.40.x (**Figure 4.6**) confirmed that samples M1 and M2 were homozygous for T-DNA insertion.

For ATMS3 mutant lines screening, the genotyping analysis for SALK_018956.27.10.x (**Figure 4.7**) showed that B5.1 and B16 as homozygous for no T-DNA insertion. Plants B13 and B14 were identified as homozygous for T-DNA insertion. DNA extraction of plants B19.2 and B19.3 failed to amplify probably due to DNA integrity or quality. Genotyping analysis results for SALKseq_088429.2 (**Figure 4.8**) showed that C11 is heterozygous for T-DNA insertion. Plants C8.2 and C19.2 were identified as homozygous for T-DNA insertion. Plant C20 was identified as homozygous for no T-DNA insertion (wild type). DNA extraction from C19.1 failed to amplify probably due to DNA integrity or quality.

The genotyping analysis of WiscDsLox356D04.0 (**Figure 4.9**) showed that E13 and E19 are heterozygous for T-DNA insertion. Plant E9 was identified as homozygous for T-DNA insertion. Plants E6 and E7 were identified as homozygous for no T-DNA insertion (wild type).

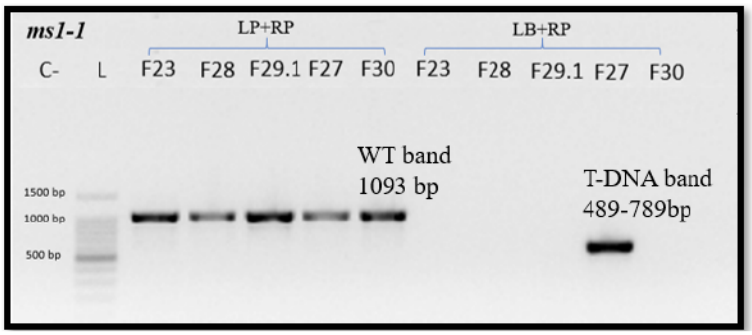

Sample	WT band	T-DNA band	Genotype
F23	+	-	WT
F28	+	-	WT
F29.1	+	-	WT
F27	+	+	Hz
F30	+	-	WT

Figure 4.2. Identification of heterozygous *ms1-1* (SALKseq_030047.2). ID "F#" stands for internal identification of plants for SALKseq_030047.2. Abbreviations correspond to LR, left genome primer; RP, right genome primer; LB, Left border primer; C-, negative control; L, ladder, WT, wild type; Hz, heterozygous; Hm, homozygous.

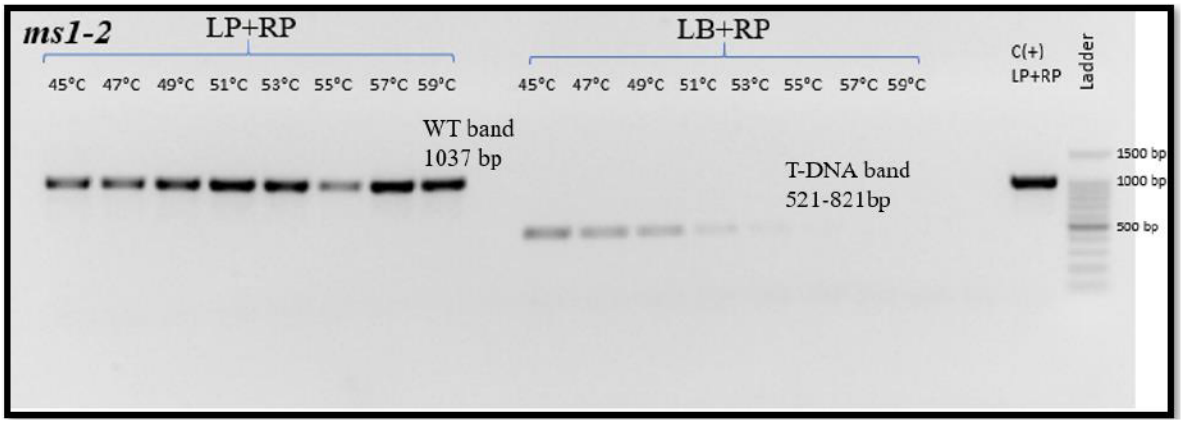

Figure 4.3. Identification of heterozygous *ms1-2* (SALKseq_138706.8). Temperature gradient to optimize the amplification of T-DNA insertion for SALKseq_138706.8. Abbreviations correspond to LR, left genome primer; RP, right genome primer; LB, Left border primer; C+, positive control; L, ladder.

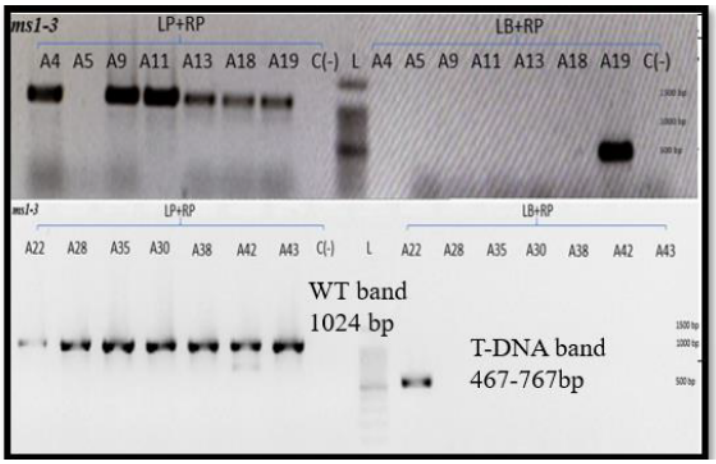

Sample	WT band	T-DNA band	Genotype
A4	+	-	WT
A5	-	-	ND
A9	+	-	WT
A11	+	-	WT
A13	+	-	WT
A18	+	-	WT
A19	+	+	Hz
A22	+	+	Hz
A28	+	-	WT
A30	+	-	WT
A35	+	-	WT
A38	+	-	WT
A42	+	-	WT
A43	+	-	WT

Figure 4.4. Identification of heterozygous *ms1-3* (SALKseq_035581.1). ID "A#" stands for internal identification of plants for SALKseq_035581.1 Abbreviations correspond to LR, left genome primer; RP, right genome primer; LB, Left border primer; C-, negative control; L, ladder, WT, wild type; Hz, heterozygous; Hm, Homozygous.

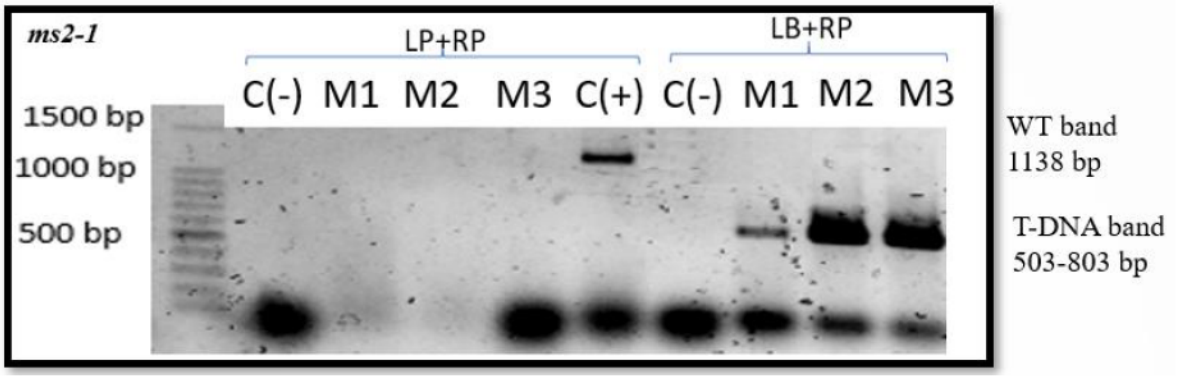

Figure 4.5 Identification of homozygous *ms2-1* (SALKseq_66232.2). ID "M#" stands for internal identification of plants for SALKseq_66232.2. Abbreviations correspond to LR, left genome primer; RP, right genome primer; LB, Left border primer; C-, negative control; C+, positive control L, ladder.

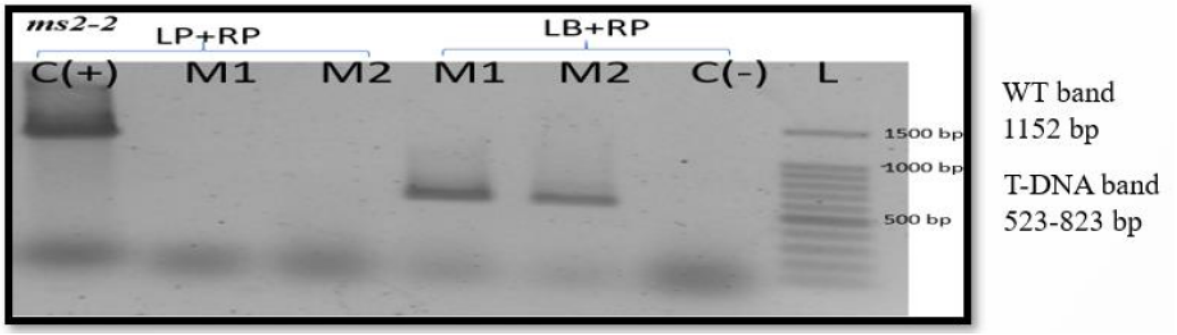

Figure 4.6 Identification of homozygous *ms2-2* (SALK_143628.49.40.x). ID "M#" stands for internal identification of plants for SALK_143628.49.40.x. Abbreviations correspond to LR, left genome primer; RP, right genome primer; LB, Left border primer; C-, negative control; C+, positive control L, ladder.

Sample	WT band	T-DNA band	Genotype
B5.1	+	-	WT
B13	-	+	Hm
B14	-	+	Hm
B16	+	-	WT
B19.2	-	-	ND
B19.3	-	-	ND

Figure 4.7. Identification of homozygous *ms3-1* (SALK_018956.27.10.x). ID "B#" stands for internal identification of plants for SALK_018956.27.10.x. Abbreviations correspond to LR, left genome primer; RP, right genome primer; LB, Left border primer; C-, negative control; L, ladder, WT, wild type; Hm, homozygous; Hz, heterozygous.

Sample	WT band	T-DNA band	Genotype
C8.2	-	+	Hm
C11	I	I	Hz
C15	+	-	WT
C19.1	-	-	ND
C19.2	-	+	Hm
C20	+	+	WT

Figure 4.8. Identification of homozygous *ms3-2* (SALKseq_088429.2). ID "C#" stands for internal identification of plants for SALKseq_088429.2. Abbreviations correspond to LR, left genome primer; RP, right genome primer; LB, Left border primer; C-, negative control; L, ladder, WT, wild type; Hm, homozygous; Hz, heterozygous.

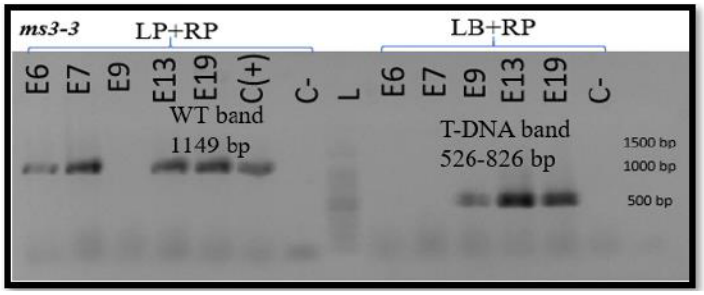

Sample	WT band	T-DNA band	Genotype
E6	+	-	WT
E7	+	-	WT
E9	-	+	Hm
E13	+	+	Hz
E19	+	+	Hz

Figure 4.9. Identification of homozygous *ms3-3* (WiscDsLox356D04.0). ID "E#" stands for internal identification of plants for WiscDsLox356D04.0. Abbreviations correspond to LR, left genome primer; RP, right genome primer; LB, Left border primer; C-, negative control; L, ladder, WT, wild type; Hm, homozygous; Hz, heterozygous.

Once genotyping analysis was completed, homozygous and heterozygous plants were isolated, and seeds were collected in separate tubes and stored at room temperature. Seeds from this harvest were used for further plate-based phenotypic and metabolic analysis. From this point to the rest of the presented work, homozygous and heterozygous genotype will be denoted as (*Hm*), and (*Hz*), respectively.

4.2 Plate-based phenotypic analysis

To investigate phenotypic differences, data from *in vitro* plants were collected and analyzed. The shoots and roots were separated from 14-days old Arabidopsis to assess their weight differences (**Figure 4.10**). Shoots weight for *Col-0* resulted in a mean value of 2.72±1.02 mg per plant (**Figure 4.10A**). Statistically significant differences in shoots weight were found in *ms1-1* and *ms3-2* mutant lines resulting in 0.55 and 0.61-fold change decrease, respectively ($P<0.05$), when compared to *Col-0* plant control. In other hand, shoots weight of *ms1-3, ms2-1, ms2-2, ms3-1*, and *ms3*-3 mutant lines were not significantly different ($P<0.05$) (**Figure 4.10A**). The root weight for control plants scored a mean value of 243.1±95.8 µg per plant. Statistically significant differences were not found for all mutant lines compared to *Col-0* (**Figure 4.10B**).

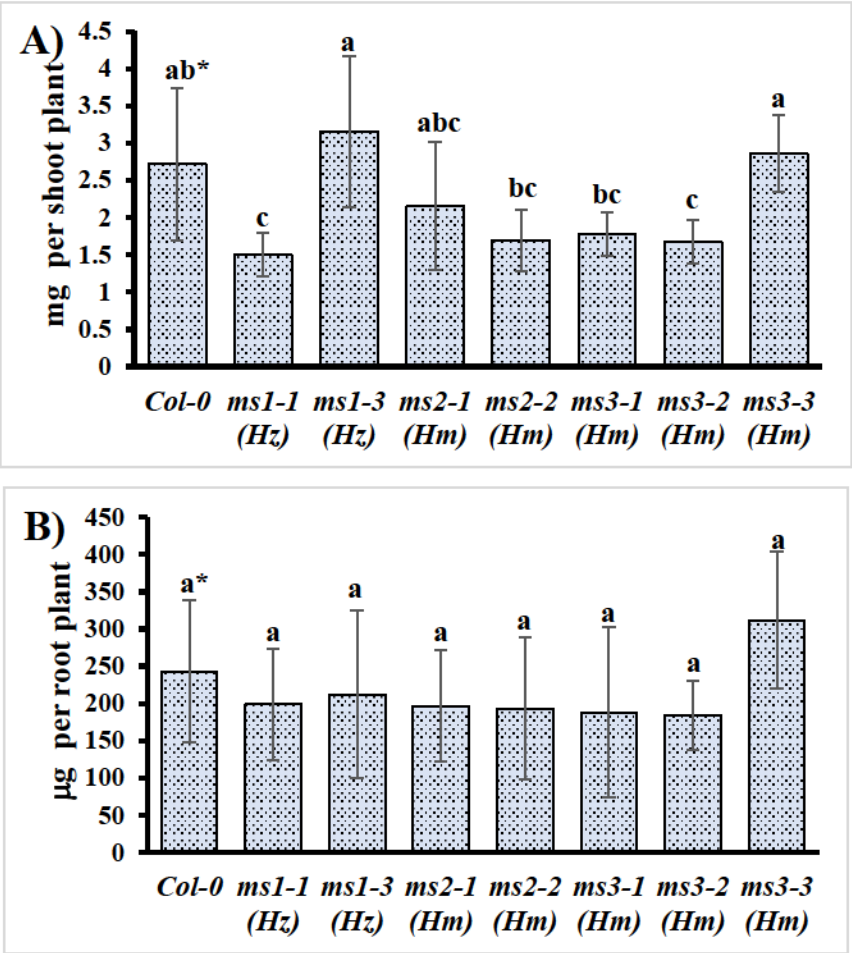

Figure 4.10. Shoots (A) and roots (B) fresh weight of 14-days old *A. thaliana* mutant lines. Data are presented as means ± SD. The number of replicates for each genotype were: *col-0* n=9, *ms1-1* n=9, *ms1-3* n=8, *ms2-1* n=8, *ms2-2* n=7, *ms3-1* 6, *ms3-2* n=9, and *ms3-3* n=9. *Letters indicate significantly differences determined by Tukey test ($P<0.05$). Hz, heterozygous; and Hm homozygous genotypes.

For root, hypocotyl and cotyledons length determination, seeds were surface sterilized as previously described in Chapter 3, but surface sterilized seeds were sown in the middle of the plate as it can be observed in Appendix Section Figures **A1, A2,** and **A3.** Root, hypocotyl and cotyledons length measures were realized at 7-days old plants. Representative images from these plates are shown next in **Figure 4.11** with zoom (200%) in order to get a better qualitative view of plants phenotype.

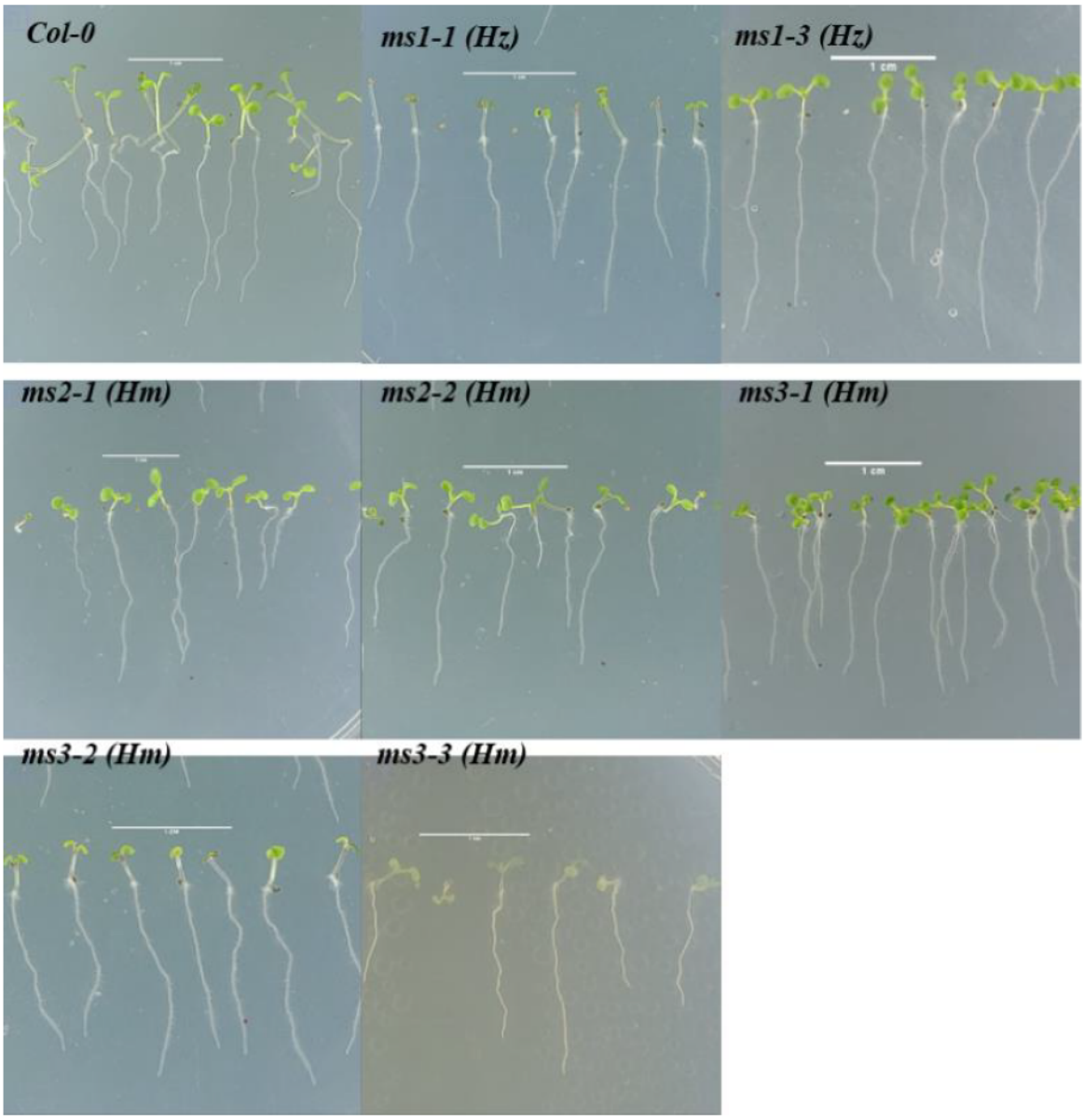

Figure 4.11. Roots phenotype of 7-days old *A.thaliana* mutant lines. Close up representative images from root length determination are showed. Scale bars for each genotype is equal to 1 cm. Hz and Hm indicates heterozygous and homozygous genotypes, respectively.

Control plants showed mean values for root, hypocotyl and cotyledons of 1.65±0.43, 0.51±0.15, and 0.27±0.05 cm, respectively. Visual inspection of T-DNA insertional mutant seedlings for ATMS1 is shown in **Figure A1**. The root length determination (**Figure 4.12 A)** found statistically significant differences ($P<0.05$) in *ms1-1* with a decrease of 0.69-fold change, whereas *ms1-3* resulted in 1.21-fold change increase when compared to *Col-0* plants. Hypocotyl length determination (**Figure 4.12 B**) showed that *ms1-1* and *ms1-3* mutant lines present a significant decline ($P<0.05$) of 0.50 and 0.34-fold, respectively. Cotyledons length

determination (**Figure 4.12 C**) only found statistically significant differences ($P<0.05$) in *ms1-1* with 0.61-fold change when compared to the control plants.

ATMS2 mutant lines are shown in **Figure A2.** For root length determination (**Figure 4.12 A**), statistically significant differences ($P<0.05$) were found only for *ms2-2* with a 0.73-fold change decrease while *ms2-1* was not different when compared to *Col-0* plants. In hypocotyl length determination (**Figure 4.12 B**), measurements showed statistically significant differences ($P<0.05$) with 0.35 and 0.32-fold change decrease when compared to control plants. Cotyledons length determination (**Figure 4.12 C**) only showed statistically significant differences for *ms2-2* mutant line with 0.78-fold change decrease while *ms2-1* was not different to control plants.

Visual evaluation for ATMS3 mutant lines is shown in **Figure A3**. Root length determination (**Figure 4.12 A**) found not statistically significant differences for *ms3-1*, *ms3-2* and *ms3-3* mutant lines when compared to *Col-0* plants. Hypocotyl length determination (**Figure 4.12 B**) demonstrated significant differences ($P<0.05$) for *ms3-1*, *ms3-2*, and *ms3-3* mutant lines with 0.35, 0.44, and 0.30-fold decrease when compared to control plants. In other hand, cotyledons length determination (**Figure 4.12 C**) showed statistically significant differences ($P<0.05$) for *ms3-1* and *ms3-2* mutant lines with 0.70 and 0.60-fold change decrease while *ms3-3* mutant line was not different when compared to *Col-0* plants.

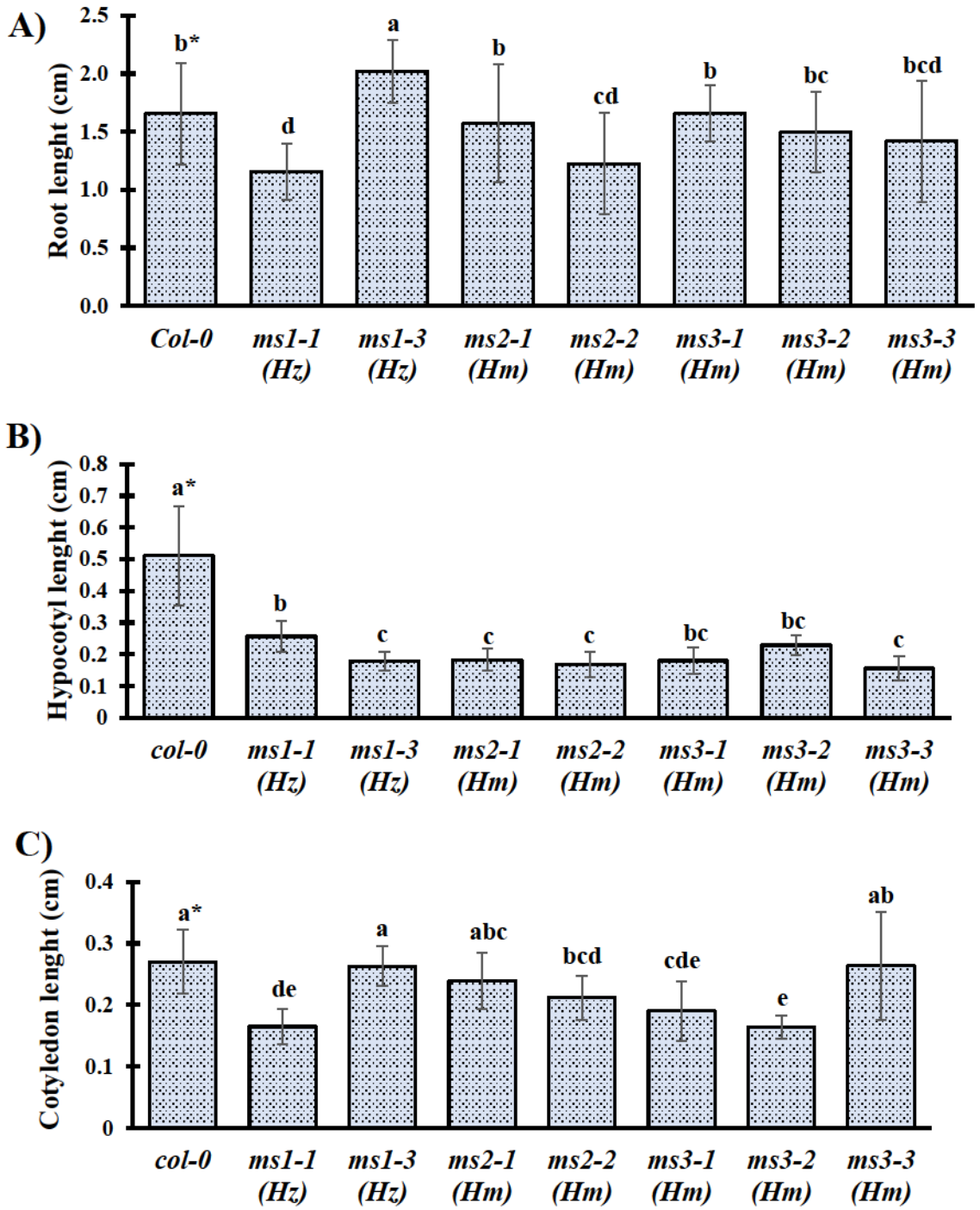

Figure 4.12. Root, hypocotyl and cotyledon length of 7-days old *A. thaliana* mutant lines. Dara are presented as means ± SD of root weight (mg) per plant. *Letters indicate significant differences determined by Tukey test ($P<0.05$). Root length determination: *col-0* n=57, *ms1-1* n=25, *ms1-3* n=31, *ms2-1* n=18, *ms2-2* n=43, *ms3-1* n=47, *ms3-2* n=23, and *ms3-3* n=16. Hypocotyl length determination: *col-0* n=22, *ms1-1* n=19, *ms1-3* n=17, *ms2-1* n=16, *ms2-2* n=26, *ms3-1* n=14, *ms3-2* n=21, and *ms3-3* n=9. Cotyledon length determination: *col-0* n=22, *ms1-1* n=19, *ms1-3* n=17, *ms2-1* n=16, *ms2-2* n=26, *ms3-1* n=14, *ms3-2* n=21, and *ms3-3* n=9. Hz, heterozygous; Hm, homozygous genotypes.

To asses development differences in T-DNA insertion mutant lines compared to *Col-0*, photographs of 4-days old plants were visual analyzed and development stage was assigned for each plant according to methodology previously described (Boyes *et al*., 2001). Data for developmental stage differences is presented in **Figure 4.13**.

Mutant lines developmental stage at 4-days old showed significant differences with respect to the *Col-0* control ($P<0.05$). The plant percentages in developmental stage 0.1 (dormant seed) were 28, 42, 3, 22, 23, 16, 7%, and 71%; in developmental stage 0.5 (seed protrusion) were 2, 5, 17, 5, 5, 33, 8, 7%; in developmental stage 0.7 (hypocotyl and cotyledon emergence) were 5, 22,45, 16, 29, 39, 17, 9%, whereas in developmental stage 1.0 (fully opened cotyledons) were 65, 31, 36, 57, 43, 12, 67, 14%: for *col-0, ms1-1, ms1-3, ms2-1, ms2-2, ms3-1, ms3-2, and ms3-3*; respectively (**Figure 4.13 A**).

Interestingly, T-DNA insertion mutants showed a developmental delay at 4-days old, mainly *ms3-3* line. In other hand, *ms1-3* mutant line showed a rapid germination process (less plant percentage in developmental stage 0.1), nevertheless, the percentages in developmental stages 0.7 and 1.0 were 45 and 36, respectively; compared with 5% and 65% of the control plants (**Fig 4.13 B**).

Seeds of Arabidopsis lines ($n\geq150$) were counted and weighted to determine differences in seed fresh weight. The average fresh weight per seed was determined and data are presented in **Figure 4.14**. All mutant lines did not show significant differences except for *ms3-3* mutant line; it showed a 0.71-foldchange decrease in fresh weight compared to control plants.

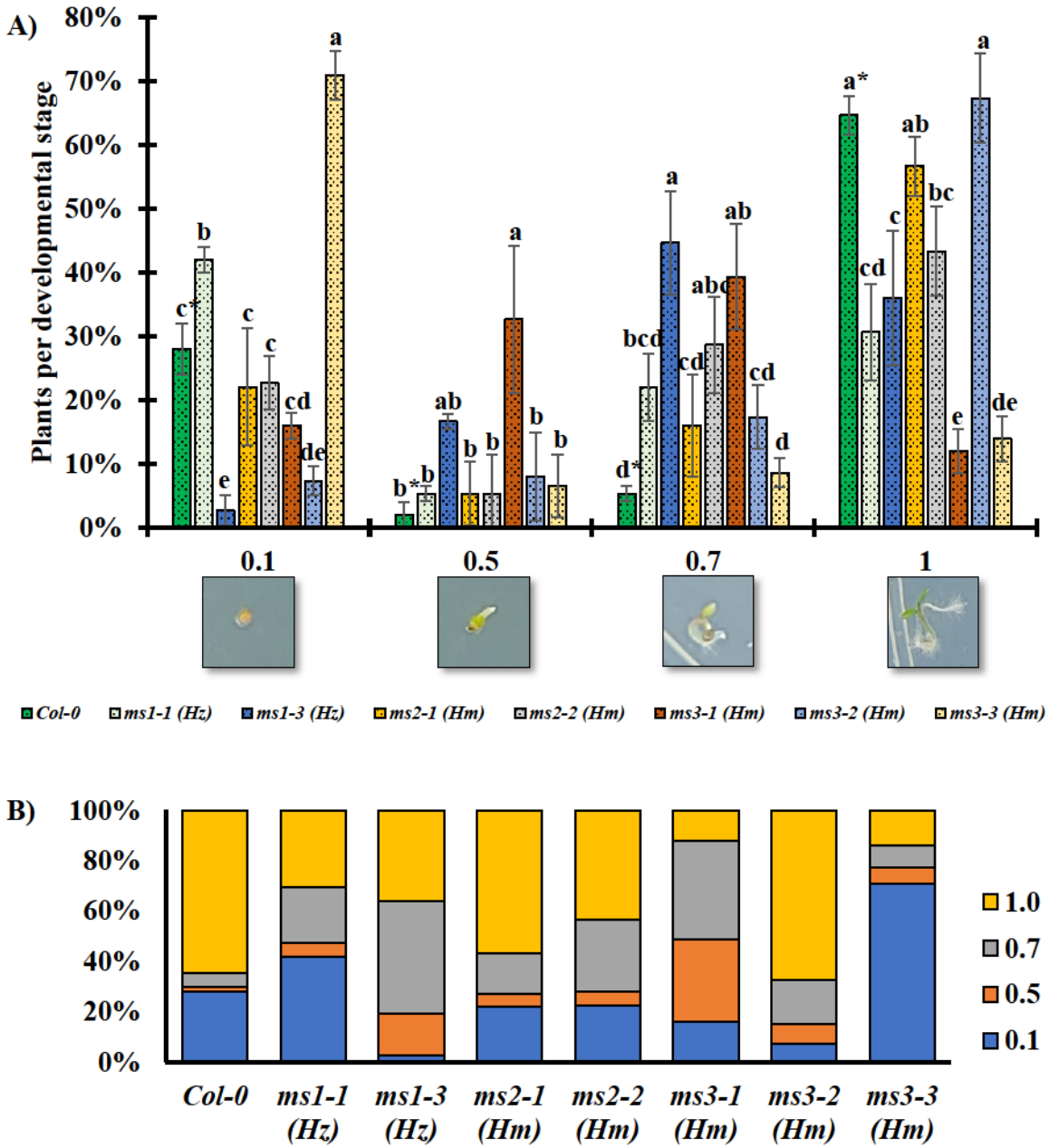

Figure 4.13. Development stage of 4-days old *A. thaliana* lines. Three representative photographs from plates of 4-days old plants were selected from each T-DNA insertion mutant line and col-0 plants. Each plate contains n=50 seeds. Seeds where scored with 0.1, 0.5, 0.7 and 1.0 for dormant seed, seed protrusion, hypocotyl and cotyledon emergence and fully opened cotyledons, respectively. (A) The plant percentage in each developmental stage per genotype was calculated. Data represents means ± SD. *Different letters indicate that are significantly different (Tukey test, $P<0.05$). (B) The composition of developmental stage per genotype to visualize the total distribution. Hz, heterozygous; Hm, homozygous genotypes.

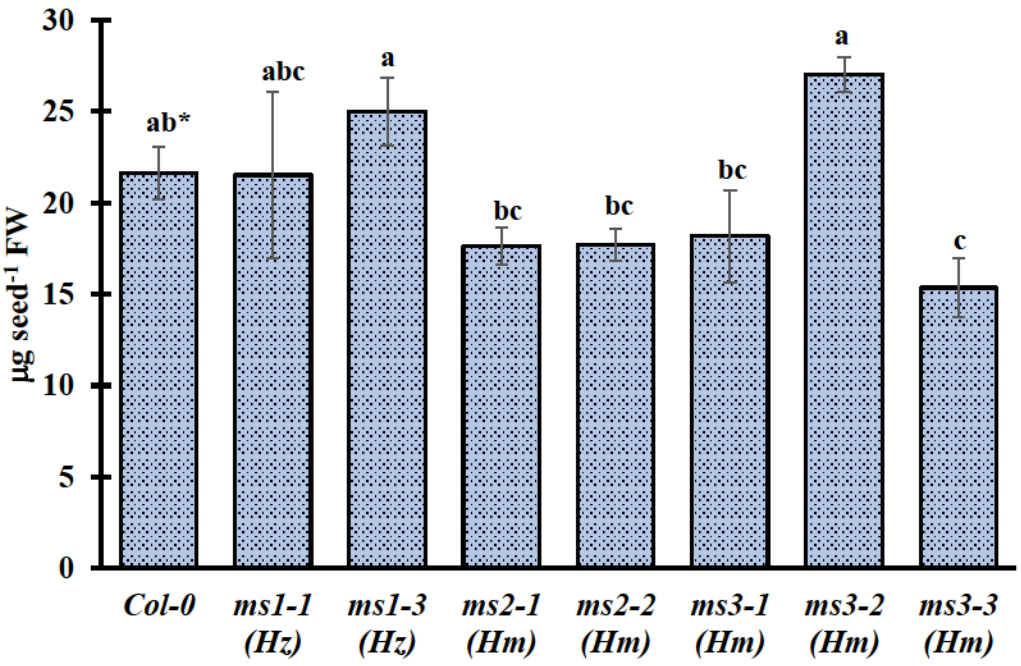

Figure 4.14. Seed fresh weight of *A.thaliana* mutant lines. Seeds were distributed in a paper sheet; a photograph was taken, and seeds were counted in Image J in order to obtain the exact number of seeds. Seeds were transferred into microtubes and were weighted. *Data represent the means ± SD for three replicates (each replicate consists in one microtube containing n≥150, the tube was weighted, seeds were counted and the mean value for each replicate was obtained). *Different letters indicate that are significantly different (Tukey test, $P<0.05$).

4.3 Amino acid analysis

Amino acid profile was evaluated in ATMS1, ATMS2, and ATMS3 mutant lines according to the methodology described in Chapter 3. In general, 16 amino acids were identified and quantified in all the Arabidopsis lines, nevertheless, differences in the distribution profiles were observed between mutant lines when compared to the plant control (**Figure 4.15**). The major amino acid in *Col-0* plant was glutamine (41%) (Gln), followed for 13.85% of threonine+arginine (Thr+Arg), 9.66% asparagine (Asn), 8.43% serine (Ser), 5.94% aspartic acid (Asp), 5.57% glutamic acid (Glu), 3.77% alanine (Ala), 3.51% glycine (Gly), 2.66% leucine+lysine (Leu+Lys), 1.15% cysteine (Cys), 1.14% valine (Val), 1.02% proline (Pro), 0.74% phenylalanine (Phe), 0.62% isoleucine (Ile),0.42% histidine (His), 0.29% tyrosine (Tyr), and 0.22% methionine (Met).

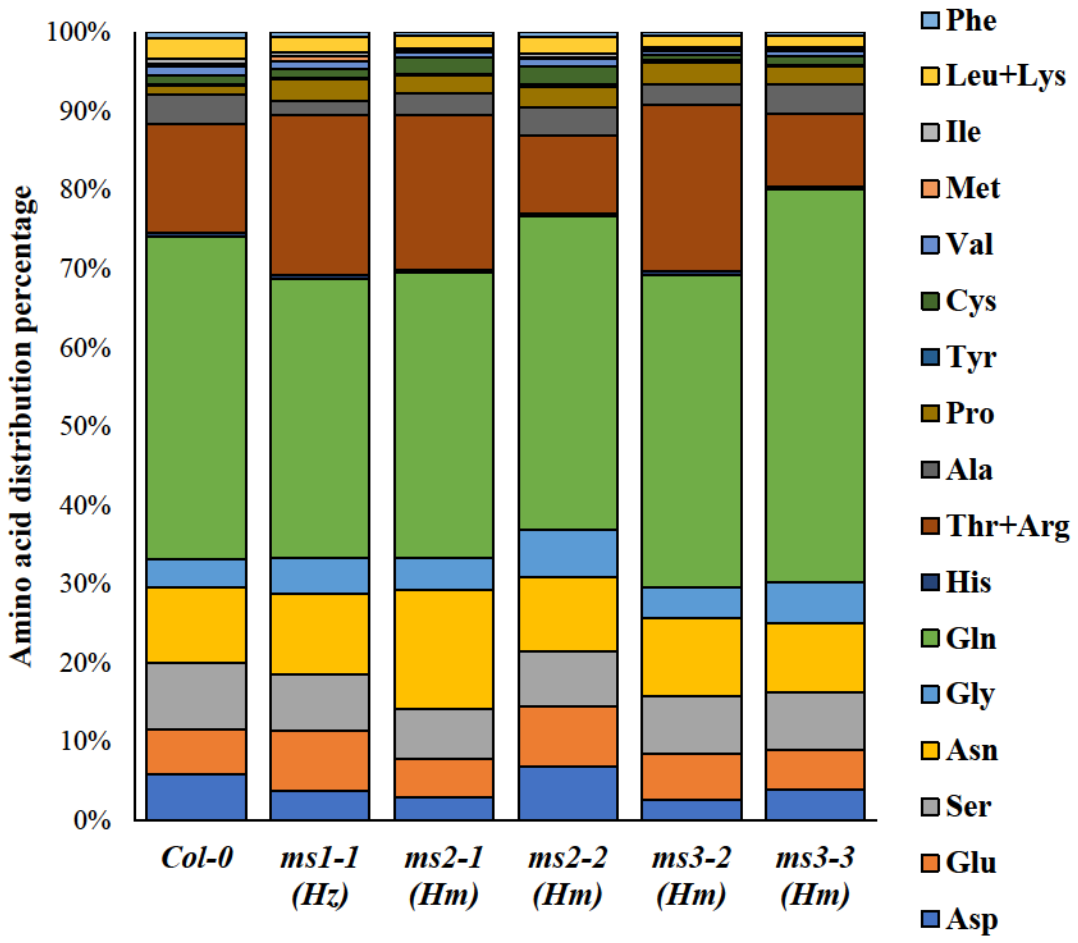

Figure 4.15. Total amino acid profile of 14-day old *A. thaliana* lines shoots. Data represent each amino acid content divided by total amino acids content. Hz, heterozygous; Hm, homozygous genotypes.

Total amino acid contents were calculated for all the evaluated Arabidopsis lines (**Table 4.1**). In general, only the homozygous *ms3-2* mutant line presented an impact on the total amino acid content with a 1.7-fold increase when was compared to *Col-0*. Amino acid profile was not statistically significant different ($P<0.05$) for all mutant lines in Ser, Gly, His, Ala, Val, Leu+Lys, and Phe contents when compared to control plants (**Table 4.1**). In other hand, interestingly changes were found in Pro, Cys and Met content (**Table 4.1, Figure 4.16**).

Table 4.1. Amino acid profile of 14 days old shoots of *Arabidopsis thaliana lines*

	nmol mg^{-1} FW																							
	Col-0				***ms1-1 (Hz)***				***ms2-1 (Hm)***				***ms2-2 (Hm)***				***ms3-2 (Hm)***				***ms3-3 (Hm)***			
aa	Mean		SD		Mean		SD		Mean		SD		Mean		SD		Mean		SD		Mean		SD	
Asp	1.14	±	0.21	b	0.94	±	0.048	b	0.81	±	0.153	b	1.60	±	0.084	a	0.86	±	0.186	b	1.08	±	0.092	b
Glu	1.06	±	0.25	b	1.97	±	0.083	a	1.33	±	0.363	ab	1.80	±	0.221	a	1.89	±	0.283	a	1.40	±	0.157	ab
Ser	1.61	±	0.64	a	1.83	±	0.229	a	1.71	±	0.491	a	1.65	±	0.209	a	2.40	±	0.167	a	1.97	±	1.008	a
Asn	1.85	±	0.24	c	2.61	±	0.333	bc	4.15	±	0.450	a	2.21	±	0.195	c	3.26	±	0.080	ab	2.41	±	0.641	bc
Gly	0.67	±	0.19	a	1.16	±	0.204	a	1.11	±	0.397	a	1.39	±	0.496	a	1.30	±	0.339	A	1.44	±	0.365	a
Gln	7.84	±	3.07	b	9.04	±	0.640	ab	9.87	±	1.723	ab	9.35	±	2.040	ab	12.99	±	1.875	ab	13.72	±	2.268	a
His	0.08	±	0.02	a	0.11	±	0.012	a	0.09	±	0.022	a	0.09	±	0.001	a	0.13	±	0.033	a	0.07	±	0.006	a
Thr+Arg	2.65	±	0.83	b	5.19	±	0.607	a	5.36	±	1.409	a	2.32	±	0.238	b	6.92	±	0.466	a	2.56	±	1.001	b
Ala	0.72	±	0.21	ab	0.48	±	0.036	b	0.77	±	0.154	ab	0.85	±	0.029	a	0.87	±	0.146	a	1.01	±	0.061	a
Pro	0.19	±	0.08	c	0.68	±	0.071	ab	0.60	±	0.157	b	0.60	±	0.032	b	0.91	±	0.048	a	0.62	±	0.161	b
Tyr	0.05	±	0.00	b	0.06	±	0.003	a	0.05	±	0.004	c	0.07	±	0.002	a	0.05	±	0.003	bc	0.05	±	0.001	bc
Cys	0.22	±	0.06	b	0.29	±	0.012	b	0.60	±	0.110	a	0.53	±	0.034	a	0.22	±	0.029	b	0.33	±	0.003	b
Val	0.22	±	0.03	ab	0.23	±	0.018	ab	0.18	±	0.031	b	0.24	±	0.009	a	0.20	±	0.018	ab	0.18	±	0.012	b
Met	**0.04**	±	**0.003**	c	**0.17**	±	**0.008**	a	**0.05**	±	**0.004**	c	**0.05**	±	**0.004**	c	**0.06**	±	**0.006**	b	**0.04**	±	**0.001**	c
Ile	0.12	±	0.004	a	0.10	±	0.003	b	0.08	±	0.003	cd	0.12	±	0.002	a	0.09	±	0.006	c	0.07	±	0.003	d
Leu+Lys	0.51	±	0.011	a	0.53	±	0.040	a	0.45	±	0.070	a	0.49	±	0.024	a	0.48	±	0.029	a	0.41	±	0.085	a
Phe	0.14	±	0.019	a	0.14	±	0.010	ab	0.10	±	0.018	b	0.12	±	0.007	ab	0.12	±	0.006	ab	0.12	±	0.018	ab
Total	19.11	±	3.86	b	25.56	±	0.65	ab	27.29	±	4.79	ab	23.48	±	1.98	ab	32.74	±	1.96	a	27.48	±	5.49	ab

Different letters in the same row indicate significant differences (Tukey test p-value ≤0.05). Values represent the mean ± SD of three biological replicates

The proline content presented statistically significant differences (P<0.05) in all the mutant lines when compared to *Col-0* plants **(Figure 4.16 A)**. The proline levels in *ms1-1*, *ms2-1* and *ms2-2* mutant lines showed a significant increase of 3.5, 3.08 and 3.06-fold change in comparison to the control plant (P<0.05). Similarly, *ms3-2 and ms3-3* lines presented proline content increases up of 4.6 and 3.1-fold, respectively.

Only *ms2-1* and *ms2-2* mutant lines showed statistically significant increases (P<0.05) in cysteine content by 2.7 and 2.4-fold change, respectively, when compared to *Col-0* control (**Figure 4.16 B**). Methionine content was quantified and the results showed a similar trend as other evaluated amino acids with significant increases of 4.09 and 1.54-fold in heterozygous m*s1-1* and homozygous *ms3-2* mutant lines (P<0.05); while the others T-DNA insertion mutants had similar (P<0.05) methionine contents as the Col-0 plant control (**Figure 4.16 C**).

Aspartic acid (Asp) levels were significantly different only in homozygous *ms2-2* mutant line with a 1.4-fold increase in comparison to the *Col-0* control (P<0.05) (**Table 4.1**). Glutamic acid content was higher in *ms1-1, ms2-2* and *ms3-2* with 1.85, 1.68 and 1.77-fold-change than the plant control. Serine, Glycine and Histidine contents were determined and not statistically significant differences between T-DNA insertion mutant lines and Col-0. Asparagine content were significantly different in *ms2-1* and *ms3-2* with 2.2 and 1.76 fold-change increases. Glutamine levels were significant different only in homozygous *ms3-3* mutant line with 1.75 fold-change increase.

Threonine and Arginine content were calculated as one peak area due to high arginine content masks threonine peak. Thus, threonine and arginine levels were significantly enhanced in T-DNA insertions *ms1-1, ms2-1,* and *ms3-2* mutants with 1.95, 2.02, and 2.61 fold-change increase respectively. Alanine content was significantly declined to 0.67-fold in heterozygous *ms1-1* mutant line with respect to *Col-0* control.

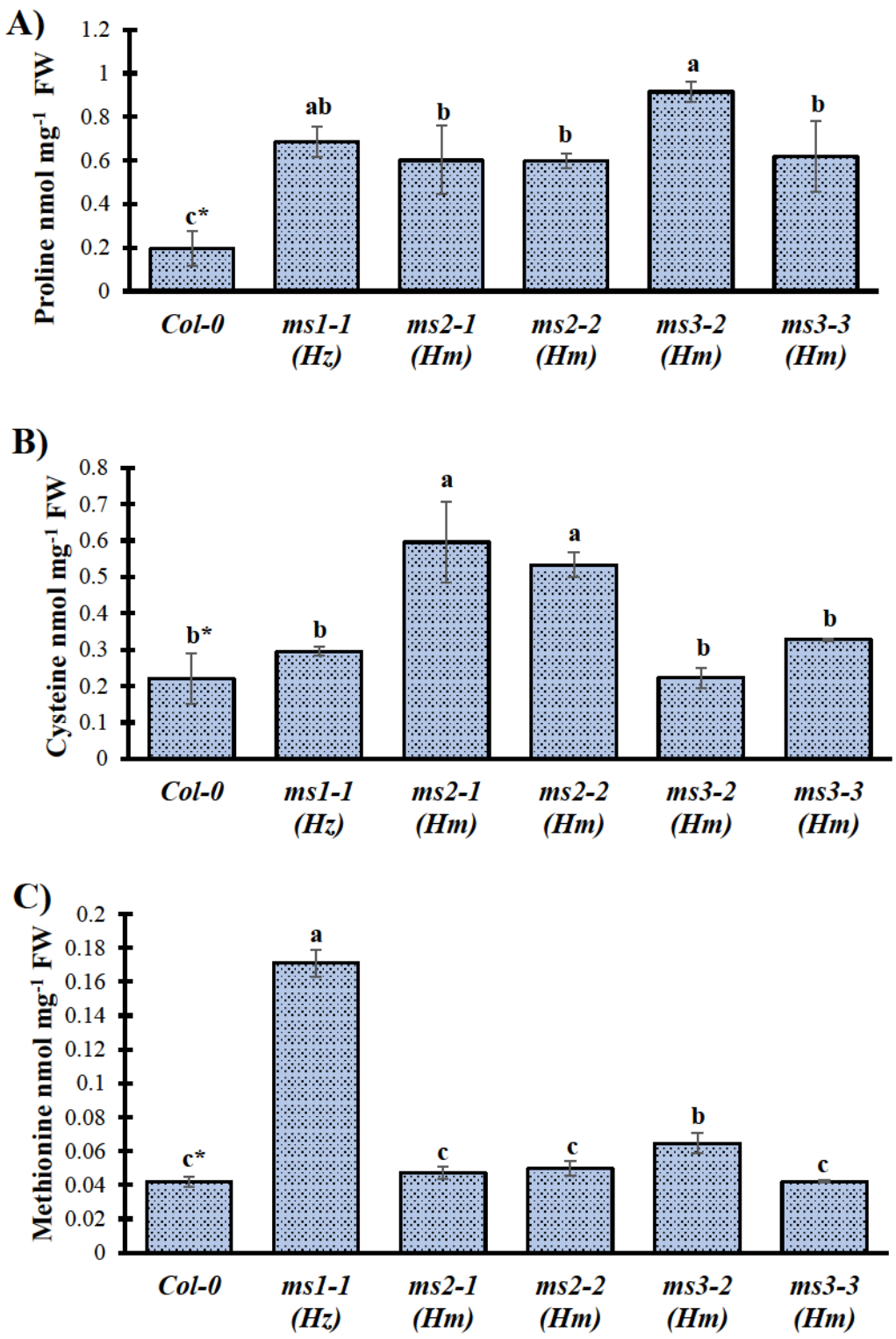

Figure 4.16. Proline, cysteine, and methionine content of 14-day old *A. thaliana* shoots. Data represent means ± SD of three independent determinations. *Different letters indicate that are significantly different (Tukey test, $P<0.05$). Hz, heterozygous; Hm, homozygous genotypes.

Tyrosine levels in *ms1-1* and *ms2-2* showed in 1.15 and 1.22-fold-change increases, while *ms2-1* showed a 0.84-fold-change decrease. Valine content only showed significant differences in *ms2-2* mutant line with 1.11-fold-change increase in comparison to the plant control. On the other hand, Isoleucine content showed a significant decrease of 0.84, 0.67, 0.74 and 0.60-fold for heterozygous *ms1-1* and homozygous *ms2-1, ms3-2, and ms3-3 mutant lines*. Leucine and Lysine levels were calculated as one peak due to chromatographic separation conditions, although no significant differences were found for all mutant lines. Phenylalanine content result in significant differences for *ms2*-1 mutant line with 0.81-fold-change decrease than the *Col-0* plants.

4.4 Folates analysis

The total folates content was identified and quantified to evaluate differences in folates profile of ATMS1, ATMS2 and ATMS3 mutant lines (**Figure 4.17**). Total folates content in control plants resulted in 1,866±262 pmol g^{-1}. Total folates content showed statistically significant differences ($P<0.05$) only for *ms3-2* mutant line with 1.37-fold change increase. Folates profile in *Col-0* plants accumulated mainly 5-CH_3-THF (53%) and 5,10-CH=THF+10-CHO-THF (32%), followed for 5-CHOTHF (13%). THF+5,10-CH_2-THF and folic acid were in minor amounts (2%).

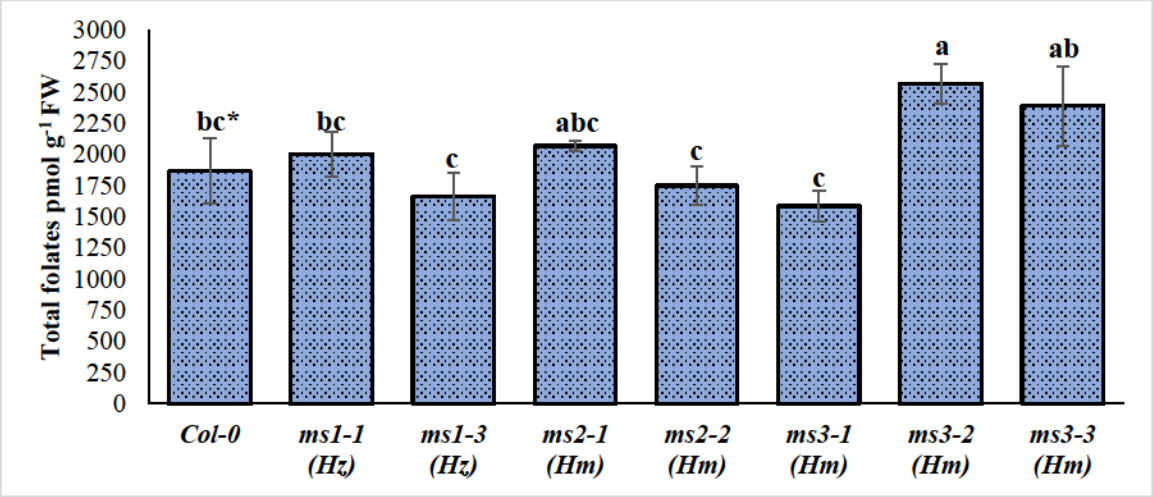

Figure 4.17. Total folate content in shoots of 14-days old *A.thaliana* mutant lines. Data represent means ± SD of three independent determinations. *Different letters indicate that are significantly different (Tukey test, $P<0.05$). Hz, heterozygous; Hm, homozygous genotypes.

Folates profile was conserved between T-DNA mutant lines and *Col-0* plants with few differences in folates species content (**Table 4.2)**. Results of 5-CH_3-THF content showed statistically significant differences ($P<0.05$) for *ms3-2* and *ms3-3* with 1.45 and 1.33-fold change increase when compared to *Col-0* plants. However, THF+5,10-CH_2 -THF, 5,10-CH=THF+10-CHO-THF, 5-CHO- THF and FA contents did not have statistically significant differences ($P<0.05$) in comparison to control plants. Furthermore, it should be noted in **Table 4.2** that 5-CH_3-THF content is significant different between T-DNA mutant lines in which *ms1-3* (822±111 pmol g^{-1} FW), *ms2-2* (864±26 pmol g^{-1} FW) and *ms3-1* (915±138 pmol g^{-1} FW) showed decreased content in comparison to *ms3-2* (1432±63 pmol g^{-1} FW) a*nd* *ms3-3* (1316±151 pmol g^{-1} FW). Similarly, 5,10-CH=THF+10-CHO-THF concentration was significant different in *ms3-1*(495±47 pmol g^{-1} FW) when compared to *ms3-2*(776±95 pmol g^{-1} FW) mutant line. For 5-CHO-THF, *ms3-1* mutant line showed decreased content (135±47 pmol g^{-1} FW) in comparison with *ms1-1* (272±37 pmol g^{-1} FW), *ms2-1* (346±45 pmol g^{-1} FW), *ms3-2* (331±56 pmol g^{-1} FW) and *ms3-3* (353±36 pmol g^{-1} FW).

Preeliminar polyglutamylation profile of 5-CH_3-THF (**Figure 4.18**) was obtained for *ms1-1*, *ms2-1*, *ms2-2*, *ms3-2*, and *ms3-3* mutant lines (n=1) due to sample availability. 5-CH3-THF polyglutamylated species identified in *Col-0* plants were 25% Glu1, 8% Glu2, 6% Glu4, 9% Glu5, 18% Glu6, 24% Glu7, and 9% Glu8 (**Figure 4.18B**). These preliminar results indicate that polyglutamylation profiles of *ms1-1*, *ms3-2* and *ms3-3* mutant lines showed a trend to increase the distribution of the forms more polyglutamylated of 5-CH_3 THF, Glu6 to Glu9, in comparison with *Col-0* plants.

Table 4.2. Folates content in 14-days old *Arabidopsis thaliana* mutant lines

	Folate content (pmol g^{-1} FW)																				
	THF+5,10-CH_2-THF				5-CH_3-THF				5,10-CH=THF + 10-CHO-THF				5-CHO-THF				Folic Acid			
Genotype	Mean		SD		Mean		SD		Mean		SD		Mean		SD		Mean		SD	
Col-0	17.28	±	15	a*	983.7	±	113	cd*	600	±	114	ab*	247	±	52	abc*	18.1	±	9.9	a*
ms1-1 (Hz)	7.1	±	12	a	1138.3	±	118	abc	576	±	39	ab	272	±	37	ab	9.69	±	0.9	a
ms1-3 (Hz)	19.98	±	2	a	822.6	±	111	d	612	±	66	ab	194	±	34	bc	15.7	±	1.8	a
ms2-1 (Hm)	38.9	±	55	a	1038	±	66	bcd	658	±	45	ab	346	±	45	a	17.7	±	4.9	a
ms2-2 (Hm)	6.54	±	5	a	864.3	±	26	cd	616	±	118	ab	244	±	22	abc	21.2	±	19.7	a
ms3-1 (Hm)	22.2	±	7	a	915.1	±	138	cd	495	±	47	b	135	±	47	c	18.6	±	3.6	a
ms3-2 (Hm)	13.66	±	13	a	1432.3	±	63	a	776	±	95	a	331	±	56	a	15.8	±	10.6	a
ms3-3 (Hm)	2.96	±	5	a	1316.6	±	151	ab	707	±	137	ab	353	±	36	a	9.48	±	0.3	a

*Different letters in the same column are significantly different (Tukey test, $P<0.05$). All values are the means ± SD of three independent determinations. Hz, heterozygous; Hm, homozygous genotypes.

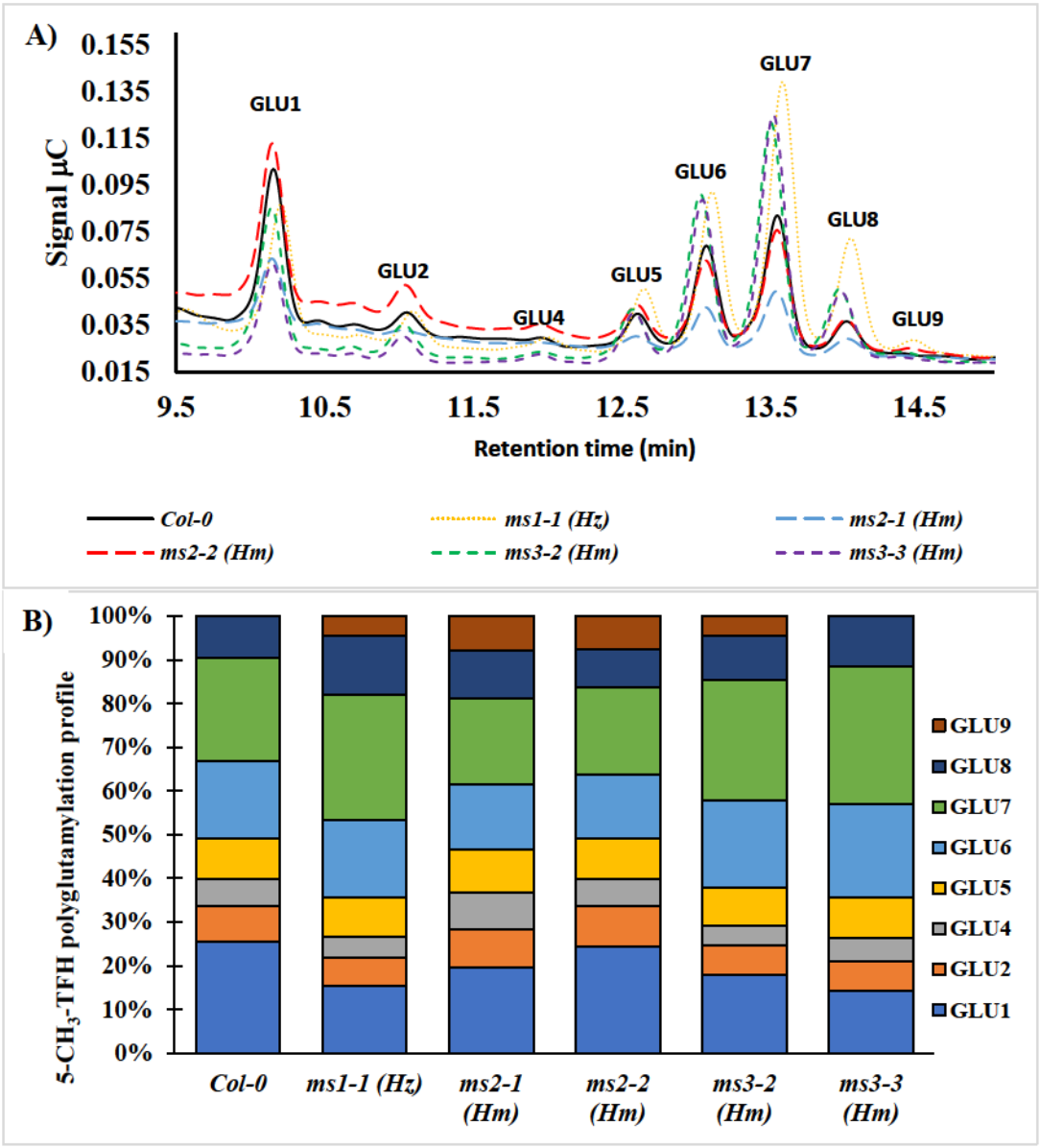

Figure 4.18. Folate polyglutamylation chromatogram (A) and distribution profile 5-CH_3 THF polyglutamy forms from 14-days old *A.thaliana* shoots. Glu_n indicates the number of glutamates residues attached to 5-CH_3 THF. Hz, heterozygous; Hm, homozygous genotypes.

5. Discussion

The three isoforms of methionine synthase in *A.thaliana* were described by Ravanel *et al*. (2004). The previous work reported that ATMS1 and ATMS2 were localized in cytosol, while ATMS3 in plastids. ATMS1 and ATMS2 share similitudes as both are 765 amino acid lengths and 92% identical between them. In another hand, ATMS3 is longer compared to ATMS1 and ATMS2, because it contains a signal peptide for plastid, and it has an 812 amino acid length. Also, ATMS3 is 79-81% similar to ATMS1 and ATMS2, respectively (Ravanel *et al,* 1998). Due to the existence of three methionine synthase isoforms, questions arise about the biological relevance of each enzyme, therefore the aim of this study was to determine the impact of *A. thaliana* mutant lines lacking each methionine synthase isoenzyme to study the role of specific cellular localization and their impact on visual and metabolic growing phenotype and metabolic profile of Arabidopsis seedlings. Principal findings about the metabolic and visual phenotype of Arabidopsis mutants of this research will be discussed next.

5.1 Although ATMS1 and ATMS2 are localized in cytosolic compartment, homozygous ATMS1 showed lethality

Although ATMS1 and ATMS2 isoenzymes share structural similitudes, in the present work was demonstrated that under our experimental growing conditions, it was not possible to identify homozygous plants for ATMS1 mutant lines, instead, for ATMS2 and ATMS3 were identified homozygous mutant lines (**Figures 4.2 to 4.9**). Therefore, it can be inferred that homozygous T-DNA mutants of ATMS1 could be a lethal phenotype while there is a functional redundancy in homozygous T-DNA mutants of ATMS2 (*ms2-1* and *ms2-2*) and ATMS3 (*ms3-1*, *ms3-2* and *ms3-3*). Similar results have been reported regarding lack of identification of ATMS1 homozygous plants (Yang *et al*, 2019). On the other hand, Ju *et al, (*2019) showed that they were able to identify homozygous plants for ATMS1 in one of three studied T-DNA mutant lines. These authors reported to obtain homozygous plants for CS480822 mutant line, while did not identify homozygous plants for CS828436 and SALK_205174, this result is in agreement with our experimental results in which from three ATMS1 T-DNA mutant lines, only were found heterozygous plants (*ms1-1*, *ms1-2*, and *ms1-3*). Also, in this work was studied the mutant line SALK_088429, ATSM3 T-DNA insertional mutant, the same germplasm used by Yan *et al*., (2019). It was possible to identify a homozygous mutant line for SALK_088429 (*ms3-2*) as previously reported in their study,

this was an interesting result because this isoenzyme is in charge of *de novo* methionine biosynthesis, thus, it was though that ATMS3 is a critical source of methionine to sustain germination and plant development.

5.2 Problems in seedling establishment and plant development were found in mutant lines

Seed germination is a key process in plant development during plant life cycle, which is characterized by the switch from quiescence to highly active metabolism in embryonic cells (Gallardo *et al*, 2002). Therefore, it is expected that methionine, as a precursor of metabolites as SAM and ethylene, is essentially required to sustain metabolic requirements for plant development. Moreover, it was demonstrated that methionine plays an essential signal role in modulating cellular events that facilitate seed germination (Ju *et al*,2019). In a proteomics analysis, it was showed that during germination, imbibed seeds accumulate methionine synthase in 4-fold and these levels return to basal content when subsequent seed drying was applied (Gallardo *et al*, 2002)

Accordingly, to Ju *et al* (2020), ATMS1 have a predominantly role in the regulation of seed germination, this is due to the high transcript levels of ATMS1 compared to ATMS2 and ATMS3, and the relationship between L-methionine-dependent germination due to the activation of AtGLR3.5 with cytosolic Ca^{2+} signal. They reported that homozygous knock-down of ATMS1 results in decreased germination when compared to control. Although, in this study it was only possible to find heterozygous T-DNA insertional mutant lines for ATMS1, this could explain why *ms1-1*, *ms1-3* showed delayed germination when compared to control plants (**Figure 4.13**)

Although, the transcriptional levels of methionine synthase isoenzymes were not determined in this work, in order to support this observation, the expression levels of MS isoenzymes were investigated in "The Bio-Analytic Resource for Plant Biology (BAR)" Canadian database (**Figures 5.1, 5.2, A4, A5, and A6**). As it can observed in **Figure 5.1**, the expression level of ATMS1 during seed germination are remarkedly higher in comparison with ATMS2 and ATMS3, this observation supports the lack of identification of homozygous ATMS1 mutant lines with exception of previously reported CS480822 (**Figure 2.4**), but in this case, this could be explained due to the insertion position at the final position of exon 12. This expression level is followed by ATMS2 that becomes active during seed protrusion.

In this work *ms2-1* developmental stage was not significant different when compared to control but *ms2-2* showed delayed germination, although this could due to the insertion position of *ms2-1* that could be removed during splicing process, unlike *ms2-2* which is localized in exon 11(**Table A2**). In the other hand, ATMS3 expression level is below the detection limits during seed germination. Although *ms3-1* and *ms3-3* mutant lines showed delayed germination when compared to control plants indicating that AMTS3 besides its low expression level it could be essential to sustain plant development during early stages, this it is represented in **Figure 5.2** in which is demonstrated that ATMS3 is expressed during the first steps of embryo development, although its expression level is lower in comparison to ATMS2 and ATMS3. This information supports the importance of ATMS1, ATMS2 and ATMS3 during seed germination and this could explain why it was not possible to find homozygous plants for ATMS1 T-DNA mutant lines while homozygous ATMS2 and ATMS3 mutant lines were identified.

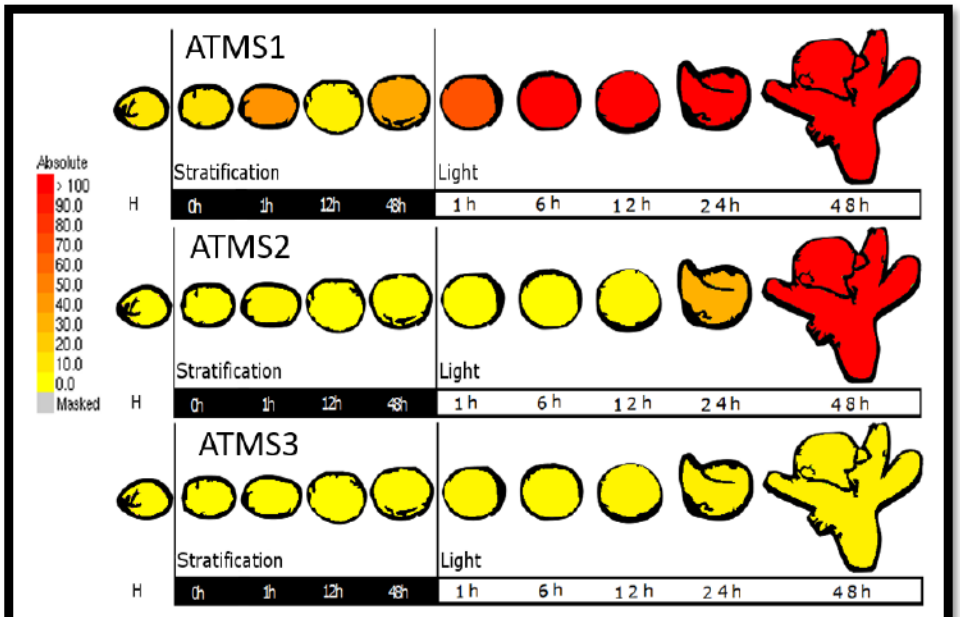

Freshly harvested ecotype Columbia seeds directly upon removal from the silique (H). Seeds desiccated for 15d in darkness (0h). Seeds stratified at 4°C in the dark: for 1h, 12h, and 48h. Stratified seeds were then transferred into continuous light and further collected at 1, 6, 12, 24, 48h into the light.
Narsai *et al*., 20011. Plant physiol. 157(3):1342-62

Figure 5.1. Expression levels of methionine synthase isoenzymes during seed germination. This scheme represent the expression levels during seed germination of *A.thaliana* seeds. (Narsai *et al*.,2011)

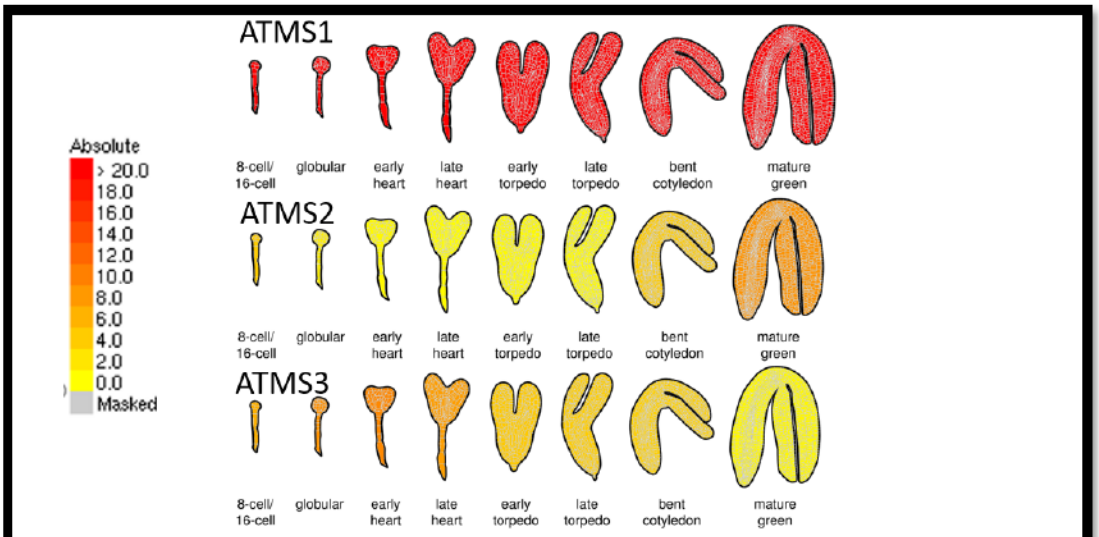

Col-0 seeds were grown in a climate-controlled growth chamber set at 20-22°C temperature with a 16h- light/8-h dark cycle. The pseudo-aligner Kallisto was used for quantification of all mRNA-seq datasets [v0.44.0, (Bray *et al*., 2016)]. Before quantification, the aproppiate adapter sequences for each mRNA-seq library were trimmed from the FASTQ files using Cutadapt with a minimum match length of five nucleotides [v1.9.1, (Martin 2011)]. Cutadapt was also used to trim all oligo-A or oligo-T sequences that were at least five nucleotides long from the ends of reads. All reads longer than 18 nucleotides after trimming were used as input for kallisto quant. Kallisto quant was run on paired-end samples using default settings. For single-ends samples, the arguments -fragment-length 200-sd 100 were used. Gene-level transcripts per million (TPM) were estimated by combining the TPM of all isoforms of protein-coding genes. Gene IDs mapping to mitochondria and chloroplast genomes, as well as the 270 kilobase mitochondrial insertion on chromosome 2(Stupar *et al*., 2001), were discarded. Last, abundances were renormalized to a sum of 1 million for each sample

Figure 5.2. Expression levels of methionine synthase isoenzymes during embryo development. This scheme represent the expression levels during embryo development of *A.thaliana* seeds. (Hofmann *et al*.,2019)

Plant growth is a metabolic process regulated by several factors such as temperature, light intensity, water, hormones, nutrient availability and root growth. Primary root growth relies on cell division in the apical root meristem, subsequent elongation is due to newly divided cells, therefore it is a high metabolite demanding process (Pelagio-Flores *et al*., 2020). Due to the biological importance in plant development of methionine synthase as it is demonstrated by their differential expression during plant development (**Figure 5.1, 5.2, A4, A5, and A6**), phenotypic analysis was performed, and significant differences were found for shoots weight, root, hypocotyl and cotyledon length. The plate-based phenotypic analysis demonstrated significant decreases in shoots weight of 14-days old plants from *ms1-1* and *ms3-2* (**Figure 4.10 A**), whereas roots weight of 14-days old seedlings did not show significant differences in comparison to control plants (**Figure 4.10 B**), although this could

be attributed to root harvest methodology because higher standard deviations were obtained for this determination.

Moreover, root length determination of 7-days old seedlings (**Figure 4.12 A)** showed that *ms1-1*, *ms1-3*, *ms2-2* had a significant difference of 0.69, 1.21, and 0.73-fold in comparison to plant control. Hypocotyl length determination of 7-days old seedlings (**Figure 4.12 B)** resulted in a general decrease in all mutant lines compared to control plants. Some studies demonstrated that hypocotyl length can be regulated by photoreceptors of phytochrome family under light treatments such as grown in darkness and blue light (Menon, Klose, & Hiltbrunner, 2019); and in response to plant hormones such as ethylene, ACC, auxins, etc.; (Choi *et al*., 2019; Okushima *et al*., 2005; Xiong *et al*., 2019)), although in this study it was demonstrated that all insertional mutant lines had smaller hypocotyls compared to control plants, this could be explained as delayed development which is demonstrated also in cotyledon length measurements (**Figure 4.12 C)** that showed smaller size for *ms1-1*, *ms2-2*, *ms3-1* and *ms3-2* with 0.61, 0.78, 0.70, and 0.60-fold change respectively.

Moreover, differences in plant development are shown in **Figure 4.13**, significant differences were obtained for *ms1-1*, *ms1-3*, *ms2-2*, *ms3-1* and *ms3-3* during the seedling establishment. Differences in weight of fresh seeds were determined to assess if this could lead to germination problems, but only *ms3-3* mutant line showed significant differences with a decrease of 0.71-fold change (**Figure 4.14**). A summary of the significant differences in plant growth and development phenotype of studied mutants is presented in **Figure 5.3** next. As a general view, ATMS1 T-DNA mutant lines showed significant differences in plant germination, shoots weight, cotyledons and roots length, and delayed development. For ATMS2 T-DNA mutant lines, significant differences were found in plant germination, cotyledons and roots length, seeds weight and delayed development. Finally, ATMS3 T-DNA mutant lines showed significant differences in plant germination, shoots and seeds weight, cotyledons length and delayed development. The observed phenotypic differences of T-DNA insertion mutants remark the importance of methionine synthase isoenzymes during *Arabidopsis* development, in **Figures A4, A5** and **A6** it is demonstrated that these isoenzymes are expressed differentially, this could be to specific roles of each isoenzyme in plant development. Although these mechanism remain to be discover.

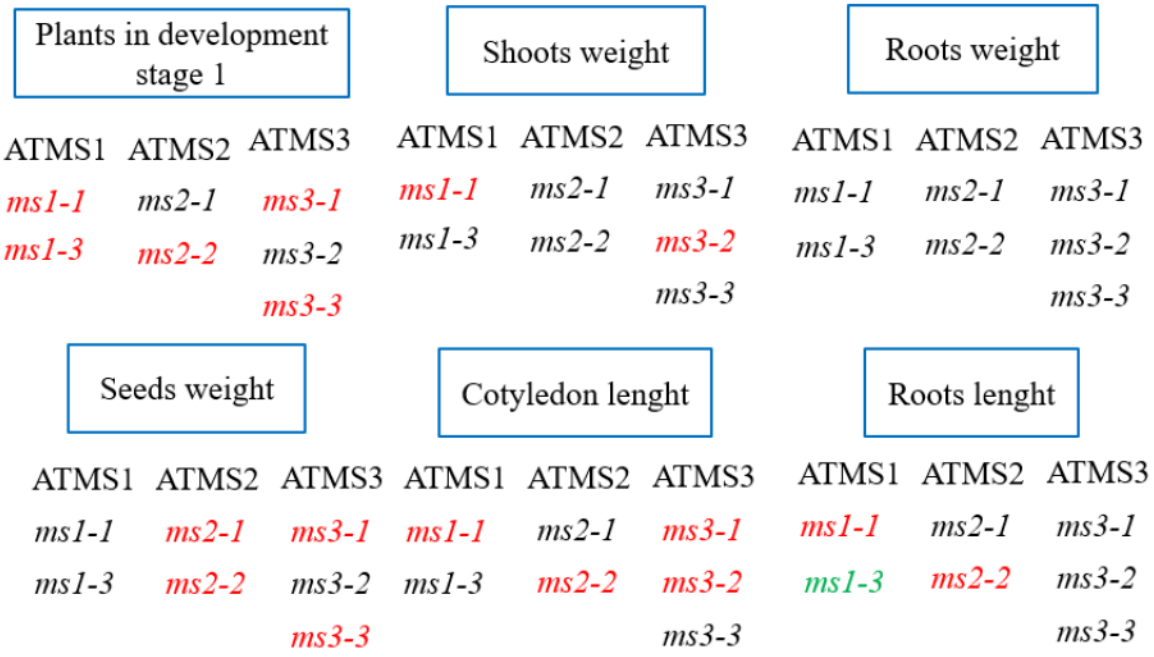

Figure 5.4. Summary of plate-based phenotypic analysis of *A.thaliana* mutant lines. In this scheme is presented all studied mutant lines in each test evaluated. Plants in development stage one refers to number of plants that reached this development stage (**Figure 4.14**). **Red Color** and **Green Color** indicates significant **decreases** and **increases** ($P<0.05$), respectively; when compared to control plants. **Black color** indicates that no significant differences were found.

5.4 Total amino acid content was significant different in ms3-2 mutant

As previously described, amino acids serves as a building blocks for proteins, thus their importance in cellular reactions and their influence in plant growth and development, intracellular pH control, production of metabolic energy, and resistance to abiotic and biotic stress cannot be underestimated (Hildebrandt *et al.*, 2015) Since methionine synthase is the enzyme in charge of methionine production, and this amino acid serves as a substrate to several destinations (as described in Chapter 2.1 and 2.2) it would be expected to find significant differences in amino acid content in the *A. thaliana* mutant lines. Although, total amino acid content of *Arabidopsis* mutant lines was only significant different for *ms3-2* with a 1.7-fold increase when was compared to control plants. Amino acid profile of 7-d-old *Arabidopsis* control plants is composed of Gly, Asp, Ser, Glu, Ala, Asn, Gln, Arg, Thr, Phe, Lys, Met, Tyr, Cys, Ile, Leu, Val, and proline based on their relative values from highest to lowest (Srivastava *et al.*, 2011), which was similar to amino acid profile obtained for *col-0* control plants in this work with slight differences due to growing conditions and plant age. A summary of amino acids which present significant differences when compared to control

plants is presented in **Figure5.4**. In general, amino acid profile was conserved for all mutant lines in Ser, Gly, His, Ala, Val, and Leu+Lys contents when compared to control plants. Although it should be noted that methionine belongs to aspartate biosynthesis family, and the amino acids from this family (Asn, Asp, Thr, and Ile) showed significant differences. Moreover, significant differences were found also in amino acids from aromatic (Phe and Tyr) and glutamate (Gln, Glu, Pro, and Arg) biosynthesis families. The ATMS1 T-DNA mutant line (*ms1-1*) showed significant differences in Glu, Thr+Arg, Pro, Tyr, Met and Ile. For AMTS2 T-DNA mutant lines, significant differences were found in Asp, Glu, Asn, Thr+Arg, Pro, Tyr, Cys, Ile and Phe. ATMS3 T-DNA mutant lines showed significant differences in Glu, Asn, Gln, Thr+Arg, Pro, Met, and Ile. All T-DNA mutant lines showed an accumulation of Pro, moreover, all T-DNA mutant lines have decreased content of Ile with exception of *ms2-2*.

5.5 Amino acid pool was affected differentially

Some studies have suggested that lysine, a nutritionally important amino acid, when is present at significant increment levels in Arabidopsis seeds can causes delayed germination, mostly due to alterations in transcriptome, primarily affecting transcriptional programs required for seed establishment (Choi *et al*., 2019). Nevertheless, in this work leucine+lysine content did not differ between analyzed mutant lines compared to control plants. Also, it was reported a relationship between catabolism of aspartic family amino acids and the onset of photosynthesis (Angelovici, Fait, Fernie, & Galili, 2011). In agreement with literature, in this work, amino acids from aspartic family Asp, Asn, Ile, Thr and Met were affected at different levels (**Figure 5.4**) and Pearson correlations were determined and are presented in **Table 5.1 to Table 5.6** in order to visualize differences and relationship between amino acids, folates and plant development. All significant Pearson correlations for Col-0 plants were between metabolites while in T-DNA mutant lines were found also with phenotypic parameters. For example, in *ms1-1* the content of 5FTHF demonstrate positive correlation with plant development and seed weight, also the content of Gln was positive correlated with seed weight.

Table 5.1. Pearson correlations for *Col-0* control plants

Variable 1	Variable 2	N	C.C	P-value
5,10-CH=THF+10-CHO-THF	5MTHF	3	1	0.003
5,10-CH=THF+10-CHO-THF	Pro	3	-0.999	0.024
5FTHF	Phe	3	-0.999	0.027
5MTHF	Pro	3	-0.999	0.021
Ala	Gly	3	-0.999	0.029
Ile	Ser	3	-1	0.001
Leu+Lys	Gln	3	1	0.009
Met	His	3	1	0.002
THF+5,10-CH2-THF	Cys	3	0.998	0.041
Total aa	Gly	3	0.999	0.032
Total aa	His	3	0.998	0.037
Total aa	Met	3	0.999	0.035
Val	Tyr	3	1	0.004

C.C stands for correlation coefficient

Table 5.2 Pearson correlations for *ms1-1* (Hz) T-DNA mutant line

Variable 1	Variable 2	N	C.C	P-value
10-CHO-THF	5MTHF	3	0.998	0.037
10-CHO-THF	Phe	3	1.000	0.012
5,10-CH=THF+10-CHO-THF	5,10-CH=THF	3	0.999	0.03
5,10-CH=THF+10-CHO-THF	Glu	3	-0.998	0.037
5,10-CH=THF	Glu	3	-1.000	0.007
5FTHF	Development stage 1	3	-0.999	0.028
5FTHF	Weight/seed	3	1.000	0.002
5MTHF	Phe	3	0.999	0.025
FA	5,10-CH=THF+10-CHO-THF	3	0.998	0.038
FA	5,10-CH=THF	3	1.000	0.008
FA	Glu	3	-1.000	0.001
Gln	Weight/seed	3	-0.998	0.042
His	Ser	3	0.999	0.033
Leu+Lys	Pro	3	0.998	0.036
Total folates	Ala	3	-0.997	0.046
Val	Ala	3	-0.998	0.039
Weight/seed	Development stage 1	3	-0.999	0.025

C.C stands for correlation coefficient

For *ms2-1* mutant lines were found Pearson positive correlations between the Met content with plant development and Thr+Arg content; Phe content show positive correlation with plant development, Met and Thr+Arg content; Serine and total aa were positive correlated with seed weight. Regarding to folate content, 10-CHO-THF was negative correlated with Ala content, while 5,10-CH=THF demonstrate negative correlations with Gly, THF+5,10-CH_2-THF, and Val content; in the other hand 5MTHF content was positive correlated with Thr+Arg content.

Table 5.3 Pearson correlations for *ms2-1* (Hm) T-DNA mutant line

Variable 1	Variable 2	N	C.C	P-value
10-CHO-THF	Ala	3	-0.999	0.03
5,10-CH=THF	Gly	3	-1	0
5,10-CH=THF	THF+5,10-CH2-THF	3	-1	0.003
5,10-CH=THF	Val	3	-0.999	0.034
5MTHF	Thr+Arg	3	0.998	0.038
Gln	Glu	3	0.999	0.021
Leu+Lys	Gln	3	0.999	0.02
Leu+Lys	Glu	3	0.998	0.041
Met	Development stage 1	3	0.998	0.041
Met	Thr+Arg	3	1	0.019
Phe	Met	3	1	0.003
Phe	Development stage 1	3	0.998	0.044
Phe	Thr+Arg	3	1	0.017
Pro	Glu	3	0.999	0.031
Ser	Weight/seed	3	1	0.013
THF+5,10-CH2-THF	Gly	3	1	0.003
THF+5,10-CH2-THF	Val	3	0.998	0.038
Total aa	Leu+Lys	3	0.998	0.04
Total aa	Ser	3	0.999	0.031
Total aa	Weight/seed	3	1	0.018
Total folates	5,10-CH=THF	3	-1	0.013
Total folates	Gly	3	1	0.012
Total folates	THF+5,10-CH2-THF	3	1	0.016
Total folates	Val	3	0.999	0.022
Val	Gly	3	0.999	0.034

C.C stands for correlation coefficient

T-DNA mutant lines ms2-2 show significant Pearson correlations for 10-CHO-THF with Asn, Gln, Gly, and His content. Also, 5,10-CH=THF+10-CHO-THF was positive correlated with His and Thr+Arg content; while 5FTHF was positive correlated with Glu and THF+5,10-CH_2-THF. In this case 5MTHF was negative correlated with Phe content and plant development. Regarding amino acid pool, Gln show significant correlations with Asn, Gly, Ser content; while Gly with Asn content; moreover, His was correlated with Asn, Gln, and Gly content. In this case Phe content show positive correlation with plant development, while total folate content shows negative correlation with seed weight.

Table 5.4. Pearson correlations for *ms2-2* (Hm) T-DNA mutant line

Variable 1	Variable 2	N	C.C	P-value
10-CHO-THF	Asn	3	1	0.002
10-CHO-THF	Gln	3	0.999	0.024
10-CHO-THF	Gly	3	-1	0.012
10-CHO-THF	His	3	0.999	0.024
5,10-CH=THF+10-CHO-THF	His	3	0.998	0.042
5,10-CH=THF+10-CHO-THF	Thr+Arg	3	0.999	0.023
5FTHF	Glu	3	1	0
5FTHF	THF+5,10-CH2-THF	3	1	0.02
5MTHF	Phe	3	-1	0.017
5MTHF	Development stage 1	3	-0.997	0.049
FA	Cys	3	1	0.002
Gln	Asn	3	0.999	0.023
Gln	Gly	3	-1	0.012
Gln	Ser	3	-0.997	0.048
Gly	Asn	3	-1	0.01
His	Asn	3	0.999	0.025
His	Gln	3	0.997	0.048
His	Gly	3	-0.998	0.036
Leu+Lys	Met	3	0.999	0.026
Phe	Development stage 1	3	0.999	0.031
Ser	Asp	3	-0.999	0.024
THF+5,10-CH2-THF	Glu	3	1	0.02
Total aa	Asp	3	1	0
Total aa	Ser	3	-0.999	0.024
Total folates	Weight/seed	3	-1	0.009

C.C stands for correlation coefficient

Significant Pearson correlations for *ms3-2* mutant line were found for 10-CHO-THF with Asp, His, and Tyr content, while 5MTHF was correlated with Ile content and seed weight. Also, Gly and Ile content were correlated with seed weight. Ile content was positive correlated with Gly content. Ala show positive correlation with Ser, while Leu+Lys were negative correlated with His. THF+5,10-CH_2-THF was positive correlated with His content and was negative correlated with Glu and Leu+Lys.

Table 5.5. Pearson correlations for *ms3-2* (Hm) T-DNA mutant line

Variable 1	Variable 2	N	C.C	P-value
10-CHO-THF	Asp	3	0.998	0.037
10-CHO-THF	His	3	-0.997	0.047
10-CHO-THF	Tyr	3	-0.999	0.021
5MTHF	Ile	3	-0.998	0.036
5MTHF	Weight/seed	3	1	0.011
FA	Met	3	0.999	0.023
Ala	Ser	3	0.998	0.037
Gly	Weight/seed	3	-0.997	0.047
Ile	Gly	3	0.999	0.023
Ile	Weight/seed	3	-0.999	0.024
Leu+Lys	His	3	-1	0.003
THF+5,10-CH2-THF	Glu	3	-0.999	0.033
THF+5,10-CH2-THF	His	3	0.998	0.038
THF+5,10-CH2-THF	Leu+Lys	3	-0.999	0.034
Total aa	Cys	3	0.998	0.04
Total folates	5FTHF	3	0.998	0.043
Tyr	Asp	3	-1	0.016

C.C stands for correlation coefficient

For *ms3-3* T-DNA mutant lines significant Pearson correlations were found for folates pool. The content of 10-CHO-THF was positive correlated with Gln, Pro, and Tyr content; 5,10-CH=THF+10-CHO-THF content was positive correlated with Leu+Lys, Ser, and Val; while 5,10-CH=THF was positive correlated with Leu+Lys and Ser content. In this case 5FTHF show positive correlation with Thr+Arg content; in the other hand, 5MTHF was positive correlated with Phe content. Regarding amino acid pool, Ala content show negative correlation with Glu content; Cys was correlated positive correlated with Gly content and negative correlated with plant development.

Similarly, Gly content show negative correlation with plant development; His content was positive correlated with seed weight, while Leu+Lys show positive correlations with Ser and Val content. Met content was negative correlated with Gln. Phe content was positive correlated with Val content, while Tyr show positive correlation with Pro content.

Summarizing, Pearson correlations demonstrate that phenotypic and metabolic parameters were affected differentially between control plants and T-DNA mutants of methionine synthase isoenzymes.

Table 5.6. Pearson correlations for *ms3-3* (Hm) T-DNA mutant line

Variable 1	Variable 2	N	C.C	P-value
10-CHO-THF	Gln	3	0.999	0.03
10-CHO-THF	Pro	3	0.998	0.038
10-CHO-THF	Tyr	3	0.997	0.046
5,10-CH=THF+10-CHO-THF	Leu+Lys	3	0.999	0.03
5,10-CH=THF+10-CHO-THF	Ser	3	1	0.013
5,10-CH=THF+10-CHO-THF	Val	3	0.998	0.043
5,10-CH=THF	Leu+Lys	3	0.997	0.046
5,10-CH=THF	Ser	3	1	0.002
5FTHF	Thr+Arg	3	1	0.009
5MTHF	Phe	3	0.999	0.03
Ala	Glu	3	-1	0.019
Cys	Gly	3	0.999	0.023
Cys	Development stage 1	3	-1	0.01
Gly	Development stage 1	3	-1	0.014
His	Weight/seed	3	0.999	0.026
Leu+Lys	Ser	3	0.998	0.044
Leu+Lys	Val	3	1	0.013
Met	Gln	3	-0.998	0.038
Phe	Val	3	0.998	0.039
Total folates	5MTHF	3	0.997	0.046
Total folates	Leu+Lys	3	0.998	0.035
Total folates	Phe	3	1	0.016
Total folates	Val	3	0.999	0.022
Total aa	Gln	3	0.997	0.049
Total aa	Met	3	-1	0.012
Tyr	Pro	3	1	0.008

C.C stands for correlation coefficient

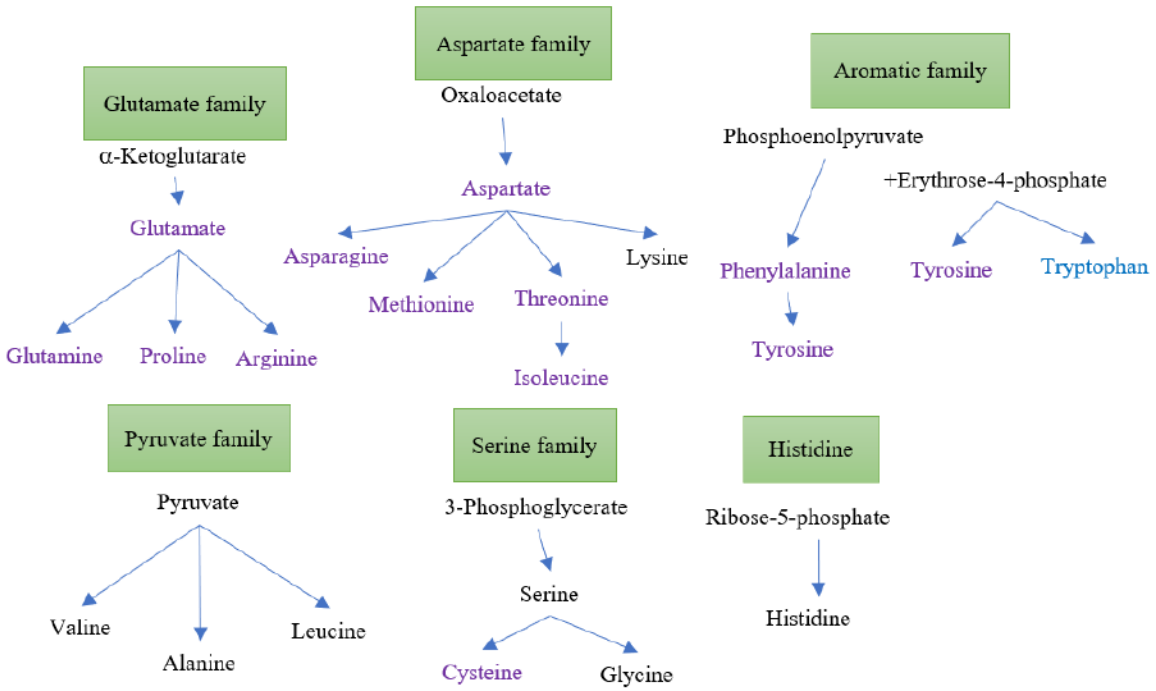

Genotype	Asp	Glu	Asn	Gln	Thr+Arg	Pro	Tyr	Cys	Met	Ile	Phe
ms1-1 (Hz)	=	++	=	=	++	++	++	=	++	--	=
ms2-1 (Hm)	=	=	++	=	++	++	--	++	=	--	--
ms2-2 (Hm)	++	++	=	=	=	++	++	++	=	=	=
ms3-2 (Hm)	=	++	++	=	++	++	=	=	++	--	=
ms3-3 (Hm)	=	=	=	++	=	++	=	=	=	--	=

Figure 5.4. Metabolic results of amino acid families based on biosynthetic pathways**.** Amino acids in **Purple Color** indicate significant differences (P<0.05) while **Black Color** denote amino acids that doesn't present significant differences. Symbol "++" denote significant increase and "--" denote significant decrease when compared to control plants. Tryptophan is indicated in Blue Color due to this amino acid was not quantified in this work.

Methionine content was evaluated by Yan *et al.* (2019), and these authors showed significant decreases on the contents of this amino acid in the ATMS mutant lines, mainly in ATSM1 and followed for ATMS2, ATMS3. Other study reported that S-methyl-methionine in vegetative tissue is transported to seeds and then is used for generation on additional methionine (Lee *et al.*, 2008). In the present work was expected a decrease in methionine content in mutant lines in comparison to control plants, however, it was obtained a significant

increase in methionine levels of *ms1-1* and *ms3-2* mutant lines with 4.09 and 1.54-fold, which is contradictory to the results obtained by Yan *et al* (2019). Differences between the results of the present project and literature could be attributed to the age of the plants and nutrients availability. In this study, we used 14-d old plants while in Yan *et al.* (2019) work the plants were harvested at 10-d old; also, they sown seeds in 1X MS medium in comparison to 0.5X MS used in this work.

A summary of methionine and cysteine biosynthesis in *A.thaliana* is showed in **Figure 5.5**. Cysteine along with methionine belongs to sulfur amino acids, due to they are in charge of sulfur assimilation, also cysteine serves as precursor molecule for the biosynthesis of glutathione, a predominant non-protein thiol, which is essential during plant stress responses (Domínguez-Solís *et al*., 2004). Domínguez-Solís and collaborators (2004) demonstrated a strong relationship between the accumulation of cysteine and cadmium in plant leaf trichomes when these were treated with different concentrations of cadmium, and they concluded that increasing cysteine content and number of trichomes in plant leaves could be a potential tool to improve heavy metal tolerance in plants. Also, Cysteine is a precursor molecule for cystathionine, as it is showed in **Figure 5.5,** cystathionine is required for homocysteine biosynthesis which acts as substrate for methionine biosynthesis. In this work, cysteine levels showed significant increase in *ms2-1* and *ms2-2*, ATMS2 is a cytosolic enzyme, as it is denoted in **Figure 5.5** cysteine can be biosynthesized at mitochondria, cytosol and plastids, thus, ATMS2 T-DNA mutant lines affect in some manner cysteine accumulation.

Proline is a protagonist amino acid in stress response, it has been extensively described and reported that proline accumulation is obtained when plants are treated with heat, salt, and water stress (Verslues *et al*., 2014; Liu *et al*., 1997; Chiang *et al*., 1995). In this study it was demonstrated that proline content resulted in an accumulation in all studied mutant lines, therefore it could be inferred that lacking methionine synthase isoenzymes could induces a stress response in plant growth and development.

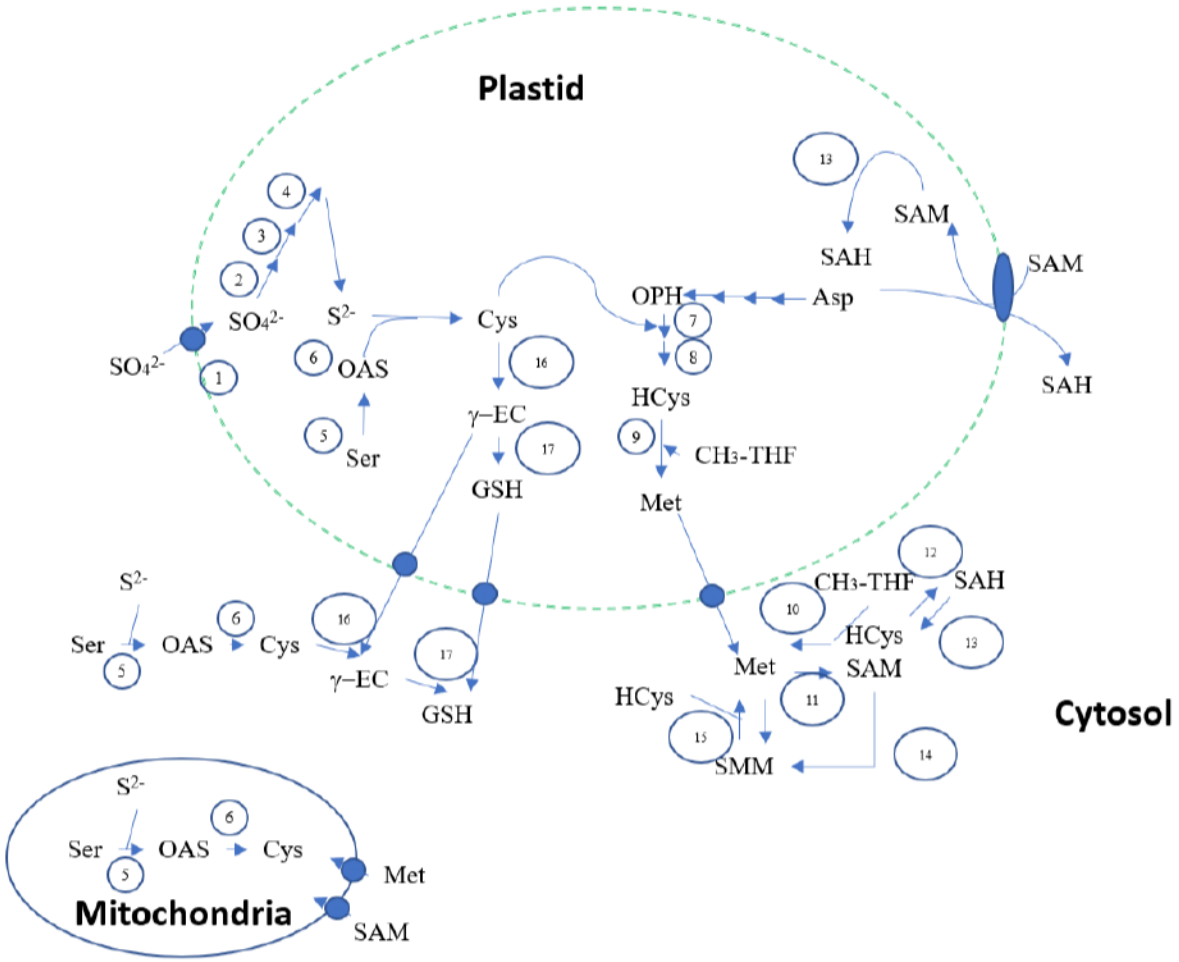

Figure 5.5. Biosynthesis pathway of sulfur amino acids in plants *A.thaliana*. The scheme summarizes the biosynthesis pathways by cell compartment of methionine and cysteine. Enzymes are listed as follow: 1, sulfate transport; 2, ATP sulfurylase; 3, ATP reductase; 4, sulfite reductase; 5, serine acetyltransferase; 6, O-acetylserine (thiol) lyase; 7, cystathionine c-cynthase; 8, cystathionine β-lyase; 9, methionine synthase 3; 10, methionine synthase 1 and methionine synthase 2; 11, SAM synthethase; 12, S-adenosyl-homocysteine hydrolase; 13, S-SAM dependent methylase; 14, SAM-methionine methyltransferase; 15, S-methylmethionine-homocysteine methyltransferase; 16, γ-glutamyl-cysteine syntethase; 17, glutathione syntethase. Molecules are: Asp: aspartate; SAH, S-adenosylhomocysteine; SAM, S-adenosyl methionine; Cys, cysteine; γ-GC, γ-glutamylcysteine; GSH, glutathione; HCys, homocysteine; OAS, O-acetylserine; OPH, O-phosphohomoserine; THF, tetrahydrofolate polyglutamate; Ser, serine; SMM, S-methylmethionine;. Modified from (Wirtz & Droux., 2005).

5.5 Folate content showed and accumulation of 5-CH_3-THF only in *ms3-2* and *ms3-3* mutant lines

Studies involving mutant lines of folates genes like methenyltetrahydrofolate cyclohydrolase (MTHFD1) showed decreased content of oxidized tetrahydrofolates and display genome-wide DNA hypomethylation, H3K9me1 decreases, and transposon activation (Groth *et al*, 2016). Some studies involving Salicylic acid (SA), which acts as a signal molecule for genes expression, demonstrated a relationship between SA treatment and folate biosynthetic and catabolic genes. Among folates biosynthetic genes, a common trend of up-regulation was observed after 24 h of SA treatment in ATMS1 and formyltetrahydrofolate deformylase (At5FCL, At4G17360), and this up-regulation was maintained until 120 h, this give arise to an increase in folates content of 2-fold (Puthusseri, 2018).

In this work, only the *ms3-2* mutant line increased the total folate and 5-CH_3-THF levels up to 1.37 and 1.45-fold, respectively, compared to *Col-0* control. Also, *ms3-3* mutant line has higher content of 5-CH_3-THF with 1.33-fold change increase in comparison to control plants. Thus, our results suggested that insertion T-DNA mutant lines of the plastic isoform in *ms3-2* and *ms3-3* mutant lines shown a significant impact on 5-CH_3-THF contents this could be attributed to impact on gene transcript levels or structural changes in ATMS3 affecting enzyme activity.

De novo methionine biosynthesis is the major metabolic flux of 5-CH_3-THF, thus, it would be expected that the lack of MS isoforms in Arabidopsis could impact its accumulation. However no significant Pearson correlation was observed between 5-CH_3-THF and Met in control plants and T-DNA mutant lines (**Tables 5.1** to **5.6**). The present results are in agreement with the information reported by Ju et al. (2019) in which they stated that homozygous ATMS3 mutant lines could survive by methionine recycling mediated by ATMS1.

5.6 Preliminary results could indicate that the folate glutamylation profile is altered in *ms1-1*, *ms3-2* and *ms3-3*

Preliminary results from polyglutamylated folates profile were obtained and showed that *ms1-1*, *ms3-2*, and *ms3-3* mutant lines accumulate predominantly Glu6, Glu7, Glu8 residues, in addition, Glu9 was found in the ms1-1 mutant line. These results were consistent

with the methionine synthase activity because it is known that the enzyme requires triglutamylated 5-CH_3-THF form (Ravanel *et al.,* 2004). Therefore, in **Figure 4.18 A** it can be noted that the increase in glutamate moieties of 5-CH_3-THF could affect the bioavailability of this cofactor for methionine synthase activity, thus, this arise questions about the mechanism behind the promotion of FPGS activity, enzyme responsible to add glutamate residues in the folate molecule, in *ms1-1, ms3-2, and ms3-3* mutant lines

6. Conclusions

In this work the phenotypic characterization of *Arabidopsis* with different T-DNA insertion positions for each MS isoenzyme was performed. Each T-DNA mutant line generated different visual and metabolic phenotypes. The most relevant visual phenotypes for ATMS1 T-DNA mutant lines were shoots weight, plant development, cotyledon and roots length; for ATMS2 mutant lines visual phenotypes were plant development, seeds weight, cotyledon and roots length; in the other hand, ATMS3 mutant lines relevant visual phenotypes were shoots weight, plant development, cotyledon length and seeds weight.

Regarding to homozygous knockout or knockdown lethality, genotyping screening of T-DNA mutants found homozygous plants for ATMS2 and ATMS3. These results suggest that ATMS3, which is responsible of *de novo* methionine biosynthesis, was not essential to sustain plant growth and development because plants are capable of survive, although it has an impact in visual phenotype and metabolic level. Indicating that methionine regeneration cycle with ATMS1 and ATMS2 has an important role in plant development, although there is the question why it is possible to find the homozygous plants for ATMS2 while ATMS1 shows lethality and both are cytosolic isoenzymes. Accordingly, to the current knowledge this could be explained due to the high expression level reported of ATMS1 in Arabidopsis database, however, further experiments will be needed, including gene expression, protein concentration and enzymatic activity to corroborate these conclusions.

It was expected that knockout or knockdown of methionine synthase genes could lead to decreased levels of methionine in Arabidopsis plants. Consequently, during the developmental stage analysis, T-DNA mutant lines should present delayed germination when compared to control plants. All mutant lines presented delayed plant development with

exception of *ms2-1* and *ms3-2*, in agreement with the results observed in shoots weight and cotyledon length for mutant lines.

The amino acid pool was differentially affected in mutant lines. The principal changes were present in glutamate, aspartate, and aromatic biosynthesis amino acid families in all mutant lines, and additionally, ATMS2 mutant lines were the only ones with significant increases of cysteine levels up to 2.7 and 2.4 for *ms2-1* and *ms2-2*, respectively. These results could be useful to contextualize the metabolic changes of amino acid pools in *A. thaliana* mutant lines, but, in order to get a complete metabolic context, it is required to perform experiments to evaluate other metabolites related to methionine metabolic flux such as homocysteine, SAH, SAM, ethylene, etc.

Total folate content was conserved in all T-DNA mutant lines in comparison to control plants with exception of *ms3-2* mutant line with 1.37 increase. 5MTHF content was increased in *ms3-2* and *ms3-3* up to 1.45 and 1.33 higher concentrations, respectively. This result could indicate an important bottleneck in 5MTHF metabolic pathway related to MS in *Arabidopsis* Moreover, preliminary results of polyglutamylation profile of folate presented evidence of accumulation of 5-CH_3-THF forms more polyglutamylated (Glu6-Glu9) in the mutant lines, thus, it could suggest that methionine synthase isoforms can participate in the polyglutamyl folates balance.

These results indicate that methionine synthase isoforms can affect in different extent to *A. thaliana*, and not only in methionine pools, involving an unknown mechanism affecting several aspects of plant growth, development and metabolites regulation in plants. Undoubtedly, this enzyme will be the subject of future research projects.

7. Future work

The original purpose of this research was to perform a functional genomic study of methionine synthase 1,2 and 3 isoforms in *A.thaliana*, although it was not possible to achieve certain goals and experiments on time, in order to get a complete functional genomic approach, this study could serve as initial steps and demonstrate an interesting role of ATMS1 in plant development and growth contrary to the plastidic isoform ATMS3. Some questions about why it was possible to find homozygous ATMS2 and ATMS3, while homozygous

ATMS1 apparently showed lethality. At the phenotype level, it is desirable to obtain the following experiments:

- Soil-based phenotypic analysis
    - Number of rosette leaves >1mm in length produced over time (Boyes *et al*., 2001)
    - Maximum rosette radius over time (Boyes *et al*., 2001)
    - Plant height over time (Boyes *et al*., 2001)
    - Growth stage progression (Boyes *et al*., 2001)
    - Time to bolting (Boyes *et al*., 2001)
    - Time to 1st flower onset (Boyes *et al*., 2001)
    - Comparison of silique area and the number of seed per half-silique (Boyes *et al*., 2001)
    - Comparison of silique number and yield per plant (Boyes *et al*., 2001)
- Plate-based phenotypic analysis
    - Seed germination with DL-propargylglycine and L-methionine (Gallardo *et al*., 2002)
    - Root phenotype characterizations (Boyes *et al*., 2001)
    - Embryo developmental stage (Collakova *et al*., 2008)
- Genomic analysis
    - Expression profiles of methionine synthase 1,2 and 3 mRNA (Stéphane Ravanel et al., 2004)
    - DNA methylation profiles (Groth *et al*., ,2016*)*
- Proteomic analysis
    - Dry seeds vs imbibed seeds over time (Gallardo *et al*., 2002)
    - Plants grown *in soil* (Gallardo *et al*., 2002)
    - Plants grown *in vitro* (Gallardo *et al*., 2002)
- Metabolite analysis
    - Methionine synthase 1,2 and 3 enzymatic activity (Ravanel *et al*., 2004)
    - SAM, S-methylmethionine and Hcy content (Kim *et al*., 2002; Yan *et al*., 2019)
    - Chlorophyll content (Ishibashi *et al*., 2015)
    - Folates and amino acid profile of roots

The result of these experiments could shed light to discover the unknown aspects of methionine synthase role in plant development and growth. Also, the generation of double mutants could help to discover the impact on the overall plant phenotype. This knowledge of basic science could be used to find new ways to use metabolic engineering in order to generate more efficient and to improve nutritional content of food crops. Undoubtedly, methionine synthase is going to be subject of future research works.

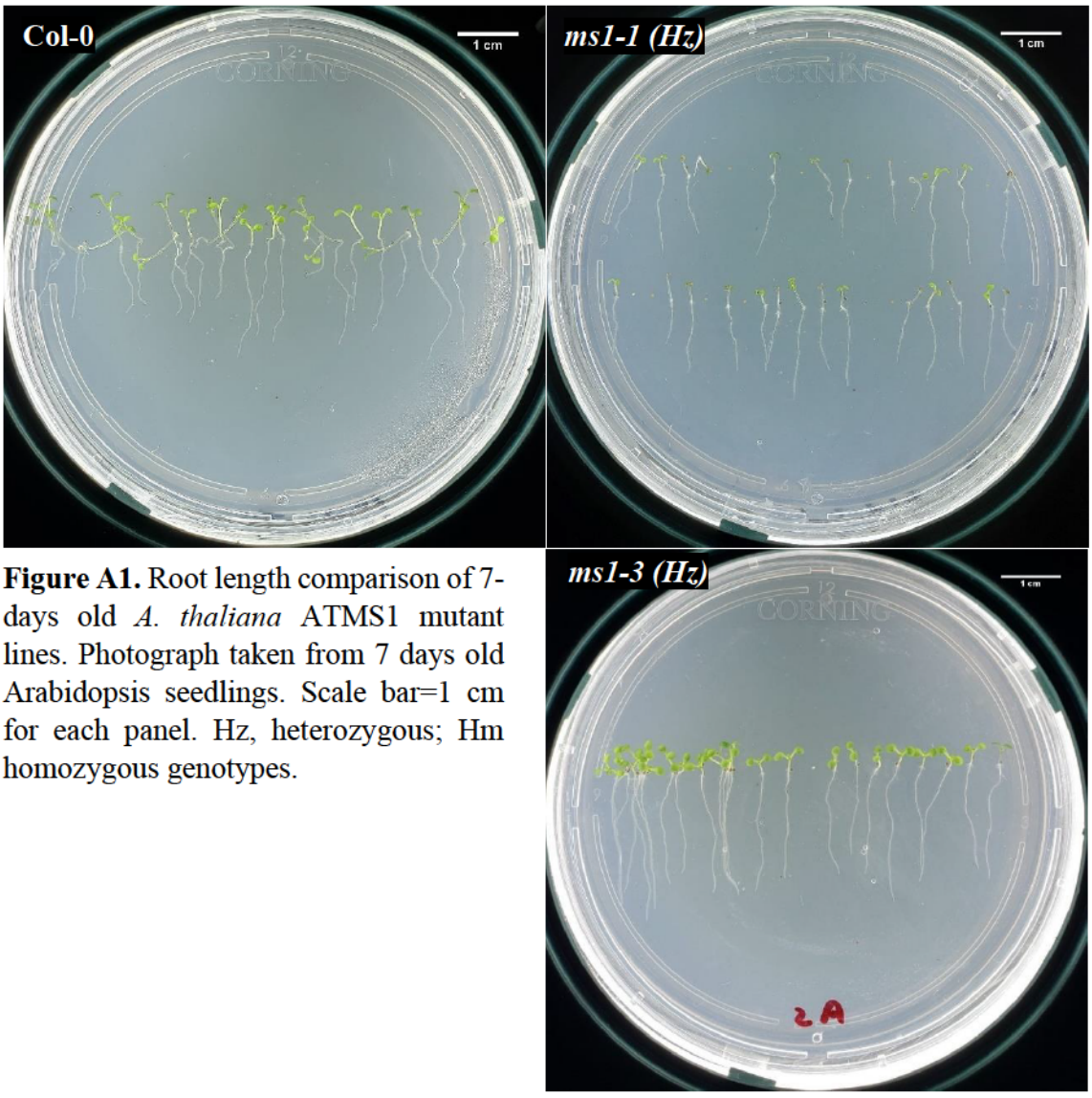

Figure A1. Root length comparison of 7-days old *A. thaliana* ATMS1 mutant lines. Photograph taken from 7 days old Arabidopsis seedlings. Scale bar=1 cm for each panel. Hz, heterozygous; Hm homozygous genotypes.

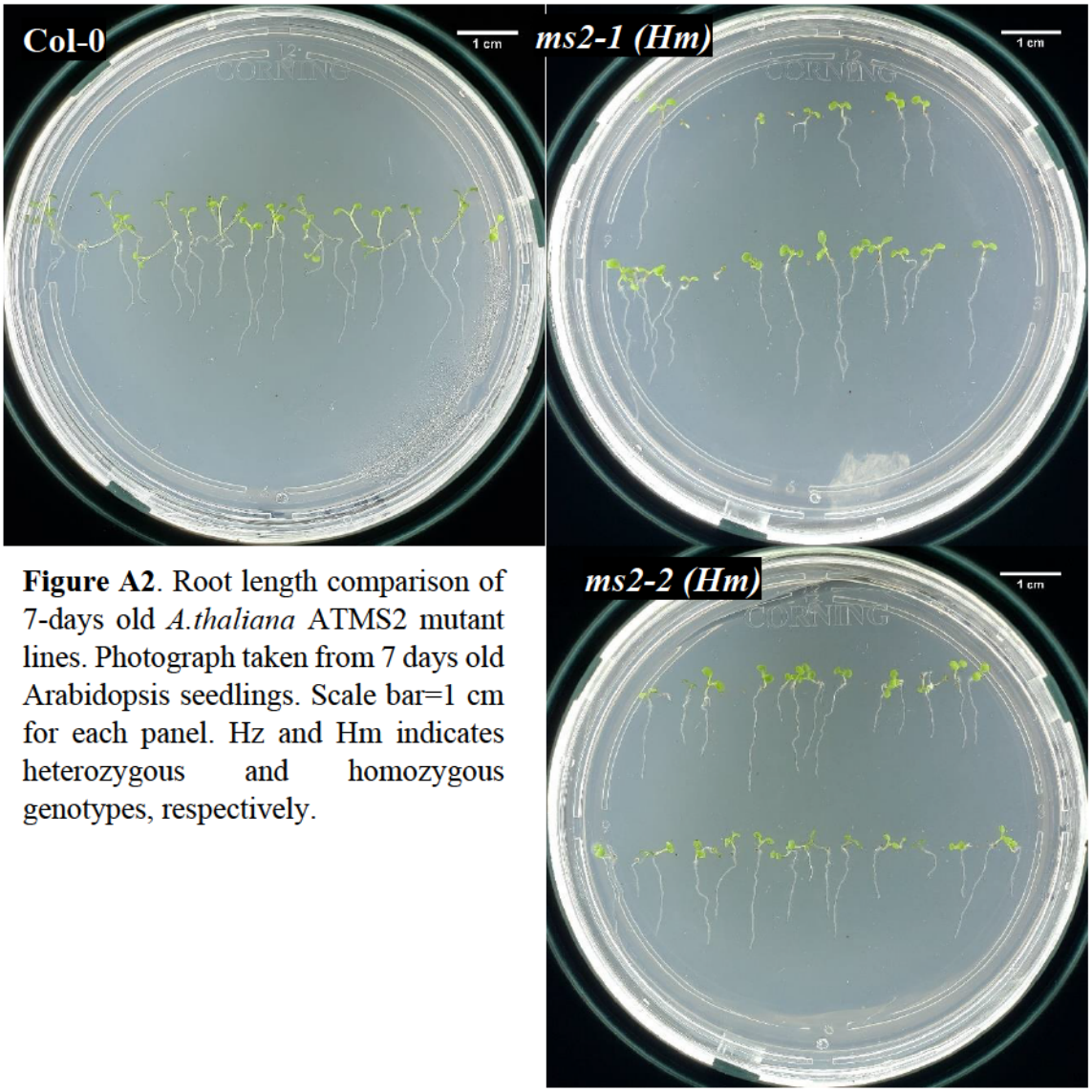

Figure A2. Root length comparison of 7-days old *A.thaliana* ATMS2 mutant lines. Photograph taken from 7 days old Arabidopsis seedlings. Scale bar=1 cm for each panel. Hz and Hm indicates heterozygous and homozygous genotypes, respectively.

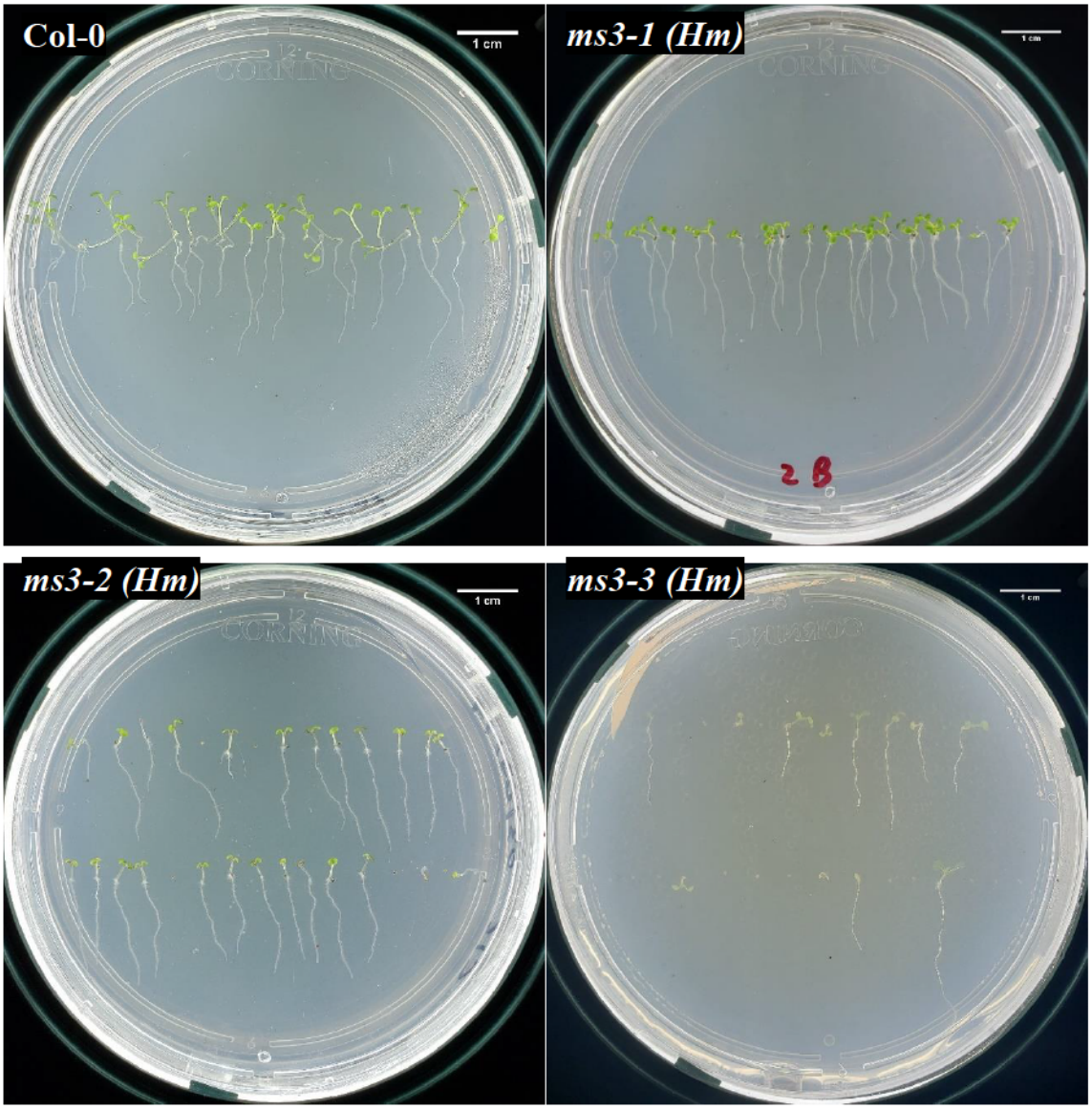

Figure A3. Root length comparison of 7-days old *A. thaliana* ATMS3 mutant lines. Photographs taken from 7 days old Arabidopsis seedlings. Scale bar=1 cm for each panel. Hz and Hm indicates heterozygous and homozygous genotypes, respectively.

Table A1. Seed stocks and germinated plants results					
Genotype	**Storage time at RT (months)**	**Germinated plants**			
		Mean		**SD**	
Col-0	~7	32.89	±	5	ef
ms1-1 (Hz)	<1	30.44	±	2.7	f
ms1-3 (Hz)	<1	48.63	±	3.1	ab
ms2-1 (Hm)	~6	36.63	±	5.3	de
ms2-2 (Hm)	~6	39.57	±	2.6	cd
ms3-1 (Hm)	<1	49.83	±	0.4	a
ms3-3 (Hm)	<1	43.77	±	2.3	bc
ms3-3 (Hm)	<1	15.33	±	2.6	g

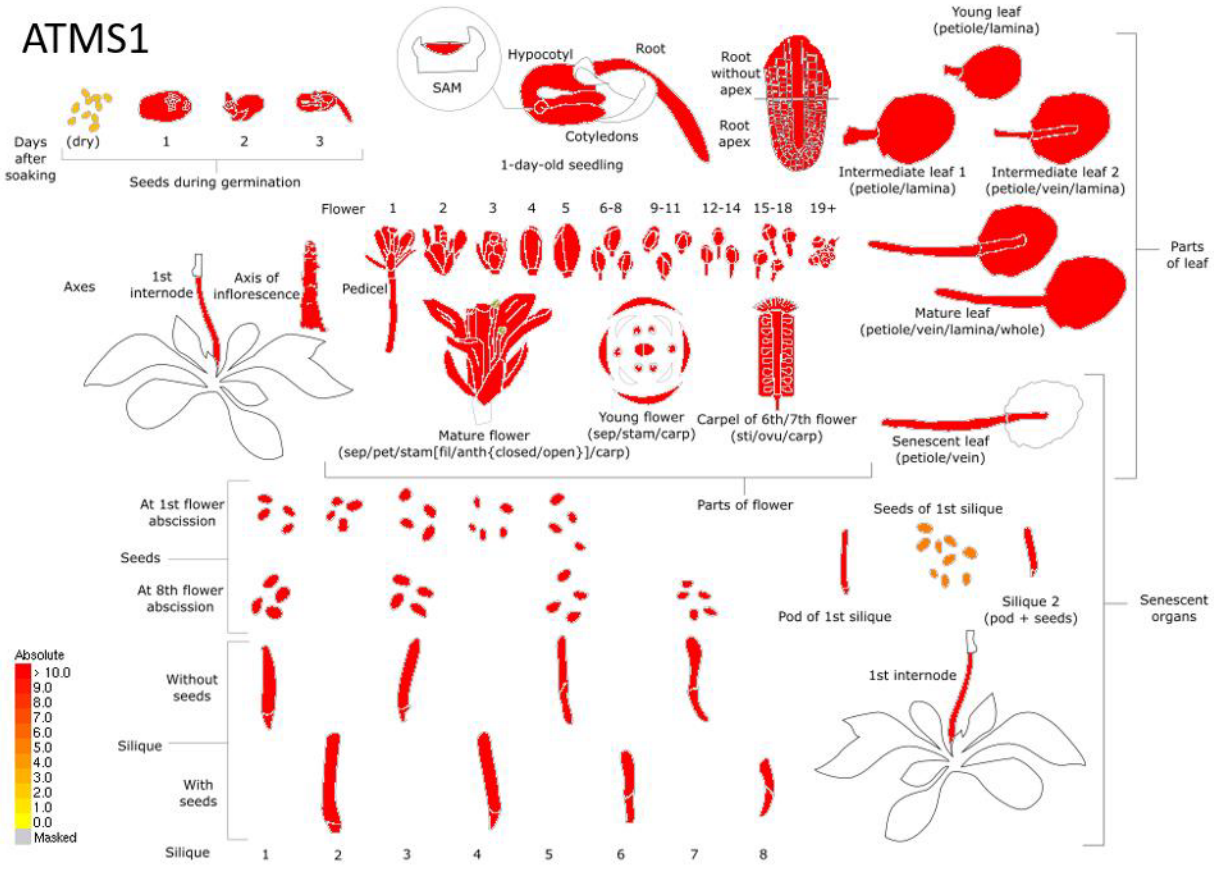

Figure A4. Expression levels of methionine synthase 1 during plant development. This scheme represent the expression levels during plant development of *A.thaliana* (Klepikova *et al*.,2016)

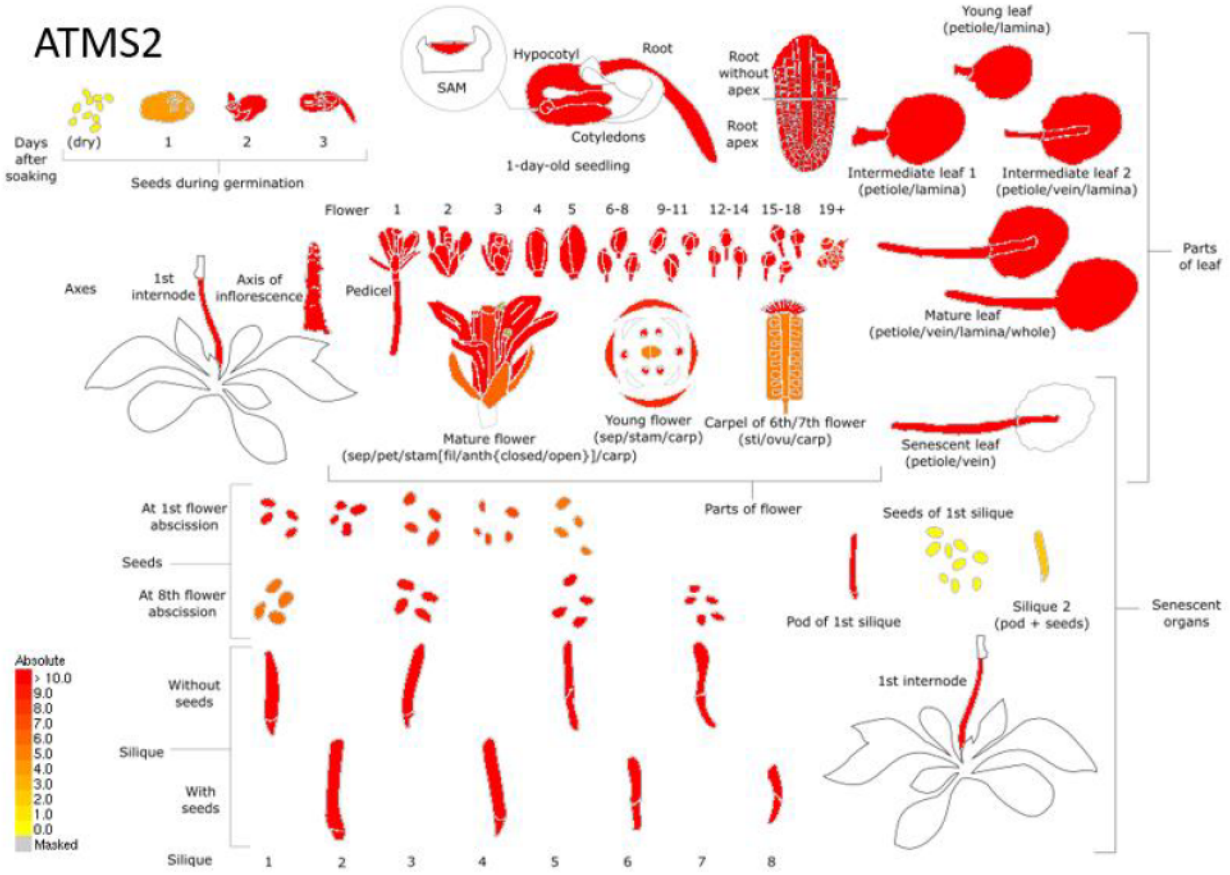

Figure A5. Expression levels of methionine synthase 2 during plant development. This scheme represent the expression levels during plant development of *A.thaliana* (Klepikova *et al*.,2016)

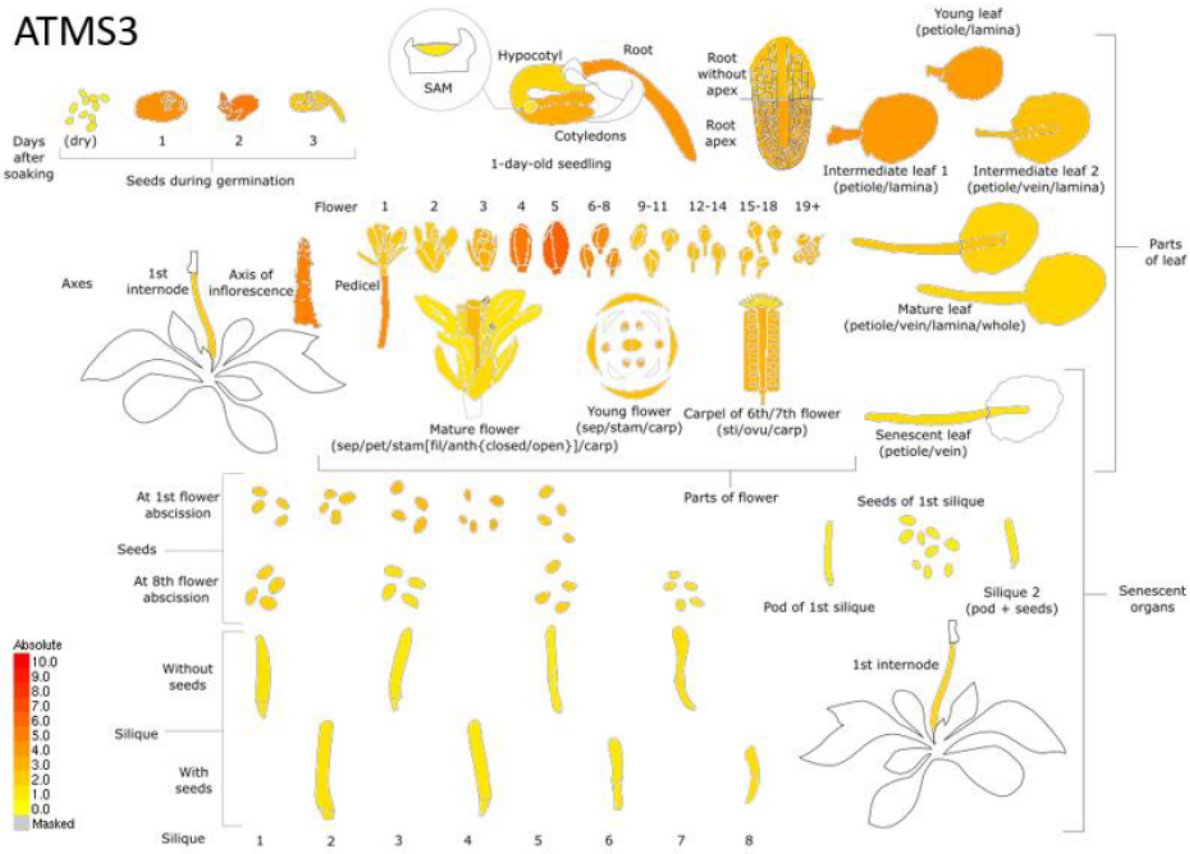

Figure A6. Expression levels of methionine synthase 2 during plant development. This scheme represent the expression levels during plant development of *A.thaliana* (Klepikova *et al*.,2016)

Table A2. Insertion position of A. thaliana T-DNA mutant lines and isoenzyme domains

Germplasm	Mutant line	Insertion position	Isoenzyme domains
SALK_035581	*ms1-1*	Intron 3	Region: 437-439 :L-homocysteine binding site
SALK_030047	*ms1-2*	Intron 5	
SALK_138706	*ms1-3*	Exon 9, Protein position: I467	Region: 521-522: 5MTHF binding site
CS881177	*ms2-1*	Intron 4	Region: 437-439 :L-homocysteine binding site
SALK_143628	*ms2-2*	Exon 11, Protein position: I670	Region: 521-522: 5MTHF binding site
SALK_018956	*ms3-1*	Exon 11, Protein position: C628	Region: 485-487 :L-homocysteine binding site
SALK_088429	*ms3-2*	Exon 10, Protein position: R624	Region: 569-570: 5MTHF binding site
CS852575	*ms3-3*	5'-UTR	

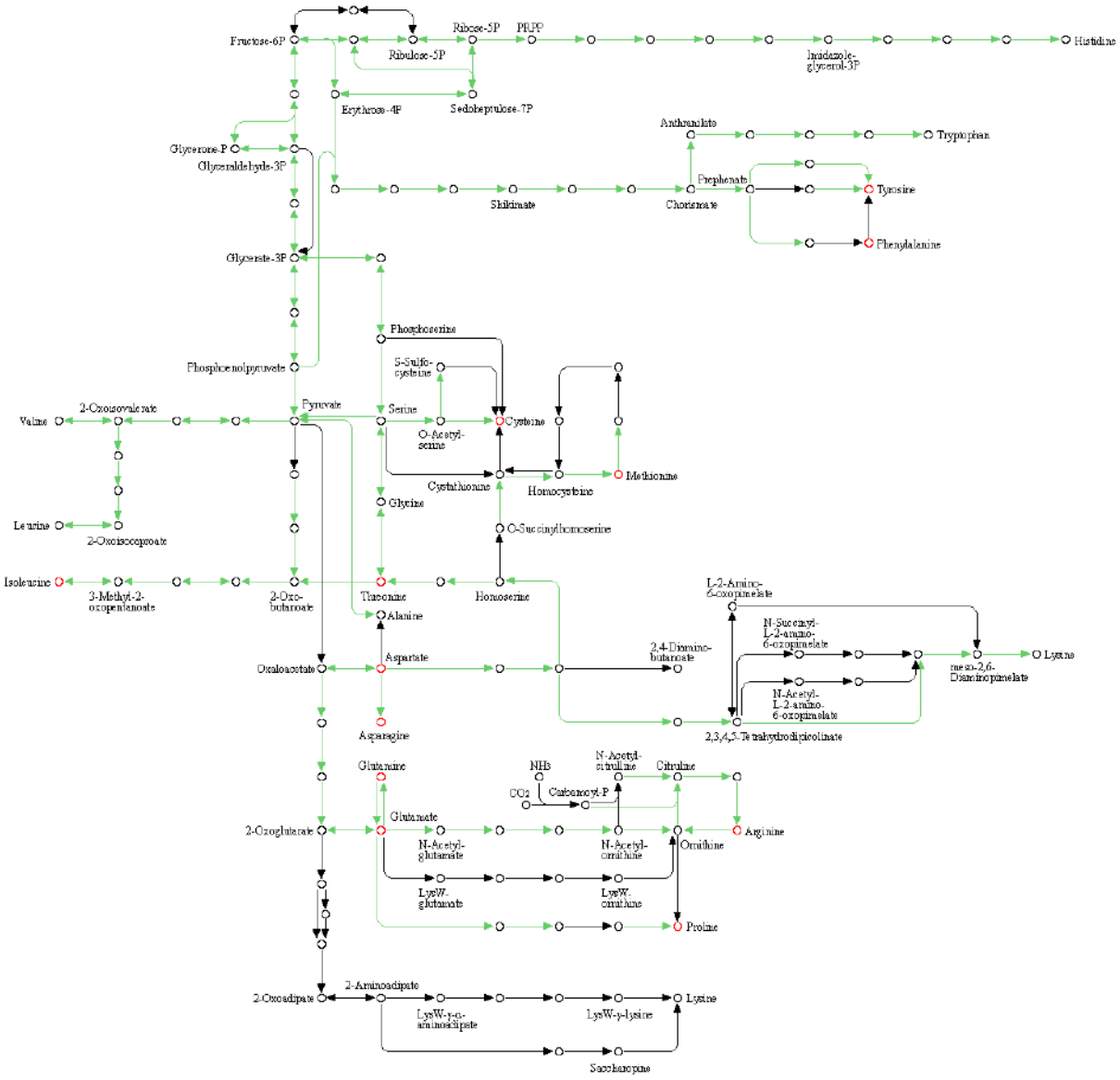

Figure A4. Amino acids biosynthesis pathways in *A. thaliana*. This scheme summarizes all the amino acid biosynthesis routes in *A.thaliana*, the circles in red indicate the amino acids which present significant differences in this study. The scheme was obtained from Kyoto Encyclopedia of Genes and Genomes at https://www.genome.jp/kegg/

References

Aarnes, H. (1977). Partial purification and characterization of methionine adenosyltransferase from pea seedlings. *Plant Science Letters, 10*(4), 381-390.

Allaway, W. (1970). Sulphur-selenium relationships in soils and plants. *Sulphur Institute Journal, 6*(3), 3-6.

Angelovici, R., Fait, A., Fernie, A. R., & Galili, G. (2011). A seed high-lysine trait is negatively associated with the TCA cycle and slows down Arabidopsis seed germination. *New Phytologist, 189*(1), 148-159.

Araghi, S. O., Kiefte-de Jong, J. C., Van Dijk, S. C., Swart, K. M., Van Laarhoven, H. W., Van Schoor, N. M., ... & Van Der Velde, N. (2019). Folic acid and vitamin B12 supplementation and the risk of cancer: long-term follow-up of the B Vitamins for the Prevention of Osteoporotic Fractures (B-PROOF) Trial. *Cancer Epidemiology and Prevention Biomarkers*, *28*(2), 275-282

Baggott, J., Johanning, G., Branham, K., Prince, C., Morgan, S., Eto, I., & Vaughn, W. (1995). Cofactor role for 10-formyldihydrofolic acid. *Biochemical Journal, 308*(3), 1031-1036.

Baur, A., & Yang, S. (1972). Methionine metabolism in apple tissue in relation to ethylene biosynthesis. *Phytochemistry, 11*(11), 3207-3214.

Bonner, E. R., Cahoon, R. E., Knapke, S. M., & Jez, J. M. (2005). Molecular basis of cysteine biosynthesis in plants structural and functional analysis of o-acetylserine sulfhydrylase from Arabidopsis thaliana. *Journal of Biological Chemistry, 280*(46), 38803-38813.

Boyes, D. C., Zayed, A. M., Ascenzi, R., McCaskill, A. J., Hoffman, N. E., Davis, K. R., & Görlach, J. (2001). Growth stage–based phenotypic analysis of Arabidopsis: a model for high throughput functional genomics in plants. *The Plant Cell, 13*(7), 1499-1510.

Burg, S. P., & Clagett, C. (1967). Conversion of methionine to ethylene in vegetative tissue and fruits. *Biochemical and biophysical research communications, 27*(2), 125-130.

Choi, J., Eom, S., Shin, K., Lee, R.-A., Choi, S., Lee, J.-H., . . . Soh, M.-S. (2019). Identification of Lysine Histidine Transporter 2 as an 1-Aminocyclopropane Carboxylic Acid Transporter in Arabidopsis thaliana by Transgenic Complementation Approach. *Frontiers in plant science, 10*, 1092.

Clarke, J. D. (2009). Cetyltrimethyl ammonium bromide (CTAB) DNA miniprep for plant DNA isolation. *Cold Spring Harbor Protocols, 2009*(3), pdb. prot5177.

Cohen, S. A., & Michaud, D. P. (1993). Synthesis of a fluorescent derivatizing reagent, 6-aminoquinolyl-N-hydroxysuccinimidyl carbamate, and its application for the analysis of hydrolysate amino acids via high-performance liquid chromatography. *Analytical biochemistry, 211*(2), 279-287.

Crider, K. S., Yang, T. P., Berry, R. J., & Bailey, L. B. (2012). Folate and DNA methylation: a review of molecular mechanisms and the evidence for folate's role. *Advances in nutrition, 3*(1), 21-38.

Droux, M., Ruffet, M. L., Douce, R., & Job, D. (1998). Interactions between serine acetyltransferase and O-acetylserine (thiol) lyase in higher plants: Structural and kinetic properties of the free and bound enzymes. *European Journal of Biochemistry, 255*(1), 235-245.

Eichel, J., González, J. C., Hotze, M., Matthews, R. G., & Schröder, J. (1995). Vitamin-B12-Independent Methionine Synthase from a Higher Plant (Catharanthus Roseus) Molecular Characterization, Regulation, Heterologous Expression, and Enzyme Properties. *European journal of biochemistry, 230*(3), 1053-1058.

Fox, J. T., & Stover, P. J. (2008). Folate-mediated one-carbon metabolism. *Vitamins & hormones, 79*, 1-44.

Field, M. S., Szebenyi, D. M., & Stover, P. J. (2006). Regulation of de novo purine biosynthesis by methenyltetrahydrofolate synthetase in neuroblastoma. Journal of Biological Chemistry, 281(7), 4215-4221.

Gallardo, K., Job, C., Groot, S. P., Puype, M., Demol, H., Vandekerckhove, J., & Job, D. (2002). Importance of methionine biosynthesis for Arabidopsis seed germination and seedling growth. *Physiologia plantarum, 116*(2), 238-247.

García-Salinas, C., Ramos-Parra, P. A., & de la Garza, R. I. D. (2016). Ethylene treatment induces changes in folate profiles in climacteric fruit during postharvest ripening. *Postharvest Biology and Technology, 118*, 43-50.

García-Salinas, C., Ramos-Parra, P. A., & Díaz de la Garza, R. I. (2016). Ethylene treatment induces changes in folate profiles in climacteric fruit during postharvest ripening. *Postharvest Biology and Technology, 118*, 43-50.

Giovanelli, J., MUDD, S. H., & DATKO, A. H. (1980). Sulfur amino acids in plants. In *Amino acids and derivatives* (pp. 453-505): Elsevier.

Giovanelli, J., Mudd, S. H., & Datko, A. H. (1985). Quantitative analysis of pathways of methionine metabolism and their regulation in Lemna. *Plant Physiology, 78*(3), 555-560.

González, B., & Vera, P. (2019). Folate metabolism interferes with plant immunity through 1C methionine synthase-directed genome-wide DNA methylation enhancement. *Molecular plant, 12*(9), 1227-1242.

Gregory III, J. F., & Toth, J. P. (1988). Chemical synthesis of deuterated folate monoglutamate and in vivo assessment of urinary excretion of deuterated folates in man. *Analytical biochemistry, 170*(1), 94-104.

Hanson, A. D., & Gregory III, J. F. (2011). Folate biosynthesis, turnover, and transport in plants. *Annual review of plant biology, 62*, 105-125.

Hirsch, S., de la Maza, M. P., Barrera, G., Leiva, L., & Bunout, D. (2019). Folic Acid and Colon Cancer: Impact of Wheat Flour Fortification With Folic Acid. In Flour and Breads and their Fortification in Health and Disease Prevention (pp. 413-421). Academic Press.

Jabrin, S., Ravanel, S., Gambonnet, B., Douce, R., & Rébeillé, F. (2003). One-carbon metabolism in plants. Regulation of tetrahydrofolate synthesis during germination and seedling development. *Plant physiology, 131*(3), 1431-1439.

Jones, C. E., Dancer, J. E., Smith, A. G., & Abell, C. (1994). Evidence for the pathway to pantothenate in plants. *Canadian journal of chemistry, 72*(1), 261-263.

Ju, C., Kong, D., Lee, Y., Ge, G., Song, Y., Liu, J., & Kwak, J. M. (2020). Methionine synthase 1 provides methionine for activation of the GLR3. 5 Ca2+ channel and regulation of germination in Arabidopsis. *Journal of Experimental Botany, 71*(1), 178-187.

Kastanos, E. K., Woldman, Y. Y., & Appling, D. R. (1997). Role of mitochondrial and cytoplasmic serine hydroxymethyltransferase isozymes in de novo purine synthesis in Saccharomyces cerevisiae. *Biochemistry, 36*(48), 14956-14964.

Kredich, N. M., Becker, M. A., & Tomkins, G. M. (1969). Purification and characterization of cysteine synthetase, a bifunctional protein complex, from Salmonella typhimurium. *Journal of Biological Chemistry, 244*(9), 2428-2439.

Leustek, T., Martin, M. N., Bick, J.-A., & Davies, J. P. (2000). Pathways and regulation of sulfur metabolism revealed through molecular and genetic studies. *Annual review of plant biology, 51*(1), 141-165.

Lieberman, M., Kunishi, A., Mapson, L., & Wardale, D. (1965). Ethylene production from methionine. *Biochemical Journal, 97*(2), 449-459. doi:10.1042/bj0970449

Maharaj, P. P., Prasad, S., Devi, R., & Gopalan, R. (2015). Folate content and retention in commonly consumed vegetables in the South Pacific. *Food chemistry, 182*, 327-332.

McKeon, T. A., Fernández-Maculet, J. C., & Yang, S.-F. (1995). Biosynthesis and metabolism of ethylene. In *Plant hormones* (pp. 118-139): Springer.

Mehrshahi, P., Gonzalez-Jorge, S., Akhtar, T. A., Ward, J. L., Santoyo-Castelazo, A., Marcus, S. E., . . . Beale, M. H. (2010). Functional analysis of folate polyglutamylation and its essential role in plant metabolism and development. *The Plant Journal, 64*(2), 267-279.

Okushima, Y., Overvoorde, P. J., Arima, K., Alonso, J. M., Chan, A., Chang, C., . . . Nguyen, D. (2005). Functional genomic analysis of the AUXIN RESPONSE FACTOR gene family members in Arabidopsis thaliana: unique and overlapping functions of ARF7 and ARF19. *The Plant Cell, 17*(2), 444-463.

Pelagio-Flores, R., Muñoz-Parra, E., Barrera-Ortiz, S., Ortiz-Castro, R., Saenz-Mata, J., Ortega-Amaro, M. A., . . . López-Bucio, J. (2020). The cysteine-rich receptor-like protein kinase CRK28 modulates Arabidopsis growth and development and influences abscisic acid responses. *Planta, 251*(1), 2.

Rahikainen, M., Alegre, S., Trotta, A., Pascual, J., & Kangasjärvi, S. (2018). Trans-methylation reactions in plants: focus on the activated methyl cycle. Physiologia plantarum, 162(2), 162-176.

Raman, S. B., & Rathinasabapathi, B. (2004). Pantothenate synthesis in plants. *Plant Science, 167*(5), 961-968.

Ramos-Parra, P. A., Urrea-López, R., & Díaz de la Garza, R. I. (2013). Folate analysis in complex food matrices: Use of a recombinant Arabidopsis γ-glutamyl hydrolase for folate deglutamylation. *Food research international, 54*(1), 177-185.

Ravanel, S., Block, M. A., Rippert, P., Jabrin, S., Curien, G., Rébeillé, F., & Douce, R. (2004). Methionine metabolism in plants chloroplasts are autonomous for de novo methionine synthesis and can import s-adenosylmethionine from the cytosol. *Journal of Biological Chemistry, 279*(21), 22548-22557.

Ravanel, S., Douce, R., & Rebeille, F. (2011). Metabolism of folates in plants. In *Advances in Botanical Research* (Vol. 59, pp. 67-106): Elsevier.

Ravanel, S., Gakière, B., Job, D., & Douce, R. (1998). The specific features of methionine biosynthesis and metabolism in plants. *Proceedings of the National Academy of Sciences, 95*(13), 7805-7812.

Rolfes, R. (2006). Regulation of purine nucleotide biosynthesis: in yeast and beyond. In: Portland Press Ltd.

Saini, R. K., Nile, S. H., & Keum, Y.-S. (2016). Folates: chemistry, analysis, occurrence, biofortification and bioavailability. *Food Research International, 89*, 1-13.

Saint-Girons, I., Parsot, C., Zakin, M. M., Baˇrzu, O., Cohen, G. N., & Weissbach, H. (1988). Methionine Biosynthesis in Enterobacteriaceae: Biochemical, Regulatory, and Evolutionary Aspect. *Critical Reviews in Biochemistry, 23*(sup1), S1-S42.

Sauter, M., Moffatt, B., Saechao, M. C., Hell, R., & Wirtz, M. (2013). Methionine salvage and S-adenosylmethionine: essential links between sulfur, ethylene and polyamine biosynthesis. *Biochemical Journal, 451*(2), 145-154.

Schröder, G., Eichel, J., Breinig, S., & Schröder, J. (1997). Three differentially expressed S-adenosylmethionine synthetases from Catharanthus roseus: molecular and functional characterization. *Plant Molecular Biology, 33*(2), 211-222. doi:10.1023/a:1005711720930

Witte, C.-P., & Herde, M. (2020). Nucleotide Metabolism in Plants. *Plant physiology*, pp. 00955.02019.

Xiong, F., Zhuo, F., Reiter, R. J., Wang, L., Wei, Z., Deng, K., . . . Yang, Z. (2019). Hypocotyl Elongation Inhibition of Melatonin Involves in Repressing Brassinosteroids Biosynthesis in Arabidopsis. *Frontiers in Plant Science, 10*, 1082.

Yan, X., Ma, L., Pang, H., Wang, P., Liu, L., Cheng, Y., . . . Li, Q. (2019). METHIONINE SYNTHASE1 Is Involved in Chromatin Silencing by Maintaining DNA and Histone Methylation. *Plant physiology, 181*(1), 249-261.